INVESTIGATING THE EFFECT OF THE *TOXOPLASMA* SKP1 MODIFICATIONS ON ITS INTERACTORS

by

BOWEN DENG

(Under the Direction of Christopher M. West)

ABSTRACT

Understanding the regulation of the characteristic life cycle of *Toxoplasma gondii* is key to drug development. The Skp1-cullin1-F-box protein (SCF) complex plays a major role in the regulation of the eukaryotic cell cycle. A novel O_2-dependent hydroxylation/glycosylation pathway modifies the adaptor protein Skp1 in *Toxoplasma*, but not any host proteins. In an unrelated protist, *Dictyostelium*, evidence indicates that the pathway only modifies Skp1 and enhances the association between Skp1 and F-box proteins (FBPs) to promote SCF activity. This study investigated if the *Toxoplasma* Skp1 modifications influenced the association between Skp1 and its interactors. *Toxoplasma* FbxO1 was identified as the most abundant Skp1-interacting FBP. Domain analysis revealed that *Toxoplasma* FbxO1 was conserved in apicomplexans and potentially *N*-myristoylated, supportive of its dynamic localization in cells. The *Toxoplasma* Skp1-FbxO1 association was found to be robust, however, no significant effect of the *Toxoplasma* Skp1 modifications on the association between Skp1 and FbxO1 was found.

INDEX WORDS: SCF complex, F-box protein, FbxO1, Skp1, hydroxylation-dependent glycosylation, *Toxoplasma gondii*

INVESTIGATING THE EFFECT OF THE *TOXOPLASMA* SKP1 MODIFICATIONS ON ITS INTERACTORS

by

BOWEN DENG

B.S., Muskingum University, 2015

A Thesis Submitted to the Graduate Faculty of The University of Georgia in Partial Fulfillment of the Requirements for the Degree

MASTER OF SCIENCE

ATHENS, GEORGIA

2020

INVESTIGATING THE EFFECT OF THE *TOXOPLASMA* SKP1 MODIFICATIONS ON ITS INTERACTORS

by

BOWEN DENG

Major Professor: Christopher M. West
Committee: Ronald Drew Etheridge
Robert S. Haltiwanger
Walter K. Schmidt

Electronic Version Approved:

Ron Walcott
Interim Dean of the Graduate School
The University of Georgia
May 2020

ACKNOWLEDGEMENTS

I would like to express my gratitude to Dr. Chris West for offering me the opportunity and support to study and research in his lab for the past four years. I'm indebted to the directions and advice he has provided to me, which had shaped me in every way to become a better science researcher. I would like to say thank you to all former and current members of our lab for their friendship and support, especially Dr. Elisabet Gas-Pascual, who helped me tremendously with the majority of the co-immunoprecipitation/mass spectrometry (co-IP/MS) experiments, Dr. Travis Ichikawa, a former postdoctoral researcher who supervised me when I joined the lab and guided me through all the molecular biology and cell culture methods necessary for performing the work in this thesis, and Dr. Kazi Rahman, a former graduate student who set the groundwork for investigating the *Toxoplasma* Skp1 modification. I also appreciate the members of Dr. Ira Blader's lab who have been collaborating with us on this project, especially Dr. Gustavo Baptista who performed the knockdown and immunofluorescence studies of FbxO1. The reagents and materials their lab generously shared with us were invaluable. I would also like to thank the members of Dr. Silvia Moreno's lab who generously gifted me the tagging plasmids and shared their valuable experience with me. Last but not least, I am very grateful to my thesis advisory committee members, Dr. Drew Etheridge, Dr. Robert Haltiwanger and Dr. Walter Schmidt, for unreservedly providing insightful comments on my project as well as valuable personalized advice on my graduate career development.

TABLE OF CONTENTS

LIST OF TABLES

Page

LIST OF FIGURES

Page

CHAPTER 1

INTRODUCTION

1.1 General background on *Toxoplasma gondii*

Toxoplasma gondii is a protozoan and apicomplexan parasite that infects most warm-blooded animals [1]. Members of family Felidae are the definitive hosts of *Toxoplasma* that harbor its sexual replication. Infectious *Toxoplasma* tachyzoites undergo asexual replication, during which they are haploid, in intermediate hosts including human, poultry and livestock [1]. Human can get infected mainly through the ingestion of meat, produce and water contaminated with *Toxoplasma* oocysts, contacting cat litter, and receiving blood from infected people (cdc.gov, Figure 1A). *Toxoplasma* is estimated to have latently infected around 50% of the world population [2]. The disease caused by infection with *Toxoplasma* is known as toxoplasmosis, which is usually asymptomatic in healthy people but imposes severe risks for pregnant women and people with suppressed immune systems [1, 2].

Tachyzoites, which are the infectious form of the parasite, infect host cells via the lytic cycle that employs invasion, intracellular replication, and egress. Under stressful conditions, tachyzoites convert into bradyzoites which are dormant and responsible for latent infection and reactivation in immunodeficient hosts [3, 4] (Figure 1B). *Toxoplasma* has a characteristic replication mechanism known as endodyogeny, in which two daughter cells emerge inside a maternal cell by equal nuclear division and parallel plasma membrane formation [3, 4]. The *Toxoplasma* cell possesses a unique peripheral membrane structure known as the inner

membrane complex (IMC) which provides rigidity to the cell and is dynamically turned over during endodyogeny, such that the complex is synthesized *de novo* on the new daughter cells and recycled from the maternal cell afterwards during endodyogeny [5]. A model of endodyogeny shows that it is initiated by the formation of the apical end daughter cell scaffold (DSC) which involves a number of proteins such as striated fiber assembling (SFA), a small GTPase (Rab11b), inner membrane complex (IMC) proteins, IMC sub-compartment protein 1 (ISP1), centrin2, and membrane occupation and recognition nexus protein 1 (MORN1) [3]. These factors likely contribute to the dynamic DCS throughout the initiation and elongation phases of endodyogeny. So, the expression, degradation, and localization of these factors are likely regulated by protein turnover mechanisms to properly mediate intracellular replication of the parasite.

A

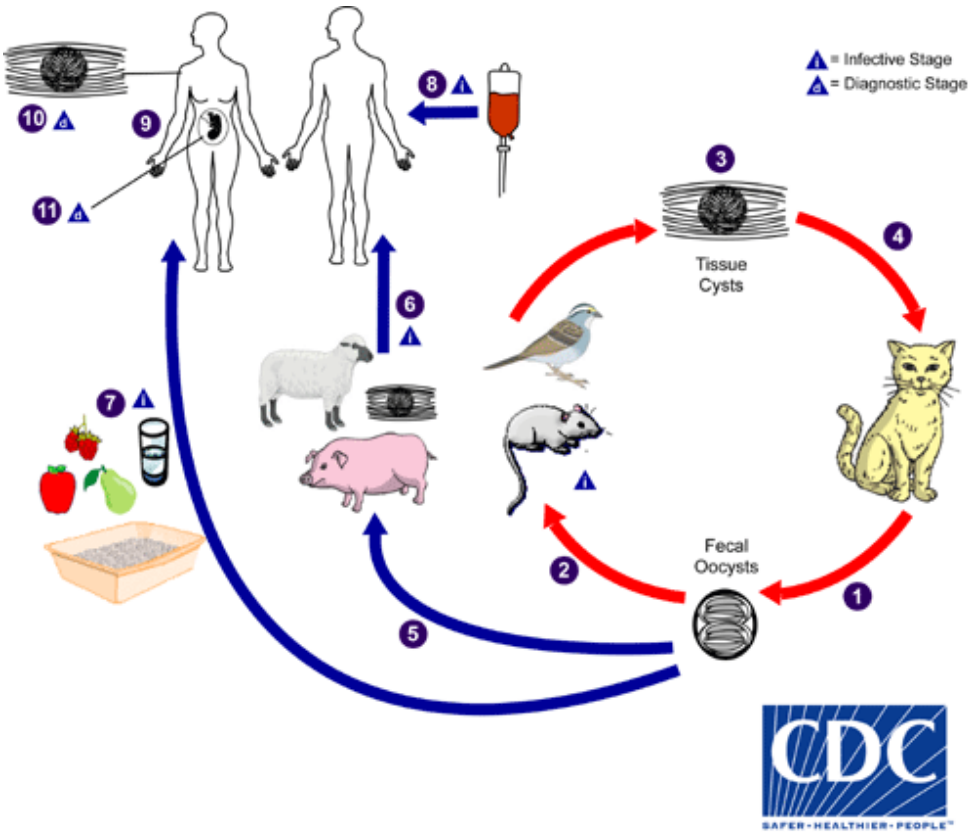
= Infective Stage
= Diagnostic Stage
Tissue Cysts
Fecal Oocysts
CDC
SAFER·HEALTHIER·PEOPLE™

B

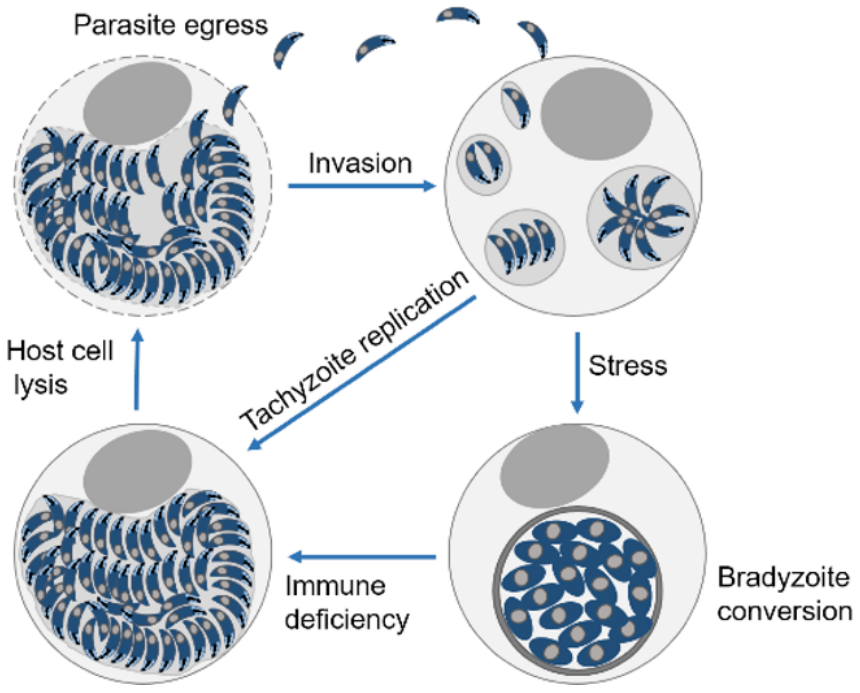
Parasite egress
Invasion
Host cell lysis
Tachyzoite replication
Stress
Immune deficiency
Bradyzoite conversion

Figure 1. *Toxoplasma* life cycle and replication. (A) *Toxoplasma* life cycle involves cats as the definitive hosts and most other warm-blooded animals as intermediate hosts. Artwork courtesy of cdc.gov. **(B)** *Toxoplasma* lytic cycle employs invasion, replication, and egress. Bradyzoite cysts form under stressful conditions and can reactivate in immune deficient hosts. The replication mechanism is known as endodyogeny. Artwork courtesy of Dr. Msano Mandalasi, West lab.

1.2 The SCF class of E3 ubiquitin ligase

Cell cycle progression requires certain proteins to be expressed and degraded at specific time points, and the majority of protein degradation is regulated by targeted proteolysis [6]. A well-known pathway of proteolysis is through polyubiquitination of protein substrates by E3 ubiquitin ligases, which comprise a class of multi-component enzyme complexes that targets substrates for signaling and proteasomal degradation in eukaryotic systems including *Toxoplasma* [6, 7]. The SCF complex is a family of E3 ubiquitin ligase that has been well-characterized in many eukaryotic systems including human and yeast [8]. Skp1 is an essential protein that functions as an essential adaptor protein that interacts with both cullins and F-box proteins (FBPs), to help bridge FBPs and the catalytic subunit of the SCF [8] (Figure 2). Free Skp1 in the cell can form either homodimers, which inhibit binding with FBPs, or form Skp1-FBP subcomplexes [9], which constitute the substrate recognition component of the SCF complex [8]. In *Toxoplasma*, Skp1 is modified by an O_2-dependent hydroxylation/glycosylation pathway [10], which supports the potential regulation of Skp1 function and the SCF complex assembly through environmental cues.

Cullin1 (Cul1) serves as the essential scaffold of SCF and binds to the RING box protein (Rbx1) to form the catalytic core of the SCF [8]. More importantly, Cul1 is subject to neddylation by a factor known as Nedd8 and deneddylation by COP9 signalosome, and the neddylation/deneddylation cycle functions as a switch for SCF activity [11]. Rbx1 recruits E2 ubiquitin-conjugating enzyme to the SCF to initiate ubiquitination of phosphorylated substrates [8]. Another crucial factor, Cullin-associated Nedd8-dissociated protein 1 (Cand1), also binds Cul1-Rbx1 and interplays with the neddylation cycle, and it has been described as an FBP

exchange factor that responds to FBP-specific substrate availability in cells and preferentially engage the necessary Skp1-FBP subcomplexes [12].

FBPs are characterized as substrate receptors that recognize specific phosphorylated substrates for polyubiquitination and proteasomal degradation by the SCF [13]. They contact Skp1 through a conserved region known as the F-box motif [14-16]. In *Toxoplasma*, 18 genes have been predicted to encode proteins with an F-box motif, and five of these predicted FBPs have either WD40 repeats (FbxW) or leucine-rich-repeats (LRR) (FbxL) that represent them as putative substrate receptors (SR); the others (FbxO) are also predicted to interact with Skp1 through the F-box motif but their functions are less obvious [17-19]. There are two common models for the functions of the SCF complex pertaining to the roles of FBPs, one is that the SR-type FBPs target their specific substrates to mediate substrate depletion, and the other is that the autoubiquitination of FBPs leads to FBP depletion. The predicted FBPs in *Toxoplasma* are hypothesized to participate in either type of SCF function (Figure 2).

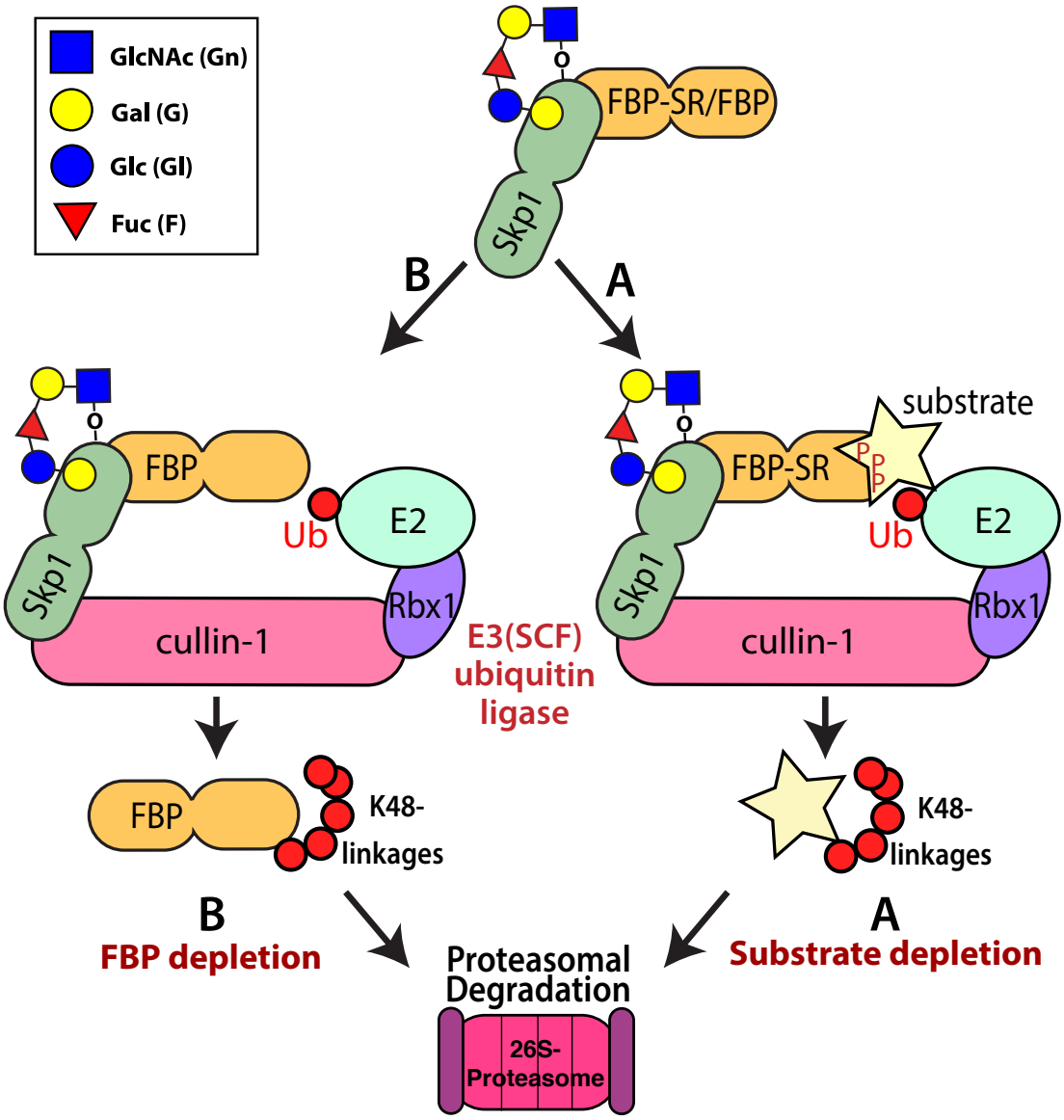

Figure 2. The *Toxoplasma* SCF model. The degradation of phosphorylated FBP-specific substrates through lysine 48 (K48)-linked polyubiquitination by the E3 SCF ubiquitin ligase and subsequent proteasomal degradation is illustrated in path A on the right, and the degradation of FBPs through autoubiquitination by the SCF complex is shown in path B on the left. FBP-SR: substrate receptor-type FBP.

1.3 Regulation of the SCF complex by the Skp1 modifications

In *Dictyostelium*, a protozoan cellular slime mold, the prolyl hydroxylase homolog (PhyA) of animal hypoxia inducible factor α (HIFα) has been shown to specifically hydroxylate *Dictyostelium* Skp1 proline 143 and modulate cellular responses to O_2 concentration [20, 21]. Knockout (KO) of *Dictyostelium phyA* significantly increases the O_2 requirement for the cells to culminate, and conversely, overexpression of *phyA* decreases the O_2 requirement [22]. Interestingly, overexpression of either *Dictyostelium* Skp1A or Skp1B results in similar phenotype to KO of *phyA*, and KO of Skp1B decreases the O_2 requirement [23]. These findings indicate that Skp1 hydroxylation by PhyA decreases Skp1 availability while PhyA activity is required for Skp1 activation and O_2-dependent development of the cellular slime mold.

In *Toxoplasma*, *phyA* KO results in significantly slower growth, and low (0.5%) O_2 moderately slows down growth. Interestingly, *phyA* knockout further slows down wildtype growth at 0.5% O_2, indicating that *Toxoplasma* deficient for Skp1 hydroxylation has decreased fitness. Thus, the hydroxylation is important for *Toxoplasma* proliferation especially at low O_2 [24, 25]. The Skp1 hydroxylation is also the priming step for a novel glycosylation pathway in protists, in which the conserved Skp1 proline is modified by a cytoplasmic hydroxylation-dependent glycosylation pathway that was initially discovered in *Dictyostelium* [10, 25, 26]. *Dictyostelium* Skp1 hydroxyproline 143 is modified by sequential addition of 5 monosaccharides by multiple cytoplasmically-localized glycosyltransferases to form a linear pentasaccharide [21, 26]. In *Toxoplasma*, the modification is on the conserved Skp1 proline 154, although the specificity of PhyA activity on *Toxoplasma* Skp1 needs to be confirmed by mutating Skp1 proline 154 and comparing the growth phenotype with that of Δ*phyA*. The Gnt1-mediated addition of O-α-GlcNAc is identical and the bifunctional PgtA-mediated addition of galactose

and fucose is conserved in both protists other than swapping the N and C domains of PgtA. However, the *Toxoplasma*-specific pathway diverges from *Dictyostelium* in the last two steps, as it utilizes Glt1 to add the fourth sugar, which is a glucose instead of a galactose in *Dictyostelium*, and it utilizes Gat1 to add the terminal galactose, as opposed to AgtA in *Dictyostelium* that adds the final two galactose [25, 27] (Figure 3). Similar to *phyA* knockout, *gnt1* knockout in *Toxoplasma* also results in slow growth, indicating the importance of the glycosylation [25]. An interaction between *gnt1* knockout and low O_2 is yet to be investigated.

The Skp1 modifications have been shown in *Dictyostelium* to promote the interaction between Skp1 and several FBPs by immunoprecipitation studies [28]. NMR and molecular dynamics analysis have shown that the linear pentasaccharide chain on hydroxyl-Skp1 promotes the formation of Skp1-FBP subcomplex, such that the glycan functions as a structural component to stabilize the disordered region between the two C-terminal helices of Skp1 to open the docking site for FBPs, thus promoting the binding between Skp1 and FBPs [29, 30] and SCF assembly. Overall, the Skp1 hydroxylation and glycosylation in selected protist species likely regulates Skp1-FBP interactions and is specifically important to protist biology. The loss of the Skp1 modifications in higher eukaryotes makes the pathway an attractive target for drug development to treat parasitic infections.

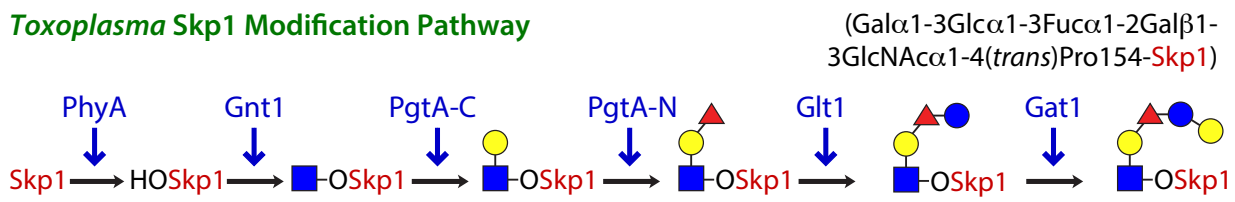

Figure 3. The O_2-dependent hydroxylation/glycosylation of *Toxoplasma* Skp1. The pathway is primed by hydroxylation of Skp1 proline 154 by PhyA, and five sequential glycosylation steps further modify the hydroxyl-Skp1 to build the linear pentasaccharide. The symbols for monosaccharides are the same as Figure 2. The image is modified from a previous publication [10].

1.4 A robust Skp1 interactor revealed by Skp1 co-IP/MS

To interrogate the components and functions of the SCF complex in *Toxoplasma*, Skp1 co-immunoprecipitation experiments coupled with mass spectrometry analysis (co-IP/MS) were performed to verify the presence of known SCF components and to discover relevant FBPs and potential SCF substrates in *Toxoplasma*. One type of co-IP/MS experiment was based on the specific interaction between Skp1 and its anti-serum (UOK75) generated previously [24]. Another type of co-IP/MS utilized a strain whose endogenous Skp1 was C-terminally tagged with a Strep/FLAG tag (Skp1-SF) and its recognition by an anti-FLAG antibody (M2). Because *Toxoplasma* cells exhibit strikingly different behaviors when they are intracellular (IC) versus extracellular (EC), such that IC cells undergo continuous replication while EC cells are arrested in interphase, *Toxoplasma* cells collected at both stages were compared in the Skp1-SF co-IP/MS experiment to examine how the Skp1 interactome would differ at distinct replication stages.

After curation of the Skp1-SF co-IP/MS results from Proteome Discoverer 2.2 (PD 2.2), a mass spectrometry data analysis software, Skp1 interactors including Cullin1 (Cul1) and Ring finger domain-containing protein 1 (Rbx1) that were expected to participate in SCF complexes [6] were detected. Several of the 18 bioinformatically predicted FBPs including FbxO1, FbxO10 and FbxL2 [17] were detected. JmjD6b, which is thought to be orthologous to one of the *Dictyostelium* FBPs, JcdI, was detected as one of the most confident interactors of Skp1 and was later determined to have a putative F-box motif [17]. One of the *Toxoplasma* Skp1 modifying enzymes, Gat1, which adds the terminal galactose of the pentasaccharide [25], was also detected as an interactor of Skp1 [17]. Interestingly, the majority of the candidate Skp1 interactors were more abundantly associated with Skp1 in the IC parasites than in the EC parasites (Figure 4A).

In an independent co-IP/MS experiment using UOK75 to capture Skp1 interactors, Cul1, Rbx1 and Gat1 were also detected, while FbxO1 was the only predicted FBP detected (Figure 4B).

The Skp1 interactome results suggested the potential formation of Skp1-FBP subcomplexes and their interaction with Cul1, which at least in part supported the assembly of SCF complexes in *Toxoplasma*. Of the predicted FBPs in *Toxoplasma*, FbxO1 was the most robustly detected interactor with Skp1 in all co-IP/MS trials. FbxO1 has a high (top 75-percentile) level of expression in tachyzoites (toxodb.org) and it is also predicted to be an essential gene for the lytic cycle [31]. Experimental results further supported the essentiality of FbxO1, such that knockout of the protein apparently led to a strong fitness defect in the parasites. A conditional knockdown of FbxO1 expression in *Toxoplasma* resulted in significantly slower growth, suggesting that *Toxoplasma* FbxO1 is important for parasite growth [17].

To visualize the localization of FbxO1 in *Toxoplasma* cells, an immunofluorescence (IFA) study was performed to label FbxO1 in actively replicating cells. The cells were fixed, stained for markers that have distinct localizations in the cells, and examined for colocalization of FbxO1HA with these markers. It was observed that in G1-phase, FbxO1 mostly localized at particular regions of the membrane of the cells, including at the apical end that did not colocalize with the inner membrane complex marker (IMC3), and at a peripheral region that colocalized with IMC3 (Figure 5, top). Starting in S-phase, FbxO1 started to disappear from the IMC and accumulated at DCS (Figure 5, middle) [17], which is a crucial protein complex that forms around the centrosome and initiates endodyogeny – a characteristic type of replication of *Toxoplasma* cells [3, 17]. During mitosis, FbxO1 at the DCS started transitioning into the apical end membrane of the newly formed daughter cells and some FbxO1 also formed foci inside the daughter cell but were clearly not associated with the nucleus throughout the cell cycle (Figure 5,

bottom). While no direct information is available regarding the co-association of Skp1, evidence presented herein is consistent with an obligatory interaction between the two proteins. This result suggested that FbxO1 is either turned over or trans-localized during the cell cycle, in order to enable its transition from the IMC to the DCS, exhibiting similar turnover pattern to the IMC complex [5].

Taken together, FbxO1 was further studied as an exemplary FBP in *Toxoplasma* to push forward understanding of the *Toxoplasma* SCF complex assembly, the effect of the Skp1 modifications on the association between Skp1 and its interactors including FBPs, and the biological relevance of these interactions and the SCF complex assembly in *Toxoplasma*.

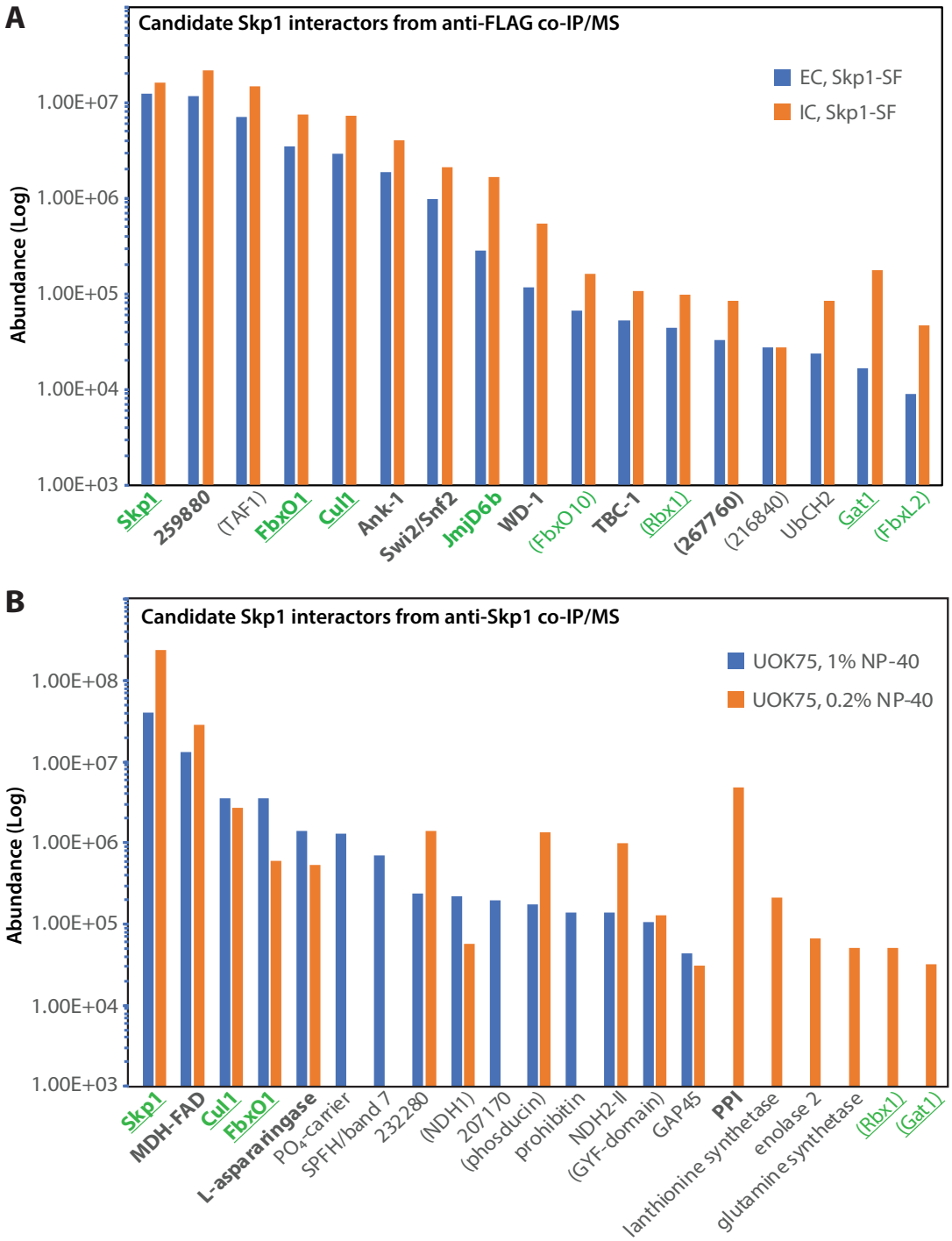

Figure 4. Candidates of Skp1 interactors revealed by Skp1 co-IP/MS. These results are adapted from a previous publication [17]. The experiments were performed by Dr. Elisabet Gas-Pascual and interpreted by Dr. Chris West and Bowen Deng. **(A)** The list of candidates of Skp1

interactors that were determined by Skp1-SF co-IP/MS using either EC or IC parasites. The quantification was based on area under the curve (AUC) calculations for all assigned peptides in PD 2.2 and all the graphed proteins were enriched ≥ 6-fold in Skp1-SF sample relative to RHΔΔ sample. The proteins in bold were selected at 1% FDR, while the ones not in bold were at relaxed FDR (5%). All the proteins had 2 or more identified peptides except for the parenthesized proteins which had only 1 identified peptide. The proteins in green were predicted to be Skp1 interactors, and the underlined proteins were species also detected in UOK75 co-IP/MS. (**B)** The list of candidates of Skp1 interactors that were determined by anti-Skp1 co-IP/MS and were enriched by ≥ 6-fold in UOK75 co-IP relative to non-specific IgG control co-IP in either 1% NP-40 or 0.2% NP-40 extractions. Protein names were categorized in the same way as in panel A. Abundance values were plotted on a logarithm scale to display the broad range of values.

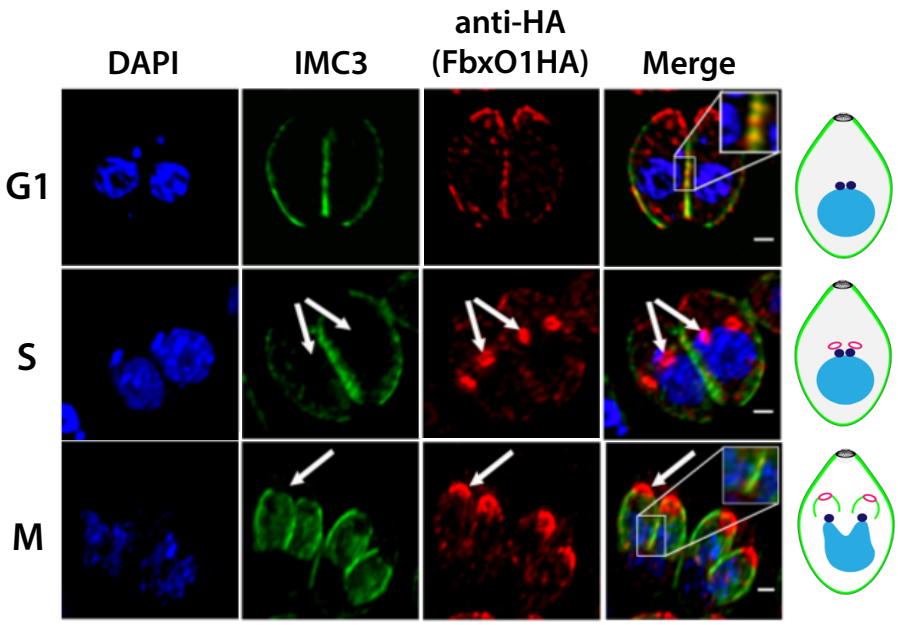

Figure 5. Localization of FbxO1 during cell cycle. This result is adapted from a previous publication [17]. The experiment was performed by Dr. Gustavo Baptista. Freshly lysed tachyzoites from the FbxO1HA strain were used to infect human foreskin fibroblast monolayers grown on coverslips. The coverslips were fixed and stained when the parasites were actively replicating. DAPI was used to stain DNA (blue), Alexa Fluor-conjugated specific antibodies were used to detect IMC3 (green) and FbxO1HA (red). The coverslips were examined under a Zeiss Axioimager M2 microscope with an Orca ER CCD camera and the images were collected as 0.2 µm z-increment serial image stacks. The images were processed and merged using the Volocity software. The white arrows pointed to the developing DCS during endodyogeny, and the boxes highlighted a location where colocalization of FbxO1 and IMC3 was observed. G1: growth phase; S: DNA synthesis phase; M: mitosis. The diagram to the right shows the morphology of *Toxoplasma* cells during the indicated stages of the cell cycle. The gray circles represent the apical end of the cell, the black dots represent the centrosome, and the red rings indicate the locale of the developing DCS.

CHAPTER 2

MATERIALS AND METHODS

2.1 FbxO1 sequence analysis

To facilitate the characterization of FbxO1 domains, a homology search was performed on the *Toxoplasma gondii* ME49 strain FbxO1 amino acid sequence (TGME49_310930) obtained from ToxoDB (toxodb.org), an online *Toxoplasma* genomic resources database. First, the full FbxO1 sequence was searched against the NCBI non-redundant database using basic local alignment search tool (BLASTP, version 2.9.0+) with the E-value cut-off at 100. Next, multiple overlapping stretches of the full sequence with better conservation that were discovered from the initial search were further searched against the NCBI non-redundant database using BLASTP with the same settings to improve the search sensitivity. From the list of identified homologs, the sequence with the smallest E-values from each genus was selected as a representative sequence, and all of the curated sequences were aligned using the constraint-based multiple alignment tool (COBALT) on NCBI and manually refined for optimal alignment of hydrophobic residues and minimal insertions/deletions except adjacent to glycine and proline residues.

To predict the conservation of the putative *N*-myristoylation motif on FbxO1 and its homologs, the neural network-based ExPASy myristoylator tool (web.expasy.org/myristoylator) was used to examine the representative sequences from each genus. A minimum of 18 N-terminal amino acids were used as the query for each selected sequence in the prediction. The

prediction tool determined the likelihood that an input sequence was *N*-myristoylated and provided a score for the confidence of the prediction.

2.2 Cell and parasite culture

A mammalian cell culture system was used for the growth and maintenance of *Toxoplasma gondii* strains [32]. Human foreskin fibroblast (HFF) and the human telomerase reverse transcriptase immortalized version of it (hTERT) were used as host cells, which were maintained in tissue culture flasks in complete Dulbecco's Modified Eagle's Medium (DMEM) supplemented with 1 or 10% (v/v) fetal bovine serum (FBS), 100 IU/ml penicillin, 100 µg/ml streptomycin and 2 mM L-glutamine. The *Toxoplasma* strains used and generated in this study, all from the RH strain, were inoculated and propagated on host cell monolayer in tissue culture flasks in DMEM containing 1% (v/v) FBS, 100 IU/ml penicillin, 100 µg/ml streptomycin and 2 mM L-glutamine. All cells and *Toxoplasma* tachyzoites were grown in humidified cell culture incubators charged with 5% CO_2 and maintained at 37 ˚C.

To grow and harvest intracellular parasites that were replicating, a confluent HFF monolayer was infected with freshly lysed tachyzoites that were quantified by counting a 100-fold dilution in media on a hemocytometer with phase contrast microscopy. The quantified tachyzoites were used to infect HFFs at ~1.5 multiplicity of infection (MOI) which was ~12 million tachyzoites for a HFF T175 (175 cm^2 growth area) flask and grown for 24 to 30 hours. Afterwards, when most of the HFFs had been infected and the tachyzoites were replicating intracellularly (Rosetta stage), the flasks were replenished with fresh media and checked with phase contrast microscopy to ensure the removal of most egressed tachyzoites. The HFF monolayer was scraped from the flask, pelleted at 2,000 × g for 10 mins and syringe lysed to

release the intracellular tachyzoites. Lastly, the tachyzoites were washed in phosphate buffered saline (PBS) for two times, pelleted at 2,000 × g for 10 mins and snap frozen in liquid N_2, before being stored at -80 ˚C. To collect extracellular parasites that were naturally egressed, the HFF monolayer was infected in the same way as for intracellular parasites but collected after 36 to 48 hours, then the media containing the extracellular tachyzoites were collected, pelleted and syringe lysed. The parasites were washed and stored as described above.

2.3 Epitope tagging

All the C-terminally 3×HA-tagged FBPs (FbxO1, FbxW1 and FbxL1) *Toxoplasma* strains (Table 1) were generated using an established CRISPR/Cas9-mediated strategy [32] in an RH parental strain that lacked the *ku80* gene and the *hxgprt* gene (RHΔΔ) to significantly improve the efficiency of homology-based repair [33]. The haploid nature of tachyzoite allows that only single targeting events are required. To target the specific region of the gene of interest, the sequence of the gene of interest was analyzed with a CRISPR gRNA design tool EuPaGDT (grna.ctegd.uga.edu) which computationally generated a list of potential gRNA sequences. Ideal gRNAs were selected based on their proximity to the target gene loci, cutting specificity, and efficiency score. The gRNA sequences were cloned into the pU6-Universal plasmid vector (Table 2) which also expressed the Cas9 gene. To generate the 3×HA tag-containing sequence that was inserted at the gRNA target site by homologous driven repair (HDR), polymerase chain reaction (PCR) was used to amplify the 3×HA tag sequence followed by a drug selection cassette (DHFR or CAT) from the 3×HA tagging plasmids (Table 2). The 5′ primer contained a 45-bp overhang sequence that was homologous to the immediate 45-bp upstream of the stop codon, and the 3′ primer contained a 45-bp overhang that was homologous to the genomic sequence

immediately downstream of the gRNA target site. The tagging process of FbxO1 is outlined in Figure 6 and the related primer sequences are shown in Table 3.

For transfection of parasites, ~10 µg of the gRNA-containing plasmid and ~1 µg of the PCR amplicon per transfection were precipitated by mixing with 2× volume of 95% ethanol and 1/9th volume of 3 M NaOAc and storing at -20 ˚C overnight. The next day, the plasmid and amplicon were centrifuged at 21,000 × g at 4 ˚C for at least 30 mins and washed in 70% ethanol. Next, the plasmid and amplicon precipitates were resuspended in cold sterile Cytomix buffer that was formulated by Dr. David Sibley's lab (10 mM potassium phosphate buffer (pH 7.6), 120 mM KCl, 0.15 mM $CaCl_2$, 5 mM $MgCl_2$, 25 mM HEPES, 2 mM EDTA) to a final concentration of 1 µg/µl and 100 ng/µl, respectively. About 10 million freshly lysed tachyzoites per transfection were harvested, washed in cold sterile Cytomix buffer, and resuspended in cold sterile Cytomix buffer supplemented with 2 mM adenosine triphosphate (ATP) and 5 mM glutathione (GSH). The plasmid, amplicon and tachyzoites required for each transfection were mixed together, transferred to an electroporation cuvette, and electroporated with a Bio-Rad Gene Pulser Xcell set at 25 µF and 1.5 kV. The transfected tachyzoites were transferred to a confluent HFF monolayer and allowed to recover in DMEM with 10% FBS, 100 IU/ml penicillin, 100 µg/ml streptomycin and 2 mM L-glutamine without selection drug for 24 hours before adding the appropriate drug. For the dihydrofolate reductase-thymine synthase (DHFR-TS) selectable marker, 1-3 µM pyrimethamine was used and for the chloramphenicol acetyltransferase (CAT) selectable marker, 20 µM chloramphenicol was used. The transfected tachyzoites that overcame drug selection were subcloned into 96-well plates by limiting dilution. The picked clones were analyzed by diagnostic PCR, Western blot, and verified by genomic sequencing for integration of the tag.

Table 1. List of *Toxoplasma* strains generated in this study.

Unique ID	Strain name	Drug resistance	Genetic background	Clone ID	Diagnostic PCR result	Sequencing result	Western blot result
BD1	RHΔΔ Δ*phyA*	DHFR	RHΔΔ	B5, B10, D4, D9, E4, E10, F5, G10, H4, H10	positive for first 6 clones, others not tested	not sequenced	not tested
BD2	Phy367 in FbxO1HA	DHFR	RHΔΔ FbxO1HA (gift from Blader lab)	D8, E3, E9, F8, G3	all negative	not sequenced	not tested
BD3	RHΔΔ FbxO1-3HA	DHFR	RHΔΔ	B12, C4, D3, D12, E10, G4, H6, H9	all positive	H6 correct, D12 has point mutation D798N, others not sequenced	H6 and D12 positive, others not tested
BD4	RHΔΔ Δ*phyA* FbxO1-3HA	DHFR	RHΔΔ Δ*phyA* pc.1 KR	A11, B11, D8, D11, F4, G5, G11, H11	all positive	A11 correct, D8 has point mutation I796K, others not sequenced	A11 and D8 positive, others not tested
BD5	RHΔΔ FbxO1-3HA-BirA*	CAT	RHΔΔ	1E5, 1H10	both positive	1E5 correct, 1H10 not sequenced	1E5 positive for HA, 1H10 not tested
BD6	RHΔΔ Δ*phyA* FbxO1-3HA-BirA*	CAT	RHΔΔ Δ*phyA* pc.1 KR	2G10, 2H5	both positive	2H5 correct, 2G10 not sequenced	2H5 positive for HA, 2G10 not tested
BD7	RHΔΔ FbxO1-FLAG-APEX2	CAT	RHΔΔ	3F4, 3D11	both positive	not sequenced	not tested
BD8	RHΔΔ Δ*phyA* FbxO1-FLAG-APEX2	CAT	RHΔΔ Δ*phyA* pc.1 KR	4D6, 4E12	both positive	not sequenced	not tested
BD9	RHΔΔ FbxW1-3HA	CAT	RHΔΔ	1C5, 1D10	both positive	both clones correct	1C5 negative, 1D10 not tested
BD10	RHΔΔ FbxW1-3HA-BirA*	CAT	RHΔΔ	2F6, 2G11	both positive	both clones correct	2F6 negative, 2G11 not tested
BD11	RHΔΔ FbxL1-3HA	CAT	RHΔΔ	6G11, 6H11	both positive	both clones retain FbxL1 stop codon, tag not expressed	6G11 negative, 6H11 not tested
BD12	RHΔΔ FbxL1-3HA-BirA*	CAT	RHΔΔ	4E6, 4E9, 4F7, 4G3	all negative	not sequenced	not tested
BD13	RHΔΔ Δ*phyA* FbxW1-3HA	CAT	RHΔΔ Δ*phyA* pc.1 KR	1D4, 1H10	not tested	not sequenced	not tested
BD14	RHΔΔ Δ*phyA* FbxW1-3HA-BirA*	CAT	RHΔΔ Δ*phyA* pc.1 KR	2E3, 2F8	not tested	not sequenced	not tested
BD15	RHΔΔ Δ*phyA* FbxL1-3HA	CAT	RHΔΔ Δ*phyA* pc.1 KR	3C5, 3G10	not tested	not sequenced	not tested
BD16	RHΔΔ Δ*phyA* FbxL1-3HA-BirA*	CAT	RHΔΔ Δ*phyA* pc.1 KR	4D11, 4G6	not tested	not sequenced	not tested

Notes: DHFR – dihydrofolate reductase-thymine synthase selectable marker; CAT – chloramphenicol acetyltransferase selectable marker; RHΔΔ Δ*phyA* pc.1 KR was generated by Dr. Kazi Rahman.

Table 2. List of plasmids used in this study.

Name	Function	Source
pU6-Universal	gRNA and Cas9 gene vector	West lab
pUC19-Linker-3×HA-LoxP-DHFR-mCherry	PCR template for epitope tagging with 3×HA	West lab
pLIC-3×HA-CmR	PCR template for epitope tagging with 3×HA	gift from Moreno lab
pLIC-3×HA-BioID-CmR	PCR template for epitope tagging with BirA*	gift from Moreno lab
pLIC-FLAG-APEX2-CmR	PCR template for epitope tagging with APEX2	gift from Moreno lab
pET15b-6His-TgFbxO1	expression of TgFbxO1	gift from Blader lab
pET15-TgSkp1	expression of TgSkp1	West lab
pET15b-6His-TgFbxO1-TgSkp1	co-expression of TgFbxO1 with TgSkp1	West lab

Table 3. List of oligonucleotides used in this study.

Name	Function	Sequence 5'-3' (cloning site)
FbxO1 219 top	FbxO1 gRNA 219 annealing	AAGTTGAACCCCCGTGGAATATCAAG (BsaI)
FbxO1 219 bottom	FbxO1 gRNA 219 annealing	AAAACTTGATATTCCACGGGGGTTCA (BsaI)
O1 left arm	FbxO1 3×HA tagging PCR amplicon primer	GGCGACATAATCGATTACTACATGAGTCAGGGCG GAGCCAATGCGAAAATTGGAAGTGGAGGACG
O1 right arm	FbxO1 3×HA tagging PCR amplicon primer	GAGCTGGTGCCCCTGAAACAGCATTGATCCCCAA AAGCGCCGTTGCATCCTGCAAGTGCATAGAAG
FbxO1 right arm 2	FbxO1 3×HA-BirA* tagging PCR amplicon primer	GAGCTGGTGCCCCTGAAACAGCATTGATCCCCAA AAGCGCCGTTGCCCTCGGGGGGGCAAGAATT
O1F1	FbxO1 tagging diagnostic PCR primer	TCTTGACTTGCCTGTACCGAATG
O1R4	FbxO1 tagging diagnostic PCR primer	GCTCCATGAAACCTTGGTGCAG
3×HA Rev	FbxO1 tagging diagnostic PCR primer	CGGTGATTAGGCATAATCTGG
DHFR Seq For	FbxO1 tagging diagnostic PCR primer	GACGCAGATGTGCGTGTATCC
BioID R	3×HA-BirA* tagging diagnostic PCR primer	TTGGTGGAGTCGATCACAGGCAG
CmR F	3×HA-BirA* tagging diagnostic PCR primer	AAGGCGACAAGGTGCTGATG
3HA_R	3×HA-BirA* tagging diagnostic PCR primer	CACATCATAGGGATAGCCAGCGTAG
APEX2_R	FbxO1 APEX2 tagging diagnostic PCR primer	CTGGTAGAAATCGGCGTAGC
FbxO1HA seq for 1 (Seq For)	FbxO1 tagging sequencing primer	TCACGTCGAGCGGTCTTCTG
FbxO1HA seq rev (Seq Rev)	FbxO1 tagging sequencing primer	CATAACTCAGTCAGGCAGTC
3HA BirA Seq Rev	3×HA-BirA* tagging sequencing primer	ACAATACCGGCACCACTTCTC
Skp1 FbxO1 Fwd XhoI	Primer for construction of pET15b-6His-TgFbxO1-TgSkp1	TACACAGACTCGAGGCGTAGAGGATCGAG (XhoI)
Skp1 FbxO1 Rev EcoRI	Primer for construction of pET15b-6His-TgFbxO1-TgSkp1	TCTACTAGGAATTCAAGCTTTAATGCGGTAG (EcoRI)

Table 3. (Continued) List of oligonucleotides used in this study.

FbxL1 14172 RC top	FbxL1 gRNA 14172 RC annealing	AAGTTGTTCCGGCTTCTGACGCTCGTG (BsaI)
FbxL1 14172 RC bottom	FbxL1 gRNA 14172 RC annealing	AAAACACGAGCGTCAGAAGCCGGAACA (BsaI)
FbxL1 left arm	FbxL1 3×HA and BirA* tagging PCR amplicon primer	CGGCCGGCGACGGCGCTGCAGCTCGGGGACGCCG CTCTGGACGACAAAATTGGAAGTGGAGGACG
FbxL1 right arm	FbxL1 3×HA and BirA* tagging PCR amplicon primer	CGTCTTCTGAGACTCGCGTCGCCTCTGCTTCCGG CTTCTGACGCTCCCTCGGGGGGGCAAGAATT
L1-F1	FbxL1 tagging diagnostic PCR and sequencing primer	GTCAGAGACTCCGATCTTCAAG
L1-R1	FbxL1 tagging diagnostic PCR and sequencing primer	CATGGATATGAGGCACGCAATG
FbxW1 8879 top	FbxW1 gRNA 8879 annealing	AAGTTGACGTCTCGCAGCCACGAGCTG (BsaI)
FbxW1 8879 bottom	FbxW1 gRNA 8879 annealing	AAAACAGCTCGTGGCTGCGAGACGTCA (BsaI)
FbxW1 left arm	FbxW1 3×HA and BirA* tagging PCR amplicon primer	CTCGCTTCCCCGCTTTCTCTCAGTGCCATCGACT CCAGGTCTGGAAAAATTGGAAGTGGAGGACG
FbxW1 right arm	FbxW1 3×HA and BirA* tagging PCR amplicon primer	TGTATAAACGAGTTCCTCGTCTCCTTCCTGCAAC GTCCGCCAAGCCCCTCGGGGGGGCAAGAATT
W1-F1	FbxW1 tagging diagnostic PCR and sequencing primer	TTCATCACGTCATGCGAACG
W1-R1	FbxW1 tagging diagnostic PCR and sequencing primer	TTAACGCCTGCTTAGTAGGCAC

Note: primers are generated by Thermo Fisher Scientific and Integrated DNA Technologies, Inc.

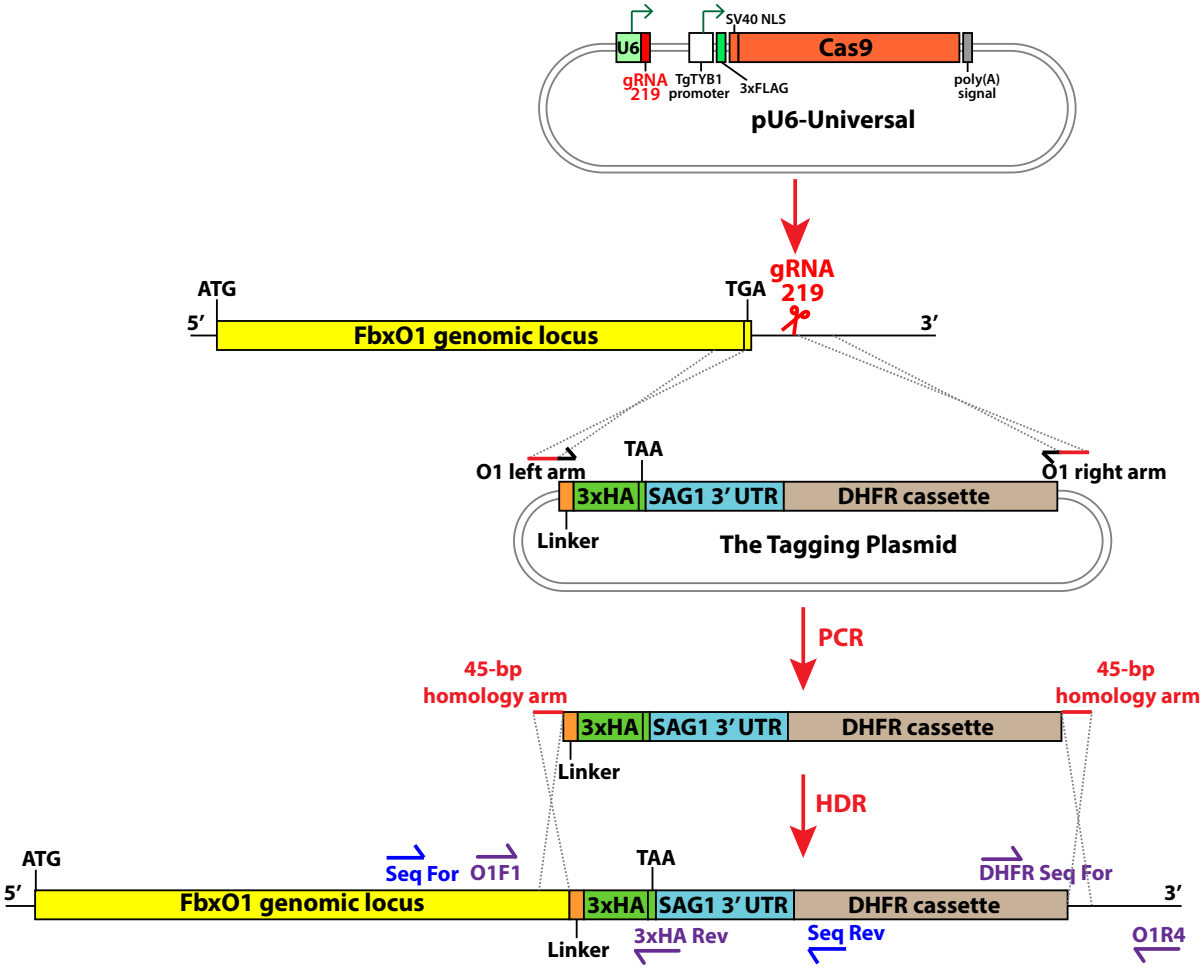

Figure 6. Epitope tagging strategy for FbxO1. From the list of FbxO1 gRNAs sequences generated by the CRISPR gRNA design tool, the DNA sequence homologous to gRNA 219 was determined as an ideal site for introducing a double-strand break (DSB) downstream of the FbxO1 stop codon (TGA) for C-terminal tagging. The DSB was repaired with the PCR amplicon generated with primers O1 left arm and O1 right arm (Table 3). Primers in purple were paired (O1F1 – 3×HA Rev, DHFR Seq For – O1R4, O1F1 – O1R4) and used for diagnostic PCR, and primers in blue (Seq For – Seq Rev) were used for sequencing verification of clones (Table 3). The gene lengths are not drawn to scale.

2.4 Diagnostic PCR and sequencing

To screen for clones that integrated the tag sequence at the desired genomic loci, the joint regions between the insert and the genomic locus were examined by PCR. Tachyzoites were collected as about 70% extracellular cells. The media from the flasks was collected, pelleted at 2,000 × g for 10 mins and briefly syringe lysed to remove host cell debris. Then the tachyzoites were washed in PBS, pelleted again, and stored at -20 ˚C. The pellet was processed for PCR using Zymo Quick-DNA Miniprep Plus Kit that extracted and purified the genomic DNA from the pellet. Primers were designed for both the genomic locus targeting sequence and the insert sequences and paired up to flank the joint regions. The primer pairs were checked using a web-based oligo analysis tool (idtdna.com/calc/analyzer) and the sequences were adjusted if necessary, to minimize the possibility of forming self-complementarity, secondary structures, or primer dimers during PCR reactions. Q5 DNA polymerase (NEB) was used for most PCR reactions and the most efficient annealing temperatures for primer pairs were determined by NEB T_m Calculator (tmcalculator.neb.com), and further empirically optimized by gradient PCR using ±5 ˚C annealing temperatures when necessary. A typical thermocycling reaction consisted of the following steps in order repeated for 30-35 cycles: denaturation at 98 ˚C for 10 seconds; annealing at primer pair-specific temperature for 30 seconds; and extension at 72 ˚C for 30 seconds/1,000 base pairs. All PCR reactions were performed using an Eppendorf Mastercycler Nexus Series. The PCR products were examined on 0.8 to 1% agarose gels containing 0.5 μg/ml ethidium bromide and imaged under ultraviolet (UV 302 nm). NEB 2-log DNA ladder was used as the size standard.

Sequencing was used to further confirm the identity of the gRNA plasmids and tagged strains. Either the gRNA plasmids or diagnostic PCR products were used as the templates for the

sequencing reactions, respectively. The gRNA plasmids were sequenced with a gRNA-specific primer and a vector-specific primer on the top and bottom strands, respectively. The diagnostic PCR products from the tagged strains were sequenced in both directions with primers that were designed as described above. All sequencing reactions were performed by Eton Bioscience, Inc. Sequencing results were checked by alignment analysis using the NCBI Nucleotide BLAST tool.

2.5 SDS-PAGE and Western blot analysis

The tachyzoite cell pellet was lysed by resuspending in an appropriate volume of NP-40 Lysis buffer containing 50 mM Tris-HCl (pH 7.4), 150 mM NaCl, 0.2%-1% NP-40, 0.5 mM ethylenediaminetetraacetic acid (EDTA), 1 mM NaF, 0.2 mM sodium orthovanadate, 10 µg/ml aprotinin, 10 µg/ml leupeptin and 1 mM phenylmethylsulfonyl fluoride (PMSF) to have a minimum cell concentration of 2.1×10^8 cells/ml. The resuspension was gently mixed on ice for 5-10 mins and centrifuged at 21,000 × g for 15 mins in a 4 ˚C centrifuge. The supernatant (S21) was recovered and mixed with 4× SDS sample buffer with DTT (200 mM Tris-HCl (pH 7.4), 8% sodium dodecyl sulfate, 40% glycerol, 0.1% bromophenol blue, 200 mM 1,4-dithiothreitol) to a final concentration of 1×, and boiled for 5 mins to denature and reduce the proteins in the sample. The pellet (P21) was solubilized by boiling in the same volume of 1× SDS sample buffer with DTT, or alternatively, homogenized by brief probe sonication before being boiled in the same way for S21. For SAG1 Western blots which required non-reduced SAG1, a duplicate set of samples were boiled in 1× SDS sample buffer without DTT. The samples were loaded on a pre-cast NuPage 4-12% polyacrylamide Bis-Tris protein SDS-PAGE gel to resolve the proteins in the sample. Novex Sharp (Invitrogen) pre-stained protein standard was used as the protein size reference. The gel was run in 1× MOPS buffer (50 mM Tris, 50 mM MOPS, 1 mM EDTA, 3.5

mM SDS) at 200V until the dye front reached the bottom of the gel. The protein gel was then transferred to a nitrocellulose membrane at 10 V for 10 mins using an iBlot 2 electrotransfer apparatus (Thermo Fisher Scientific). The membrane was blocked in 1× Tris buffered saline (TBS) containing 0.02% (w/v) sodium azide and 5% (w/v) milk for 1 hour, and incubated in appropriate primary antibody diluted in 1× TBS containing 0.02% sodium azide and 5% milk (1:500 for polyclonal anti-Skp1 (UOK75), 1:1,000 for monoclonal anti-HA (12CA5), 1:5,000 for monoclonal anti-tubulin and 1:8,000 for monoclonal anti-SAG1) at room temperature with gentle rocking overnight. The next morning, the membrane was washed in 1× TBS for 4 times, 5 mins each, and incubated in appropriate secondary antibody diluted in 1× TBS containing 0.02% sodium azide and 5% milk (1:10,000 Alexa Fluor-680 goat-anti-rabbit for UOK75, 1:10,000 Alexa Fluor-680 goat-anti-mouse for 12CA5, anti-tubulin and anti-SAG1) for 2 hours. Then the membrane was washed in 1× TBS for 4 times, 5 mins each, and scanned with a Li-Cor Odyssey CLx using auto scanning and imaged with Li-Cor Image Studio. Either a duplicate gel or the blotted gel was stained in Coomassie Blue R250 staining solution (0.25% CBB R250 (w/v), 50% MeOH, 40% H_2O, 10% HAc) for 1 hour at room temperature with gentle rocking and destained in Fast Destain (50% MeOH, 40% H_2O, 10% HAc) for 1 to 2 hours or until protein bands were clearly seen. The gel was rinsed in H_2O and scanned at 700 nm.

Densitometry analyses for Western blots were performed using Image J software. All images were adjusted to grayscale and 8 bits /channel before being opened in Image J. Images were first calibrated to the function “uncalibrated OD”, and the band of interest was outlined with a minimal box and measured. The same box was moved up or down in each lane to also outline a region without visible protein signal to serve as a scanning background control, which was later subtracted from the signal of interest. The integrated density value calculated by

ImageJ for each band was used for comparison. The same measuring procedure was used for the loading controls, and the signal in each lane was used to normalize the signal of interest. If the stained Coomassie Blue gel was used as the loading control, a horizontal region on the gel that was consistent across all lanes was outlined for each lane and used as the normalization factor.

2.6 Proximity biotin labeling (BioID)

The workflow for tagging the FBPs for BioID study was essentially the same as for epitope tagging. The BioID tagging plasmid (Table 2) is a gift from Dr. Silvia Moreno's lab, which has a 963-bp BirA* sequence in-frame between a 3×HA epitope tag and a CAT selection cassette. This plasmid was used to generate the PCR amplicon for BioID tagging with the method described above, and the tagged strains were confirmed by diagnostic PCR and sequencing. For the BioID labeling experiment, both the tagged and untagged strains were grown in DMEM containing 1% FBS with and without 150 μM d-biotin for 24 to 48 hours to examine the effects of BirA* activation and proximity based labeling. All the strains were collected, lysed in NP-40 Lysis buffer, centrifuged at 21,000 × g for 15 mins, and the S21 equivalent to ~3 to 6 million tachyzoites for each strain were loaded on an SDS-PAGE gel, Western blotted, probed for 3×HA tag with 12CA5 and probed for biotinylated proteins. For Western blot of biotinylated proteins, the membrane was blocked in 50 mM Tris-HCl (pH 7.4) with 150 mM NaCl and 3% BSA for 1 hour at room temperature with gentle rocking and incubated in 1:4,000 streptavidin-Alexa Fluor-680 diluted in the fresh blocking buffer at room temperature for 2 hours. Afterwards, the membrane was washed in 50 mM Tris-HCl (pH 7.4) with 300 mM NaCl and 0.05% NP-40 for 4 times, 5 mins each, before being scanned and image as above. To assess if the streptavidin-Alexa Fluor-680 was specific to the biotinylated proteins, a negative control was

included, in which 1:4,000 streptavidin-Alexa Fluor-680 diluted in the fresh blocking buffer was incubated with ~1.5 µM biotin for 30 mins before incubation with the membrane.

2.7 Cellular fractionation

To biochemically investigate the solubility of FbxO1, a cell pellet containing ~1.2×10^8 IC parasites from the FbxO1HA strain was used. This strain is previously generated by and a gift from Dr. Ira Blader's lab that has FbxO1 C-terminally tagged with 3×HA using a double homologous recombination method [17]. The pellet was first resuspended in 300 µl of Sucrose buffer containing 50 mM Tris-HCl (pH 7.4), 250 mM sucrose, 4 mM $MgCl_2$, 0.5 mM EDTA, 12 µg/ml DNase I from bovine pancreas, 12 µg/ml RNase A from bovine pancreas and protease/phosphatase inhibitors (10 µg/ml aprotinin and leupeptin, 1 mM PMSF, 0.2 mM Na_3VO_4 and 1 mM NaF). Next, the cell resuspension was lysed and homogenized on ice by probe sonication at 25% amplitude with a 1/8-inch probe installed on a Qsonica Sonicator Q500 (Fisher Scientific) for at least 20 pulses or until at least 80% of the tachyzoites were lysed as observed by phase contrast microscopy. Then the lysate was centrifuged at 1,000 × g for 5 mins to remove any undisrupted cells. The supernatant (S1) that contained all the released cellular material was collected and equally divided into three, and the pellet (P1) was washed in 300 µl of Sucrose buffer and centrifuged at 1,000 × g for 5 mins again. The divided S1 fractions were centrifuged at 200,000 ×g for 30 mins to obtain the soluble and insoluble fractions. After the centrifugation, all three soluble supernatants (1-S100) were collected and pooled, and all three pellets (1-P100) were gently surface washed once in 100 µl of Sucrose buffer. Then the first of the 3 pellets was resuspended in 100 µl of Hypertonic buffer containing the same ingredients as Sucrose buffer with 600 mM NaCl instead of sucrose; the second pellet was resuspended in 100

µl of Hypotonic buffer containing 4 mM $MgCl_2$, 0.5 mM EDTA, and the same nucleases and protease/phosphatase inhibitors as in Sucrose buffer; and the third pellet was resuspended in 100 µl of Detergent buffer containing the same ingredients as Sucrose buffer with 100 mM NaCl instead of sucrose and supplemented with 1% NP-40. Then the 3 resuspended pellets were homogenized by probe sonication on ice with the same settings and centrifuged at 200,000 × g for 30 mins. After the centrifugation, the supernatants from the 3 subsequent extractions (2-S100, 3-S100 and 4-S100, respectively) were collected and all 3 pellets (2-P100, 3-P100 and 4-P100, respectively) were washed once in 100 µl of their respective buffer. Afterwards, 3-P100 was extracted again with 100 µl of Detergent buffer, and 4-P100 is extracted again with 100 µl of Hypotonic buffer, to further obtain the soluble fractions from each. After the centrifugation, the soluble supernatants were collected as 34-S100 and 43-S100, respectively. The remaining pellets were denoted as 34-P100 and 43-P100, respectively.

As a negative control, a cell pellet from the RHΔΔ strain with similar number of cells was resuspended directly in 300 µl of Detergent buffer, probe sonicated on ice with the same settings, and centrifuged at 200,000 × g for 30 mins. The soluble (RHΔΔ S100) and insoluble (RHΔΔ P100) fractions were collected. Lastly, all of the insoluble fractions (P1, 2-P100, 34-P100, 43-P100 and RHΔΔ P100) were solubilized by boiling in 1× SDS sample buffer without DTT. All of the samples were analyzed by SDS-PAGE followed by anti-HA and anti-Skp1 Western blots.

2.8 Co-immunoprecipitation and interactome analysis

Tachyzoite extracts were analyzed with a protocol combining co-immunoprecipitation (co-IP) and Western blotting or nano-liquid chromatography/mass spectrometry (nLC/MS) that was adapted from a previous publication [28]. To investigate the FbxO1 interactome, the

FbxO1HA and the untagged RHΔΔ strains were compared by co-IP/MS. The monoclonal anti-HA antibody (12CA5) purified from the hybridoma culture medium was stably cross-linked through dimethyl pimelimidate to protein A/G magnetic agarose beads (Pierce) at 4 mg IgG protein per milliliter of beads [17]. The optimal bead to sample ratio at which most of the FbxO1 (>80 %) in the cell extract was captured by the least number of beads, was tittered by incubating 1 µl of crosslinked anti-HA magnetic agarose beads against a series of S21 equivalent to between 5×10^6 and 5×10^7 tachyzoites. The beads from all co-IP incubations were then washed sufficiently in NP-40 Lysis buffer and eluted with 8M urea. The eluates were analyzed by SDS-PAGE and anti-HA (12CA5) Western blot, and the optimal bead to sample ratio was determined as ~2×10^7 cells/µl of the crosslinked anti-HA magnetic agarose beads.

Typically, for co-IP/MS experiments, about 100 µl of S21 equivalent to 1.2 to 2×10^8 tachyzoites was incubated with 10 µl of the anti-HA magnetic agarose beads in 1.5-ml Lo-Bind tubes (Eppendorf) at 4 ˚C for 1 hour with gentle mixing. The beads were collected by placing the tubes on a DynaMag-2 magnetic stand (Life Technologies) and the unbound supernatants were aspirated. The beads were washed 3 times with NP-40 Lysis buffer, 3 times with 10 mM Tris-HCl (pH 7.4) containing 50 mM NaCl, and once with 50 mM NaCl to remove non-specifically bound species and detergent. For nLC/MS analysis, the beads with bound proteins were eluted twice with 60 µl of 133 mM triethylamine (TEA, Pierce) by incubating for 15 min at room temperature and immediately neutralized by transferring to a new tube with 200 mM acetic acid.

The Skp1 interactome analysis workflow was performed as previously reported [17]. Briefly, the anti-Skp1 antibody (UOK75) was affinity-purified against *Toxoplasma* Skp1 as described previously [24]. UOK75 and rabbit IgG (negative control) were independently crosslinked to protein A/G magnetic agarose beads in the same way as for 12CA5 and used for

UOK75 co-IP. For co-IP of the C-terminally tagged Skp1-Strep/FLAG (Skp1-SF), a monoclonal anti-FLAG antibody (M2) was crosslinked as described above. The optimal bead to sample ratio for each type of crosslinked beads was determined by a tittering as described above. Tachyzoites from the RHΔΔ and the Δ*phyA* strains for UOK75 co-IP, and from the Skp1-SF strains in both RHΔΔ and Δ*phyA* background for anti-FLAG co-IP, were all lysed according to the general protocol described above. All co-IP incubations were at 4 ˚C for 1 hour with gentle mixing. And all washing and elution steps were identical as for FbxO1 co-IP.

For MS analysis, the eluted samples were vacuum dried, reconstituted in 10 mM Tris-HCl (pH 7.4), 8M ultrapure urea, reduced in 10 mM DTT for 40 mins at room temperature, and alkylated in 50 mM 2-chloroacetamide for 30 mins at room temperature in the dark. The sample was then diluted 4-fold with 10 mM Tris-HCl (pH 8.0) to 2M urea followed by addition of 10 µg/ml trypsin (Promega, MS grade) and incubation at room temperature overnight with gentle mixing. The next day, trypsin activity was stopped in 1% trifluoroacetic acid (TFA, Pierce) for 15 mins on ice and centrifuged at 1,800 × g for 15 mins at 4 ˚C to remove precipitates, and the supernatant were enriched for peptides by passing through a C18 zip-tip column (Agilent) for adsorption. Then, peptides were eluted with 50% (v/v) acetonitrile (ACN, Thermo Fisher Scientific, LC/MS grade), 0.1% formic acid (Pierce, LC/MS grade), followed by elution with 75% (v/v) ACN, 0.1% formic acid. The eluted peptides were vacuum dried and resuspended in 40 µl 5% ACN, 0.05% TFA. The resuspended sample was transferred to an auto-sampler vial and separated with an Ultimate 3000 RSLCnano ultrahigh performance liquid chromatography (UHPLC, Thermo Fisher Scientific) system equipped with a C18 matrix, and sent directly to the nano-electrospray ion source of an Orbitrap QE plus mass spectrometer (Thermo Fisher Scientific) coupled to the UHPLC for tandem mass spectrometry analysis as described [17]. The

output raw spectra files were analyzed using Sequest HT in Proteome Discoverer 2.2 (PD 2.2, Thermo Fisher Scientific). The proteome database employed for protein identification in PD 2.2 was a merge of the *Toxoplasma gondii* (strain ATCC 50853/GT1) proteome (ID: UP000005641) acquired from Uniport (uniport.org) with a list of common protein contaminants from co-IP/MS sample preparation. Variable modifications were Met oxidation, Glu and Asn deamidation, and N-terminal acetylation, and fixed modification was Cys carbamidomethylation. The peptide-spectrum match (PSM) was filtered at 1% false discovery rate (FDR) with relaxation to 5% FDR at protein level. Protein abundance was determined from the area under the curve (AUC) quantification method in PD 2.2, summed over all assigned peptides. The initial list of candidate interactors was selected based on their relative enrichment in protein abundance in the experimental groups compared to their respective negative control groups, then the list was further manually filtered to exclude contaminants and background.

To test the effect of the Skp1 modifications on the interaction between FbxO1 and Skp1, the 2 proteins were reciprocally co-IPed from both the RHΔΔ and Δ*phyA* extracts and analyzed by Western blot. About 10 to 20 million tachyzoites per co-IP were lysed in 0.2% NP-40 Lysis buffer as described above. About 35 to 70 µl of S21 equivalent to 10 to 20 million tachyzoites was incubated with ~1 µl of the crosslinked anti-HA magnetic agarose beads in 1.5-ml Lo-Bind tubes (Eppendorf) at 4 ˚C for 1 hour with gentle mixing. Then the unbound supernatant was removed, and the beads were washed once in 0.2% NP-40 Lysis buffer and 4 times in 50 mM Tris-HCl, pH 7.4. The beads were eluted by boiling in 1× SDS sample buffer for 5 mins. All the S21, co-IP flow-throughs, and co-IP eluates were analyzed by SDS-PAGE and Western blot. The FbxO1HA co-IP samples were probed with both 12CA5 and UOK75, and the Skp1 co-IP

samples are probed with both UOK75 and 12CA5 to examine their relative steady state levels. α-tubulin was used as the loading control.

2.9 Recombinant FbxO1 expression and purification

To generate FbxO1 anti-serum and conduct biochemical and structural analysis on FbxO1, *Toxoplasma* FbxO1 was recombinantly expressed in *E. coli* with and without *Toxoplasma* Skp1 that might serve as a chaperone for FbxO1, to produce FbxO1 and FbxO1-Skp1 complex, respectively. For independent expression, pET15b-6His-TgFbxO1 was used as the expression plasmid (gift from Dr. Ira Blader's lab, Table 2). This plasmid contains the *Toxoplasma gondii* ME49 FbxO1 cDNA led by an N-terminal 6×Histidine (6His) tag followed by a thrombin cleavage site. The co-expression construct was made by first linearizing pET15b-6His-TgFbxO1 plasmid with restriction endonucleases XhoI and EcoRI to remove the fragment between FbxO1 3′ end and the start of the AmpR cassette and to create non-compatible sticky ends. The *Toxoplasma* Skp1 coding sequence followed by a T7 terminator sequence was PCR amplified from the pET15b-TgSkp1 plasmid (Table 2) with forward and reverse primers that had 5′ and 3′ overhangs containing the recognition sequences for XhoI and EcoRI, respectively. Next, the PCR amplicon was digested with XhoI and EcoRI and ligated with the linearized pET15b-6His-TgFbxO1 plasmid using T4 DNA ligase (NEB) at 37 ˚C for 2 to 4 hours. The ligation products were transformed into TOP10 competent *E. coli*, plated on LB-Ampicillin (100 mg/ml) selection media, and grown overnight at 37 ˚C. Afterwards, several ampicillin resistant colonies were expanded by culturing in liquid LB-Ampicillin and miniprepped to extract the ligated plasmid. The identity of the ligated plasmid was verified by dual restriction digestion with SpeI that is part of the TgSkp1 insert, and PvuI that is part of the AmpR cassette in the

pEt15b-6His-TgFbxO1 vector. The digested plasmid was run on an agarose gel and imaged to confirm the sizes of the expected fragments.

The pET15b-6His-TgFbxO1 plasmid and the co-expression plasmid were independently transformed into Gold and ER2566 competent *E. coli* strains and expressed using a 48-hour autoinduction protocol. Briefly, a starter culture was prepared by inoculation with cells from the frozen stock of each expression strain into 40 ml of terrific broth with 100 µg/ml ampicillin and growth overnight at 37 ˚C with vigorous shaking till the cultures reached a density that could not be seen through. Then each of the starter cultures was transferred to 1 L of autoinduction media consisting of terrific broth with 5 g/L NaCl, 0.05% (w/v) glucose, 0.2% (w/v) lactose, 100 µg/ml ampicillin and 0.6% (v/v) glycerol. The cultures were incubated with vigorous shaking at 37 ˚C for 2 hours and at 18 ˚C for 46 hours to induce expression. Each of the cultures were harvested at 5,000 × g for 10 mins at 4 ˚C, supernatant in each was aspirated, and the pellets were stored at -80 ˚C. The yield was about 20 grams of wet pellet from a 1 L culture.

Each of the *E. coli* pellets was resuspended in ~1.66 ml cold *E. coli* Lysis buffer (20 mM sodium phosphate pH 7.4, 0.5 M NaCl, with freshly added 5 µg/ml aprotinin, 5 µg/ml leupeptin, 0.5 µg/ml pepstatin A, 5 mM benzamidine, 1 mg/ml lysozyme, 0.5 mM PMSF) per gram of pellet by stirring at 4 ˚C. The resuspended cells were lysed by probe sonication on ice for 5 to 8 mins at 25% amplitude with a 1/4-inch probe or until completely homogenized when the lysate was more translucent by visual inspection. Right after sonication, each of the lysates was supplemented with 5 mM $MgCl_2$, 10 µg/ml DNase I and 50 µg/ml RNase A, incubated on ice for 10 mins, and centrifuged at 200,000 × g for 30 mins at 4 ˚C. The supernatant (S100) was carefully removed, and the pellet (P100) was further extracted by 1× SDS sample buffer without

DTT. Aliquots of the S100 and the extracted P100 were analyzed by SDS-PAGE and Western blotting with a monoclonal anti-His antibody (1:1,000; Novagen).

The S100 (~25 ml from the 1 L culture) was incubated with ~1.8 ml of prepared nickel charged Sepharose resin (GE Healthcare) in the presence of 5 mM imidazole at 4 ˚C for 45 mins with gentle mixing. The beads were pelleted at low speed (3,500 × g), and the supernatant was collected as the unbound material. The resin was first washed with 20 ml cold *E. coli* Lysis buffer containing 5 mM imidazole, followed by a wash with 20 ml cold *E. coli* Lysis buffer containing 60 mM imidazole, and bound proteins were eluted stepwise with 5 ml cold *E. coli* Lysis buffer containing 120 mM, 240 mM, 360 mM and 500 mM imidazole, with low speed centrifugation after each step. The eluates were analyzed by SDS-PAGE and anti-His Western blot to determine the fractions enriched the most for FbxO1. The amount of total proteins in each eluate was determined by UV spectroscopy at 280 nm wavelength on NanoDrop One (Thermo Fisher Scientific), and the amount of the recombinant FbxO1 in each eluate was estimated by densitometry analysis of the protein gel. The selected eluates were dialyzed in 10 kDa molecular weight cut-off (MWCO) dialysis tubing into Thrombin Cleavage buffer (20 mM Tris-HCl (pH 8.3), 150 mM NaCl) overnight with constant stirring, pooled, and digested with human α-thrombin (Haematologic Technologies) at an optimized condition of 1:50 enzyme to substrate molar ratio at 4 ˚C for 6 hours, with gentle mixing after every 2 hours. The digested sample was passed through a 1 ml benzamidine column (GE Healthcare) for affinity capture of α-thrombin, followed in series by a 1 ml subtractive Ni-Sepharose column (GE Healthcare) to remove undigested 6His-FbxO1 and non-specifically bound material. The cleaned-up sample was flash frozen and stored at -80 ˚C for future use.

2.10 Generation of FbxO1 anti-serum

The digested recombinant FbxO1 sample was further purified by boiling in 1× SDS sample buffer with DTT for 5 mins and running on a home-made 15-20% polyacrylamide Bis-Tris large slab gel (19cm × 20 cm) that had a single well to contain ~1.5 ml of sample. The gel was run in a slab gel apparatus in 25 mM Tris with 190 mM glycine and 0.1% SDS (pH 8.5) at 25 mA for ~90 mins, and at 35 mA till the dye front was at bottom of the gel. Then the gel was stained in CBB R250 for 20 mins, rinsed and destained in Fast Destain overnight. Afterwards, the gel was rinsed again and scanned using Li-Cor Odyssey CLx at 700 nm. The protein band containing FbxO1 was carefully excised using a clean razor blade, further destained in Fast Destain in a 15 ml tube to remove residual CBB, and rinsed in deionized H_2O for three times, 45 min each before sending to Cocalico Biologicals, Inc. for anti-serum generation in rabbits. Before the immunization, a pre-bleed from each of the two rabbits were screened with RHΔΔ lysate to ensure there was no cross-reactivity. Immunization of the rabbits followed a 56-day protocol with three boost inoculations after the initial inoculation. Two test bleeds were collected 20 days apart from each rabbit. The test bleeds were diluted to 1:100 in 5% milk in 1× TBS and incubated with purified FbxO1 antigen (100 ng loading) as the positive control and with RHΔΔ S21 from 2% SDS whole cell extract (from about 3 million tachyzoites) to evaluate the test bleeds for anti-serum specificity and titer, and probed with 1:10,000 dilution of Alexa Fluor-680 goat-anti-rabbit 2nd antibody using the SDS-PAGE and Western blot protocol described above. Exsanguinations from both rabbits were obtained at the end of the project after a final boost.

CHAPTER 3

RESULTS AND DISCUSSION

3.1 Sequence-based domain and phylogenetic analyses of FbxO1

To understand the evolution of FbxO1 and how it was related to FBPs in other systems, *Toxoplasma gondii* ME49 FbxO1 amino acid sequence (TGME49_310930, 808 amino acids) (Figure 7A) was acquired from ToxoDB and analyzed by BLASTP against all non-redundant sequences in NCBI's database. Interestingly, the searches only discovered sequence homologs from alveolates even when the E-value was relaxed to 100, suggesting that evolutionarily, FbxO1 is a highly conserved protein specifically required for the function of the alveolate clade. Based on the manually curated COBALT alignment (Figure 7C) of FbxO1 sequence and the representative homologous sequences from other alveolates, the full FbxO1 sequence was organized into three domains including the N-terminal domain (N), the F-box domain (F) and the C-terminal domain (C) (Figure 8).

The generally weakly-conserved N-terminal domain spanned the first 430 amino acids, and it contained regions of higher and lower conservation (Figure 8B, blue and gray patches, respectively). This weak sequence conservation was only seen in coccidian species, *Vitrella* and several ciliates, except for the first 20-25 amino acids that were also conserved in the other apicomplexans, including *Plasmodium*, as indicated by the BLASTP search. The F-box domain was ~45 amino acids and was conserved among all the discovered alveolates. It had a sequence feature of hydrophobic and hydrophilic sequences organizing into three α-helices interspaced by

secondary structure breaking residues such as proline and glycine (Figure 7C), which suggested that the F-box domain in FbxO1 possibly folds into a series of short helices connected by conformational turns. The C-terminal domain was ~330 amino acids and spanned the rest of the FbxO1 sequence. It was also conserved among all the discovered alveolates and was much more conserved compared to the N-terminal region as observed in the sequence alignment, suggesting potential functional relevance of FbxO1 protein in addition to the F-box. These observations support the hypothesis that the C-terminal region could be important for protein-protein interactions between FbxO1 and its potential interactors aside from Skp1.

Despite the low overall conservation of the N-terminal domain, the higher conservation of the first 20-25 amino acids suggested a functional relevance. Indeed, the N-terminal GxxxS motif on FbxO1 was predicted as the putative site for the major 14-carbon lipidation known as *N*-myristoylation [34]. Based on the ExPASy myristoylator tool prediction results, the *Toxoplasma* FbxO1 was myristoylated, although with low confidence. All the FbxO1-like sequences in other coccidian species possessed the motif and were predicted to be *N*-myristoylated with even higher confidence (Table 4, marked in green). An exception was the *Cystoisospora suis* homolog, which had the N-terminal GxxxS motif but was not predicted to be *N*-myristoylated (Table 4, marked in red). A potential explanation was that the double proline following the GxxxS motif interferes with the prediction algorithm. Interestingly, several other sequences predicted to be *N*-myristoylated had variable GxxxP/N/T motif (Table 4, marked in orange), suggesting that S is not the only allowable amino acid at the 5th position. It has been reported that *N*-myristoylation could anchor the modified protein to membranes or the myristoyl group could also be buried inside the modified protein, thus rendering the modified protein to be soluble [35]. Evidently, substitution of the N-terminal glycine in *Toxoplasma* FbxO1 to an

alanine (G2A) made FbxO1 mainly cytoplasmic during the cell cycle as opposed to localization at the DCS and IMC in the wildtype [17]. These results suggested that the N-terminus of FbxO1 is possibly subject to posttranslational *N*-myristoylation following removal of the N-terminal Met, and that the potential *N*-myristoylation could modulate the solubility and function of FbxO1. Further studies are needed to verify the presence of the myristol group on *Toxoplasma* FbxO1 and understand the mechanism of modulation.

A. TgFbxO1 (TGME49_310930) genomic and amino acid sequences

```
tggtagactgcatccgcgggacacgctgtgcaggctcagctttgcgtaaaggacttaccc 5′ UTR

agcacatttaacgttcactaccacggaaaaaactttttctttccgtgctcaactgcgcctt 5′ UTR

ctcgctcggggtcccggaactgcgtgctttttgcccagctccctcttcgtgtccccaca 5′ UTR

ATGGGCAACACGGAATCCACGGCCGCTGAGTTGCACGACAACTACTTGGCGGTTCTTAAA   60
 M  G  N  T  E  S  T  A  A  E  L  H  D  N  Y  L  A  V  L  K    20
    . Predicted .
N-myristoylation motif

AGCGTCGAGGGTCGGTTGGGACAGTACCCAAGCCGAACGCTCTCCCCTCGGTCGCAGTCA  120
 S  V  E  G  R  L  G  Q  Y  P  S  R  T  L  S  P  R  S  Q  S    40

AGCGGTGTGGATCGGTCTCGCGCGAGGGTACGCCCCGAGGAGGCGTACCGGGATCCTGGA  180
 S  G  V  D  R  S  R  A  R  V  R  P  E  E  A  Y  R  D  P  G    60

AAACGGGGTGCTGGAAACCGCCCTCGCAACTTGCCATCCAAAGGCGAGAAGCCCTCTCGG  240
 K  R  G  A  G  N  R  P  R  N  L  P  S  K  G  E  K  P  S  R    80

TCTGCGCACAAGTCGGGATCCACTTCCTCAGTGGACCAGTTCAACAACGGGCCTGGTGCG  300
 S  A  H  K  S  G  S  T  S  S  V  D  Q  F  N  N  G  P  G  A   100

AACCGGAAACACGGAAAGGACAGCGTCCAGCGGCGCGATGATGCCCCGCCACAAGCAGAT  360
 N  R  K  H  G  K  D  S  V  Q  R  R  D  D  A  P  P  Q  A  D   120

CAGGAACACTCTTCGCTTCAACCAGCTGACGGCAAGCGCCGGCCTGCCGCGAAAGGAGAG  420
 Q  E  H  S  S  L  Q  P  A  D  G  K  R  R  P  A  A  K  G  E   140

ACTCCCAATGTGGAGTCGACTGCGACAGGATCCGACTGGGGAGACTCCGCTGTCAACGAT  480
 T  P  N  V  E  S  T  A  T  G  S  D  W  G  D  S  A  V  N  D   160

TTTGCTGAAGAGGATAGCTGCGCCGTTGAGAGTCCAGCACACTTTAAGCTTCAGACGAAG  540
 F  A  E  E  D  S  C  A  V  E  S  P  A  H  F  K  L  Q  T  K   180

GAGTCGGGTGTCAAGGCACCTTCGCCGCGCCTCTTCCCCTGTGAAACGCTGTATGAGGTC  600
 E  S  G  V  K  A  P  S  P  R  L  F  P  C  E  T  L  Y  E  V   200

ACTTCGCAGATAGACCTCGCGGATGAGAAAACGCAAGTCGAAGACGGAGAGCTCAGCTCT  660
 T  S  Q  I  D  L  A  D  E  K  T  Q  V  E  D  G  E  L  S  S   220

CTCCCGAGTTCCCCCACGGCCTCTGCAGAGGTCGCGACGGACAAGCCCGGGGAGGGACGG  720
 L  P  S  S  P  T  A  S  A  E  V  A  T  D  K  P  G  E  G  R   240

ACGGCGACGCGGGAAGACACGCGGACTGGTCGGTCAGCTGAGGGAGACAGAGGGCCTTGC  780
 T  A  T  R  E  D  T  R  T  G  R  S  A  E  G  D  R  G  P  C   260

CATACAGAGAATCAGGTCGACGGAGCAGACGCGAAGGAGAATGAGTCAGACAACTCACAC  840
 H  T  E  N  Q  V  D  G  A  D  A  K  E  N  E  S  D  N  S  H   280

GGCGAGTCAGACCAAGACCTGCGACGTCGGAGCGACGGCCGCGGTGCATCCTCCCAGAGA  900
 G  E  S  D  Q  D  L  R  R  R  S  D  G  R  G  A  S  S  Q  R   300

TCCAGGGACGAGGCCTCGAACAGTGGCGAGCCTCCGTCACAGTCGAAACCGTCGCAGCTT  960
 S  R  D  E  A  S  N  S  G  E  P  P  S  Q  S  K  P  S  Q  L   320

TCAAAGCAAATACGGAAGAAAGAACTCGCCCCGGAGCCTCTCCGCGCAGCAGATATCGAC 1020
 S  K  Q  I  R  K  K  E  L  A  P  E  P  L  R  A  A  D  I  D   340

CTTTCCTCAGATGTCCGTGTCGGAGCCTCGTTGAAGGGGGGGAAGGGAGGGAAGGGAGAC 1080
 L  S  S  D  V  R  V  G  A  S  L  K  G  G  K  G  G  K  G  D   360

GCTGAGGGTGATAATGTCGCCGACCTCACAGCTGGATTCGAGGGATTTTCGCCGTACTCG 1140
 A  E  G  D  N  V  A  D  L  T  A  G  F  E  G  F  S  P  Y  S   380

CCCTCCTACTCTCTTGGCTTCAGTCAGCCGTCGTCGAAGAAGGCTGCAAAAACGACAGCT 1200
 P  S  Y  S  L  G  F  S  Q  P  S  S  K  K  A  A  K  T  T  A   400

GAAAACTCCAAAGCACACCTACCAGGAGGAACCCGCGGCAGCGGCAACAACACTGCTGTC 1260
 E  N  S  K  A  H  L  P  G  G  T  R  G  S  G  N  N  T  A  V   420
```

```
GACCGGGACGCGTGCATCTACGGAAACAAGAAAAACCACTTTCCCTTCCTCGACGAACCT 1320
 D  R  D  A  C  I  Y  G  N  K  K  N  H  F  P  F  L  D  E  P   440
                                       .     Predicted

GCCTTGTCACTGCTTGTACCATTTCTCTTCGGCAGAAGCCTCGCGACTTGCATGACCGTC 1380
 A  L  S  L  L  V  P  F  L  F  G  R  S  L  A  T  C  M  T  V   460
                              F-box

TGTCCACACTGGTTCATGAAAATCAATCGgtacgcgacaagacgccactgcggtgaacat 1440
 C  P  H  W  F  M  K  I  N  R                                 470

agactcctacctcacatacaaagggattctaagatcttggcagtgtgatctctactaaga 1500

gcctggtcgttccctttggtccacgcatctcatttttctactcgaatcagcagtggtcct 1560

tgaaaggggtttccatccagcgtgtttcctcactgtccgctgttttttgcctgcctgac 1620

gctttctctttttcagGGCTATGGAACGCATGTGTGGGCCTGCCACAAAAGGTTTCCAGC 1680
                A  M  E  R  M  C  G  P  A  T  K  G  F  Q   484
                   domain     .

AAATGTACTCAAAATACTTGGAAGTCTGGGGAAGCGCTGTCAAACTTCAGCCTCTCCAGA 1740
Q  M  Y  S  K  Y  L  E  V  W  G  S  A  V  K  L  Q  P  L  Q   504

CAGTTGGCGATGGCGGAGTCCGCGTGGACTGGGTGATTTTTGCCAAGgtgcgtctcggtg 1800
T  V  G  D  G  G  V  R  V  D  W  V  I  F  A  K               520

ctttcctgtttgctgcgccttgccgtcgtggctgataaaggggacagtacacttgatga 1860

tatgcatgagatagccttccatacttctgcgttgattctgccagacgttcctgttcgctc 1920

tttgcgtcagcagttccgcttcataataaaagcgttccgcttccagttggttttcttctc 1980

ttcggtagctggaccttcggtttctttgcttggccagagtgaagaaccggggccggcgta 2040

cagggatgagcttccgcgaacgcatcgcaccgggcaaaatgcgtcaagaatactccgtgg 2100

tatgtttttagGTCCTCCCGGAATGTGAAGGTCACATCCTTGACATATCGTATACCTATT 2160
          V  L  P  E  C  E  G  H  I  L  D  I  S  Y  T  Y   536

CCTACATTTCCGAAAGTTCGAGTTCGACTGCTCGTCCGGTGGACGAAGCGGACAAGCCCG 2220
S  Y  I  S  E  S  S  S  S  T  A  R  P  V  D  E  A  D  K  P   556

CGGCGGGTGGGAAGAGAGATCGCGGACGGCAAGGAGAAAAAAGGCGATCCCTTTCTGCCA 2280
A  A  G  G  K  R  D  R  G  R  Q  G  E  K  R  R  S  L  S  A   576

ACTTCGACGAAGGCGTCATTCTCTCTCCGTGCGGACAGgttcgtggactggaaagcagcg 2340
N  F  D  E  G  V  I  L  S  P  C  G  Q                        589

cgtctctgagagctcgtttcttcttcagtttttgcagctccttgcgcttccaccacccat 2400

gcgagagcactggcgcgcctctcagtcgatgaggggactggaccgagaaacctacactcg 2460

cctgaagggtgcggatccagtggctctcatgttagcatggtttcgagaacagtcggtata 2520

tctggccaccgcggacaaaccgtgtgcctatcgcctgcatcgcctttcgtctcctaactc 2580

cggtgtttctgtggatgtttctctgcagCCTTGCCCGACCAACATGCCTTCGCGCGTGTT 2640
                          P  C  P  T  N  M  P  S  R  V  F   600

CACGGTGTCTTACTCGCTGGCGGCGGGTGCGGCGAAGAGCAGCCGAACGCTTTGGATGCA 2700
  T  V  S  Y  S  L  A  A  G  A  A  K  S  S  R  T  L  W  M  H   620

CCGAGACTTGTGCCGGTTCCACGGAGACGAGACTGGGGTCGCTGCCATGGGCTCCGTCTC 2760
  R  D  L  C  R  F  H  G  D  E  T  G  V  A  A  M  G  S  V  S   640

AAGTGTCTGCGTAGGAGACTTCGTGGAAGTCGCTGTCACTGTGTACAACGGAGGCGGGCG 2820
  S  V  C  V  G  D  F  V  E  V  A  V  T  V  Y  N  G  G  G  R   660

CGTTGCTCTGGACAAAGTCAAGTGGCTGCCTGCGCGAGTCGAGTGGAGACGGGAGGCTGT 2880
  V  A  L  D  K  V  K  W  L  P  A  R  V  E  W  R  R  E  A  V   680
```

```
TTCGACTCGCGGCGTCTTCAACAGAGAAATCTGTCCTCTCGAACGCTGCTCTCCCGACTG 2940
  S   T   R   G   V   F   N   R   E   I   C   P   L   E   R   C   S   P   D   W  700

GCTTCCTGCAGACCAGTTCCGCATCATGACTACGGAACGCCTGAAGGCTCCAGgtgagac 3000
  L   P   A   D   Q   F   R   I   M   T   T   E   R   L   K   A   P          717

tgtcggggactggacgggccgacgctctcctgaacgtgactcggattcgaagggtcagac 3060

agccagtcctttctgcctgcggtccaccaccgtatcactgaacactgtgcaacaagggat 3120

cgaactgcagctcgaatctgcctggtacagtgcacagagatgatgacacgcgggaccgtg 3180

gtgctgatcatcatgatcatcctagcatctgaggagctgttttctctcgctgttaatacg 3240

cgtgacaccagaaatccatgaaaccgtacgcgtgaaacgtaagcgatttttggaatactt 3300

tcagtgtcgtaagacatggaactccagcgcgtttcgctctcgtggaaagaaaacagctgg 3360

aagcgaggaagcaaagccgtgggcgaagggccaaaaagtcatgccgagggaaatgcgggg 3420

atcgaaaggacggattccaaataggaacctgcgcactgtgcagtcggcctttcgcggcaa 3480

ccctgctggaaccactgcagtgcatgaagaagatatgaaggactcctgtagcacccgtag 3540

ctgaaagaacatttctttagctgaagcaagtcccgaaagatgtccgattaactgtgcagA 3600
                                                              E  718

GGACTTCTCGCCGTGTTTGAAACATGTCAAGACAGAATTTTCCGGAATGGATGTCGCCGT 3660
  D   F   S   P   C   L   K   H   V   K   T   E   F   S   G   M   D   V   A   V  738

TCGCAAATCAACATATCGAGCAGTCCGCCAAGgtaggctgaaaccgccttcgataggaca 3720
  R   K   S   T   Y   R   A   V   R   Q                                  748

tcgcacgcatatatatatatatatatatatatgtatgtgtatgttggaaatatgtgttaa 3780

tacttctacattggattaaaacactggagttacgctataactttagcgtgattgtctcca 3840

gcatcgatggatagggcaggtgcatgggaagtctgtggacagacggcacatatacaccga 3900

acgcgcgtaggacgttggtgagcgccagttgcttgtcgttgcctacaccggaggggaatg 3960

tgaattttacgcaaacgaagtctatttttcggcagaacacaggcgtttcacatctgtttt 4020

cttccggatcgaatccttgcgacagtctgacatgcttgcctgggactaccaaagctgtct 4080

gtcctcgctgcgcatgccacagGGTCGCTGGGATCAGCAGCGTGCCGGTCTTGGGGGTTC 4140
                      G   S   L   G   S   A   A   C   R   S   W   G   F   761

CCTTGTGAGATCCTTCCTCAAGGCGTCCCTGTTGTTTGCTCCCTGACGCGCTGGGGACTC 4200
  P   C   E   I   L   P   Q   G   V   P   V   V   C   S   L   T   R   W   G   L  781

CAGCATGATCGATTCCTCTCCGTTCAGCTGCGCGAGgtgagtttcgccgattgctctcgc 4260
  Q   H   D   R   F   L   S   V   Q   L   R   E                          793

gaattgccgaaaatgtcggcccgtcgaagccaaaagagctgccgattctcagggtttccg 4320

ttttgcgagagtgctagcgagtacgagcgactttctgcggcaccgcagtggctttgagcg 4380

ttgaagtttttctaggtcgttgccggaacacagcagatgggtccagccttagacgatcgc 4440

ctgtctccacctttccggcatctgatgcccgtaaacgtatcaaattcatggcctgtctgg 4500

aatttgcttgtcgccgtagctacagagagagggtgtgtgggtgtgtgtgctgggaagatg 4560

acatgtctgaaacgacgtaagacggagaaacgcgacgtagttcaatttcggtgtagtgcc 4620

acaaacgctttactgtattcacgtcgagcggtcttctgcggagccactctgagagttaag 4680
                5'-TCACGTCGAGCGGTCTTCTG-3'                                Seq For

atatggttgaatctatatcctaagttctgtagtttggtcgcttcacccgtgttcagtgtt 4740

ttgtcttggtgctttgttttgcggtcggcctccagatggtaaagtgtagacaatcccaga 4800
```

B. Inserted 3×HA tag sequence

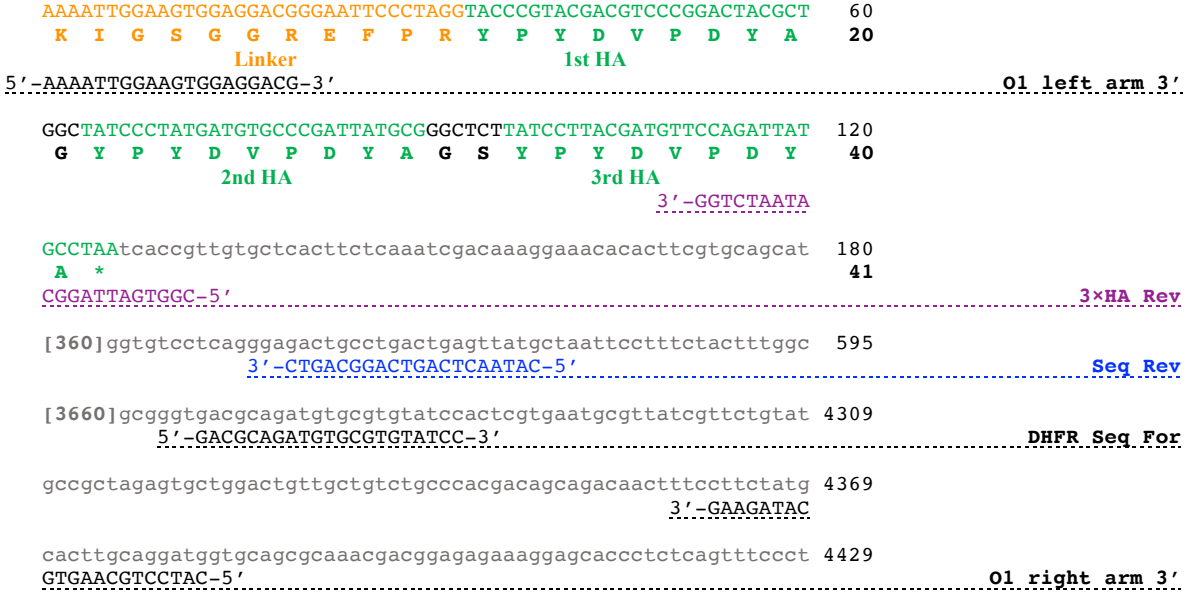

C. Manually curated COBALT alignment of FbxO1 like sequences

Code	Accession	Species	Clade	
Tg	XP_002364337.1	TGME49_310930 [*Toxoplasma gondii* ME49]	Coccidian A	Apicomplexa
Hh	XP_008885908.1	HHA_310930 [*Hammondia hammondi*]	Coccidian A	Apicomplexa
Nc	XP_003885097.1	[*Neospora caninum* Liverpool]	Coccidian A	Apicomplexa
Beb	PFH34091.1	hypothetical protein BESB_072430 [*Besnoitia besnoiti*]	Coccidian A	Apicomplexa
Cs	PHJ16413.1	hypothetical protein CSUI_009775 [*Cystoisospora suis*]	Coccidian A	Apicomplexa
Em	XP_013337306.1	oxidoreductase, putative [*Eimeria maxima*]	Coccidian B	Apicomplexa
Cc	XP_026193228.1	LOC34623623 [*Cyclospora cayetanensis*]	Coccidian B	Apicomplexa
To	XP_009689732.1	TOT_010000887 [*Theileria orientalis* strain ShIntoKu]	Piroplasmid	Apicomplexa
Bab	XP_012766453.1	hypothetical protein, conserved [*Babesia bigemina*]	Piroplasmid	Apicomplexa
Pr	CRH00939.1	conserved plasmodium protein, unknown function [*Plasmodium relictum*]	Haemosporidian	Apicomplexa
Cm	XP_002140319.1	hypothetical protein [*Cryptosporidium muris* RN66]	Conoid	Apicomplexa
Vb	CEM03254.1	unnamed protein product [*Vitrella brassicaformis* CCMP3155]	Chromerid	
Im	XP_004034674.1	hypothetical protein IMG5_116140 [*Ichthyophthirius multifiliis*]	Ciliophora	
Pt	XP_001454827.1	hypothetical protein [*Paramecium tetraurelia* strain D4-2]	Ciliophora	
Tt	XP_001028005.3	TTHERM_00498170 [*Tetrahymena thermophila* SB210]	free living ciliate	
Sc	OMJ83137.1	hypothetical protein Stecoe_15990 [*Stentor coeruleus*]	heterotrophic ciliate (heterotrich)	
Pp	KRX05854.1	hypothetical protein Ppersa_03791 [*Pseudocohnilembus persalinus*]	pathogenic ciliate	
Sl	CDW85380.1	UNKNOWN [*Stylonychia lemnae*]	Ciliate	
Ot	EJY65153.1	hypothetical protein OXYTRI_14697 [*Oxytricha trifallax*]	Ciliate	
Sm	OLQ08676.1	hypothetical protein AK812_SMIcGEnE7829 [*Symbiodinium microadriaticum*]	endosymbiotic dinoflagellate	

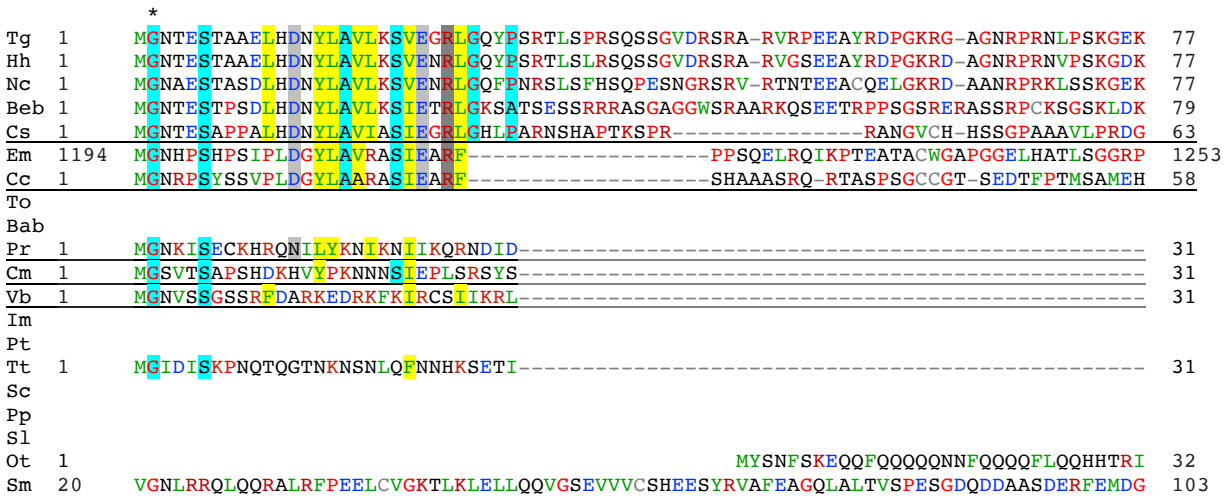

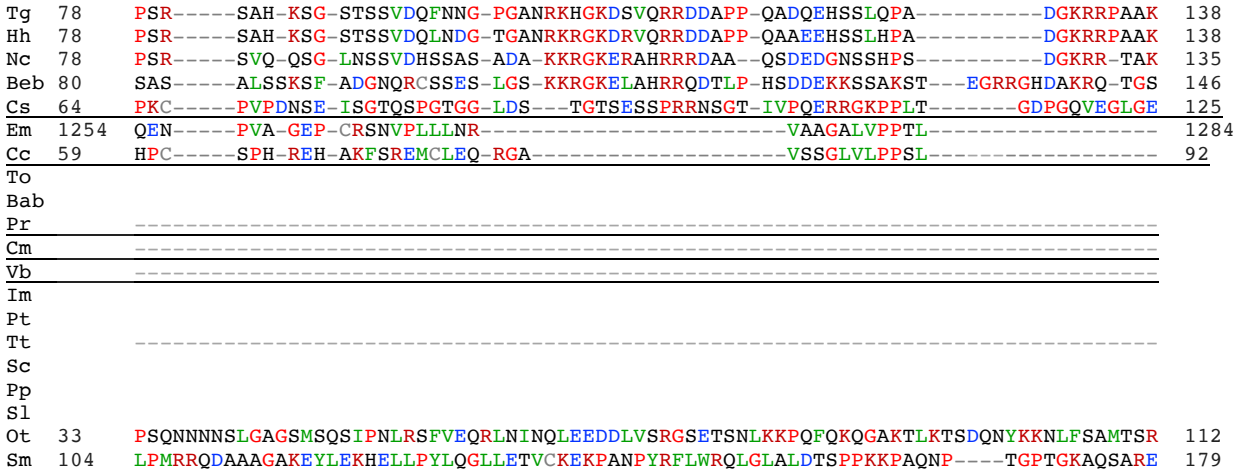

```
Tg  210   KTQVED[1]ELSSLPSSP      TAS   AEVATDKPGEGR[9]GRSAEGDRGP[9]AD    AKEN-ESDNSHGESDQDL  287
Hh  210   KTHVED[1]ALSSVPSSP      TAS   AEVATEKPGEGR[9]GRSAEGGREP[9]AD    AKEN-ESENASGESNQNL  287
Nc  207   EKTEVD[1]SLGSSPGSP      TAS   AGSVTGATG---    GRSSDARKER   AE    GKGK-DPVNTSDKSKRDP  263
Beb 215   EETQAG[3]ARESAPETP      SAF   AEGAEAQER---    ARKNSVSKKE   AK[5]SRGD-KHARHSGEQKAES  278
Cs  200   RGEEAD[1]AFHTRDDER      NGM   ATEEPEKEKE--[6]AAQIDSSLSS[9]GN[5]VTGD-SSESKPNPDMVAK  277
Em  1338  ------    -----HCSS      TVS   RKAGTHKQQLPE    -REISGSSSR    --[1]SRSN-SSGSNDGGSACST 1383
Cc  147   ------    -----NCSP      TVS   KGSDAQQAPLCN    -SSIAIINER    --[1]YTLN-SERSPNAVGC---  189
To  29    PTQATL[2]LHQPTNTQR      E--   EPPEPSKHDDNR[5]----------[5]EP[7]-----YHPYVTNYHSTEK  90
Bab 27    PTVAVP[2]--EPRPVEQ      T--   EVVEPSTTGDAS[9]PIENAQSPSS[9]EE[9]VTEDVYDPLIMNFSPKIS  111
Pr  41    NEKDLF[5]IFELYNTHE      ENT[1]KKDNENKENEEN[9]KNEKEKKKNA[9]SE[9]KRDDEGKNVKEIDEQTKK  133
Cm        ------    ----------    ---   ------------    ----------    --    ------------------
Vb        ------    ----------    ---   ------------    ----------    --    ------------------
Im
Pt
Tt        ------    ----------    ---   ------------    ----------    --    ------------------
Sc
Pp
Sl  72    PHLFR-[4]GLECTQSSP      QIN[4]SQQIKAALFGGT[9]KIQQQNKDDD[9]LK[9]QVQSqFSTNYKQKNPYKS  165
Ot  190   NNIYQP[5]GNYASQFDP      DLF[4]AMKKQYSQGVAQ[9]YYIQQNDDKI[9]QM[9]PLQEVIPQNQNQNGYAFK  285
Sm  258   EDFENV[5]ALFQSSIQQ[151]TAS[3]KVSAQEPPELAR[9]LTERILCRTA[9]EP[9]REQDaEDQGRGGKEDMPE  503
```

```
Tg  288   RRRSDGRGASSQRSR--------DEASNSGEPPSQSKPSQL    SKQIRKKELAPEPLRAADIDLSSDVRVGASLKGGK    355
Hh  288   RRRSDARRASSRGSR--------DEASNSGGRPSQAKPSQL    SKQIRKKELAPEPLRAADIDLSSDGG-GASLKGGK    354
Nc  264   RQRSNGSVASS-GTS---------GACLHTGQPHAARKSSP    PSKQSRQKEQVTQLSAADIALPSHAS-GGCTQEGK    328
Beb 279   LEREQASGSER-GSP---QKKPsRGLSCSEARRSSAKNSAS    LTNGRKKERQPQALCAEEVGLSSAAG-TGVRKKGS    349
Cs  278   LSETKVGRSLS------SKKStnSLAGTSTTRPSKSPAPGQ    PRSRGPGRNVPEPLRAEELEYAVTTA-SVCSRRG[11] 356
Em  1384  RKVYAVSAFPGPSSR----PKQLDATLVASSGGAQRPRQDR    SQQKNSSRSPPGACIADQHKAGFPVG---TRQTR[ 3]1454
Cc  190   ----------PQPKRK----PQQPAEALIAPTAG--------    ------------------------PHQTKQLGTEA     223
To  91    YAKKPTSKKVTPKSSIGEPPPPPKPPLNHAPSGPKYLE---[4]DLQTDFQKLSTETITR------------------     148
Bab 112   RLRAEAADSDTCKSPtRDVNSIsQAAATSTSSGHTAEQGVF[4]---TLFSDVGSKPMAE------------------     169
Pr  134   TNENHKKNFELDYGSFYNIEEKnNICKNNNNNKLLKKEKLL    -KHIEVKNEKSQKLKNTEKTENVLLK-KISLNKN[ 9] 215
Cm  31    ------------------SNVELPSVTPVSRSQSIQTLSAPL[2]DSVSDLIDRISSRLNKNYRIVKYLAL--ACPKDY[ 8]  95
Vb  31    ------------------------------------------    --------------------GPPGAPMPETVPPPS[ 7]  52
Im
Pt
Tt  31    ------------------------------------------    ----------------SETIQKMILRVQSQIEKG[12]  56
Sc
Sl  166   RQIS---IHTNAYLAtDVG----DSTSHKQEIFSTAQTTQM[4]NNHQRVASNT--KSFFNQTNNNTFISYDNNMINE[ 8] 243
Ot  286   RATNDSVMLSNSFHNtqAPLPKVGQNQYQNQIQDFEDSQAQ[4]QQQLLSNYERAKNLDLSQ--QNKTHTLNSSGKK-[ 6] 367
Sm  504   AASQGQGGTSPEARAKRLMELRRSFSALKQSHGLLQRKVSK[5]DEVRRNTDQAVQLLRDAFVSQRSESD--SKEEKG[10] 591
```

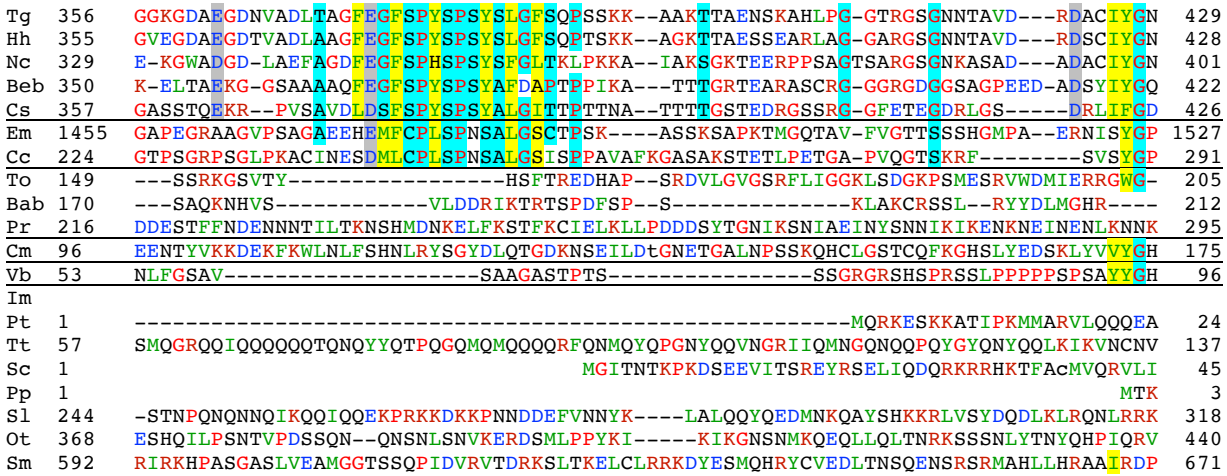


Predicted F-box domain

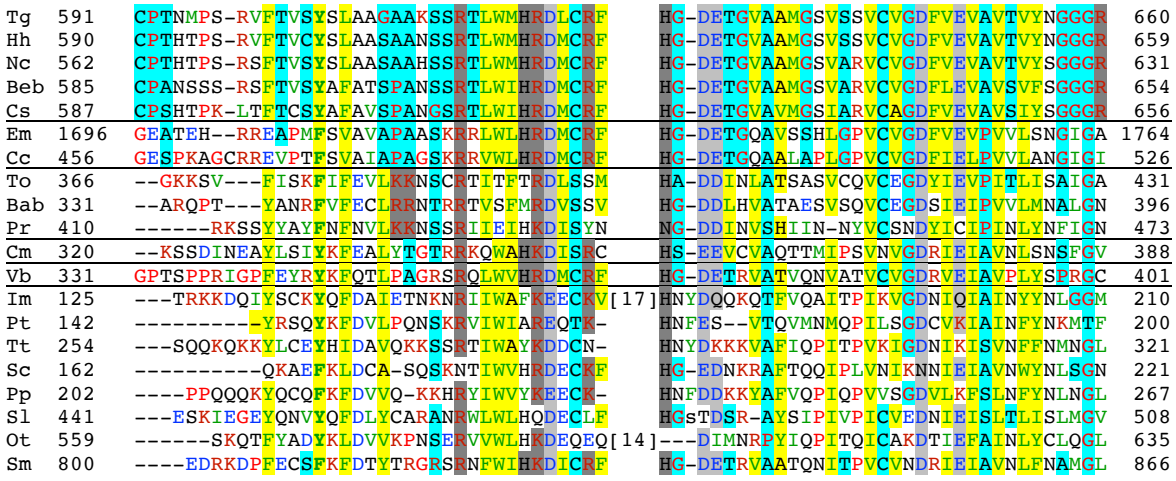

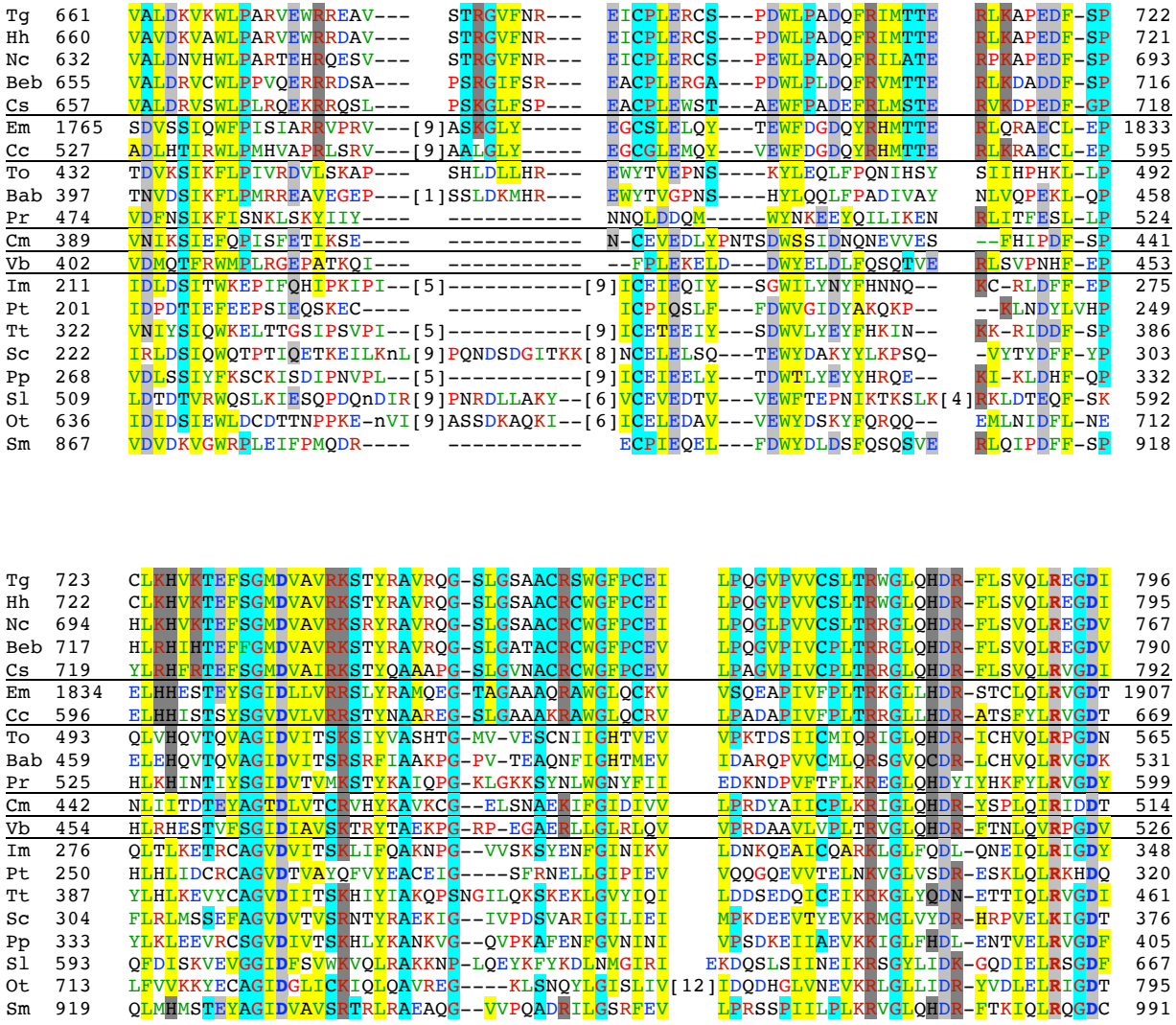

```
Tg   797   IDYYMSQGGANA*    808
Hh   796   IDYYMSQGGANA*    807
Nc   768   LDYYVSQGGATA*    779
Beb  791   VDYYLSQGGANV*    802
Cs   793   VEFYMSQGGAAV*    804
Em   1908  LESYLTIGGANV*   1919
Cc   670   LDSYLTVGGGTF*    681
To   566   LQFYITKG*         573
Bab  532   VRFYTTKG*         539
Pr   600   VVFYLIKGGNNI*    611
Cm   515   IVLYITKGGAIPE*   527
Vb   527   LYLYISQGGKIIaKR* 541
Im   349   FIFYISKGE*        357
Pt   321   LIFYLTSGD*        329
Tt   462   FVFYISSGD*        470
Sc   377   FVLYISRGG*        385
Pp   406   IIVYISKGD*        414
Sl   668   LLVYVSMGGFEK*    679
Ot   796   LVIYVQRGSS*       805
Sm   992   ILLYISQGGKMT*    1003
```

D. Comparison of the native FbxO1 coding sequence with the FbxO1 cDNA sequence used for recombinant expression in *E. coli*

```
Native FbxO1:  ATGGGCAACACGGAATCCACGGCCGCTGAGTTGCACGACAACTACTTGGCGGTTCTTAAA   60
FbxO1 cDNA:    ATGGGCAACACGGAATCCACGGCCGCTGAGTTGCACGACAACTACTTGGCGGTTCTTAAA   60
               Start

               AGCGTCGAGGGTCGGTTGGGACAGTACCCAAGCCGAACGCTCTCCCCTCGGTCGCAGTCA  120
               AGCGTCGAGGGTCGGTTGGGACAGTACCCAAGCCGAACGCTCTCCCCTCGGTCGCAGTCA  120

               AGCGGTGTGGATCGGTCTCGCGCGAGGGTACGCCCCGAGGAGGCGTACCGGGATCCTGGA  180
               AGCGGTGTGGATCGGTCTCGCGCGAGGGTACGCCCCGAGGAGGCGTACCGGGATCCTGGA  180

               AAACGGGGTGCTGGAAACCGCCCTCGCAACTTGCCATCCAAAGGCGAGAAGCCCTCTCGG  240
               AAACGGGGTGCTGGAAACCGCCCTCGCAACTTGCCATCCAAAGGCGAGAAGCCCTCTCGG  240

               TCTGCGCACAAGTCGGGATCCACTTCCTCAGTGGACCAGTTCAACAACGGGCCTGGTGCG  300
               TCTGCGCACAAGTCGGGATCCACTTCCTCAGTGGACCAGTTCAACAACGGGCCTGGTGCG  300

               AACCGGAAACACGGAAAGGACAGCGTCCAGCGGCGCGATGATGCCCCGCCACAAGCAGAT  360
               AACCGGAAACACGGAAAGGACAGCGTCCAGCGGCGCGATGATGCCCCGCCACAAGCAGAT  360

               CAGGAACACTCTTCGCTTCAACCAGCTGACGGCAAGCGCCGGCCTGCCGCGAAAGGAGAG  420
               CAGGAACACTCTTCGCTTCAACCAGCTGACGGCAAGCGCCGGCCTGCCGCGAAAGGAGAG  420

               ACTCCCAATGTGGAGTCGACTGCGACAGGATCCGACTGGGGAGACTCCGCTGTCAACGAT  480
               ACTCCCAATGTGGAGTCGACTGCGACAGGATCCGACTGGGGAGACTCCGCTGTCAACGAT  480

               TTTGCTGAAGAGGATAGCTGCGCCGTTGAGAGTCCAGCACACTTTAAGCTTCAGACGAAG  540
               TTTGCTGAAGAGGATAGCTGCGCCGTTGAGAGTCCAGCACACTTTAAGCTTCAGACGAAG  540

               GAGTCGGGTGTCAAGGCACCTTCGCCGCGCCTCTTCCCCTGTGAAACGCTGTATGAGGTC  600
               GAGTCGGGTGTCAAGGCACCTTCGCCGCGCCTCTTCCCCTGTGAAACGCTGTATGAGGTC  600

               ACTTCGCAGATAGACCTCGCGGATGAGAAAACGCAAGTCGAAGACGGAGAGCTCAGCTCT  660
               ACTTCGCAGATAGACCTCGCGGATGAGAAAACGCAAGTCGAAGACGGAGAGCTCAGCTCT  660

               CTCCCGAGTTCCCCCACGGCCTCTGCAGAGGTCGCGACGGACAAGCCCGGGGAGGGACGG  720
               CTCCCGAGTTCCCCCACGGCCTCTGCAGAGGTCGCGACGGACAAGCCCGGGGAGGGACGG  720

               ACGGCGACGCGGGAAGACACGCGGACTGGTCGGTCAGCTGAGGGAGACAGAGGGCCTTGC  780
               ACGGCGACGCGGGAAGACACGCGGACTGGTCGGTCAGCTGAGGGAGACAGAGGGCCTTGC  780

               CATACAGAGAATCAGGTCGACGGAGCAGACGCGAAGGAGAATGAGTCAGACAACTCACAC  840
               CATACAGAGAATCAGGTCGACGGAGCAGACGCGAAGGAGAATGAGTCAGACAACTCACAC  840

               GGCGAGTCAGACCAAGACCTGCGACGTCGGAGCGACGGCCGCGGTGCATCCTCCCAGAGA  900
               GGCGAGTCAGACCAAGACCTGCGACGTCGGAGCGACGGCCGCGGTGCATCCTCCCAGAGA  900

               TCCAGGGACGAGGCCTCGAACAGTGGCGAGCCTCCGTCACAGTCGAAACCGTCGCAGCTT  960
               TCCAGGGACGAGGCCTCGAACAGTGGCGAGCCTCCGTCACAGTCGAAACCGTCGCAGCTT  960

               TCAAAGCAAATACGGAAGAAAGAACTCGCCCCGGAGCCTCTCCGCGCAGCAGATATCGAC 1020
               TCAAAGCAAATACGGAAGAAAGAACTCGCCCCGGAGCCTCTCCGCGCAGCAGATATCGAC 1020

               CTTTCCTCAGATGTCCGTGTCGGAGCCTCGTTGAAGGGGGGGAAGGGAGGGAAGGGAGAC 1080
               CTTTCCTCAGATGTCCGTGTCGGAGCCTCGTTGAAGGGGGGGAAGGGAGGGAAGGGAGAC 1080

               GCTGAGGGTGATAATGTCGCCGACCTCACAGCTGGATTCGAGGGATTTTCGCCGTACTCG 1140
               GCTGAGGGTGATAATGTCGCCGACCTCACAGCTGGATTCGAGGGATTTTCGCCGTACTCG 1140

               CCCTCCTACTCTCTTGGCTTCAGTCAGCCGTCGTCGAAGAAGGCTGCAAAAACGACAGCT 1200
               CCCTCCTACTCTCTTGGCTTCAGTCAGCCGTCGTCGAAGAAGGCTGCAAAAACGACAGCT 1200

               GAAAACTCCAAAGCACACCTACCAGGAGGAACCCGCGGCAGCGGCAACAACACTGCTGTC 1260
               GAAAACTCCAAAGCACACCTACCAGGAGGAACCCGCGGCAGCGGCAACAACACTGCTGTC 1260

               GACCGGGACGCGTGCATCTACGGAAACAAGAAAAACCACTTTCCCTTCCTCGACGAACCT 1320
               GACCGGGACGCGTGCATCTACGGAAACAAGAAAAACCACTTTCCCTTCCTCGACGAACCT 1320

               GCCTTGTCACTGCTTGTACCATTTCTCTTCGGCAGAAGCCTCGCGACTTGCATGACCGTC 1380
               GCCTTGTCACTGCTTGTACCATTTCTCTTCGGCAGAAGCCTCGCGACTTGCATGACCGTC 1380
```

```
TGTCCACACTGGTTCATGAAAATCAATCGGGCTATGGAACGCATGTGTGGGCCTGCCACA 1440
TGTCCACACTGGTTCATGAAAATCAATCGGGCTATGGAACGCATGTGTGGGCCTGCCACA 1440

AAAGGTTTCCAGCAAATGTACTCAAAATACTTGGAAGTCTGGGGAAGCGCTGTCAAACTT 1500
AAAGGTTTCCAGCAAATGTACTCAAAATACTTGGAAGTCTGGGGAAGCGCTGTCAAACTT 1500

CAGCCTCTCCAGACAGTTGGCGATGGCGGAGTCCGCGTGGACTGGGTGATTTTTGCCAAG 1560
CAGCCTCTCCAGACAGTTGGCGATGGCGGAGTCCGCGTGGACTGGGTGATTTTTGCCAAG 1560

GTCCTCCCGGAATGTGAAGGTCACATCCTTGACATATCGTATACCTATTCCTACATTTCC 1620
GTCCTCCCGGAATGTGAAGGTCACATCCTTGACATATCGTATACCTATTCCTACATTTCC 1620

GAAAGTTCGAGTTCGACTGCTCGTCCGGTGGACGAAGCGGACAAGCCCGCGGCGGGTGGG 1680
GAAAGTTCGAGTTCGACTGCTCGTCCGGTGGACGAAGCGGACAAGCCCGCGGCGGGTGGG 1680

AAGAGAGATCGCGGACGGCAAGGAGAAAAAAGGCGATCCCTTTCTGCCAACTTCGACGAA 1740
AAGAGAGATCGCGGACGGCAAGGAGAAAAAAGGCGATCCCTTTCTGCCAACTTCGACGAA 1740

GGCGTCATTCTCTCTCCGTGCGGACAGCCTTGCCCGACCAACATGCCTTCGCGCGTGTTC 1800
GGCGTCATTCTCTCTCCGTGCGGACAGCCTTGCCCGACCAACATGCCTTCGCGCGTGTTC 1800

ACGGTGTCTTACTCGCTGGCGGCGGGTGCGGCGAAGAGCAGCCGAACGCTTTGGATGCAC 1860
ACGGTGTCTTACTCGCTGGCGGCGGGTGCGGCGAAGAGCAGCCGAACGCTTTGGATGCAC 1860

CGAGACTTGTGCCGGTTCCACGGAGACGAGACTGGGGTCGCTGCCATGGGCTCCGTCTCA 1920
CGAGACTTGTGCCGGTTCCACGGAGACGAGACTGGGGTCGCTGCCATGGGCTCCGTCTCA 1920

AGTGTCTGCGTAGGAGACTTCGTGGAAGTCGCTGTCACTGTGTACAACGGAGGCGGGCGC 1980
AGTGTCTGCGTAGGAGACTTCGTGGAAGTCGCTGTCACTGTGTACAACGGAGGCGGGCGC 1980

GTTGCTCTGGACAAAGTCAAGTGGCTGCCTGCGCGAGTCGAGTGGAGACGGGAGGCTGTT 2040
GTTGCTCTGGACAAAGTCAAGTGGCTGCCTGCGCGAGTCGAGTGGAGACGGGAGGCTGTT 2040

TCGACTCGCGGCGTCTTCAACAGAGAAATCTGTCCTCTCGAACGCTGCTCTCCCGACTGG 2100
TCGACTCGCGGCGTCTTCAACAGAGAAATCTGTCCTCTCGAACGCTGCTCTCCCGACTGG 2100

CTTCCTGCAGACCAGTTCCGCATCATGACTACGGAACGCCTGAAGGCTCCAGAGGACTTC 2160
CTTCCTGCAGACCAGTTCCGCATCATGACTACGGAACGCCTGAAGGCTCCAGAGGACTTC 2160

TCGCCGTGTTTGAAACATGTCAAGACAGAATTTTCCGGAATGGATGTCGCCGTTCGCAAA 2220
TCGCCGTGTTTGAAACATGTCAAGACAGAATTTTCCGGAATGGATGTCGCCGTTCGCAAA 2220

TCAACATATCGAGCAGTCCGCCAAGGGTCGCTGGGATCAGCAGCGTGCCGGTCTTGGGGG 2280
TCAACATATCGAGCAGTCCGCCAAGGGTCGCTGGGATCAGCAGCGTGCCGGTCTTGGGGG 2280

TTCCCTTGTGAGATCCTTCCTCAAGGCGTCCCTGTTGTTTGCTCCCTGACGCGCTGGGGA 2340
TTCCCTTGTGAGATCCTTCCTCAAGGCGTCCCTGTTGTTTGCTCCCTGACGCGCTGGGGA 2340

CTCCAGCATGATCGATTCCTCTCCGTTCAGCTGCGCGAGGGCGACATAATCGATTACTAC 2400
CTCCAGCATGATCGATTCCTCTCCGTTCAGCTGCGCGAGGGCGACATAATCGATTACTAC 2400

ATGAGTCAGGGCGGAGCCAATGCGTGA 2427
ATGAGTCAGGGCGGAGCCAATGCGTGA 2427
                        Stop
```

Figure 7. Sequence and evolution of *Toxoplasma* FbxO1. (A) The TGME49_310930 genomic sequence (black uppercase letter: exon; gray lowercase letter: intron and partial UTR regions) and the amino acid sequence (bold uppercase letter) translated from the +1 reading frame were obtained from ToxoDB (toxodb.org). The sequences of the primers in Figure 6 are indicated. The two dark red and underlined codons in the last exon of FbxO1 sequence marks the locations where point mutations occurred during C-terminal epitope tagging, as also shown in Figure 9B. PAM: protospacer adjacent motif. **(B)** The nucleotide sequence and amino acid sequence for the 3×HA tag. The number of abbreviated nucleotides in the SAG1 3′ UTR and the DHFR cassette are bracketed. The sequences of the primers in Figure 6 are indicated. **(C)** The manually curated COBALT alignment of *Toxoplasma* FbxO1 and its homologous sequences from other alveolates was adapted from Baptista et al, 2019 [17]. Blue: acidic residues; dark red: basic residues; red: small or proline; green: hydrophobic residues. Underlines separates phylogenetic groups: the top two groups consist of different coccidian subclades, the next two groups consist of other apicomplexans, the next group contains a chromerid (apicomplexan predecessor), and the bottom group contains non-apicomplexan alveolates including ciliates and dinoflagellates. Positions of conservation in at least one group are highlighted based on hydrophobic residues (yellow), acidic residues (light gray), basic residues (dark gray), or small and proline (teal). **(D)** Comparison of the native *Toxoplasma* FbxO1 coding sequence with the FbxO1 cDNA sequence cloned into the pET15b-6His-TgFbxO1 plasmid for recombinant expression of *Toxoplasma* FbxO1 in *E. coli*. The two sequences are identical.

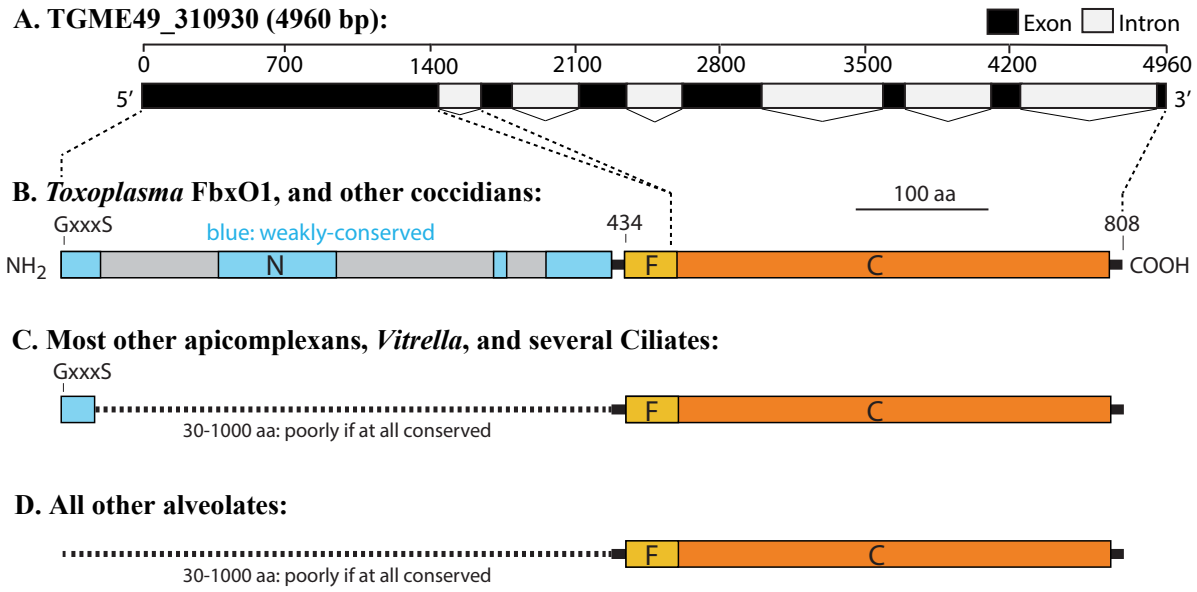

Figure 8. Predicted domain organization and conservation of *Toxoplasma* FbxO1. (A) The predicted gene model of *Toxoplasma* FbxO1. The dashed lines link the coding region (predicted mRNA; introns spliced out) of the gene sequence with the *Toxoplasma* FbxO1 protein domain structure based on translation of the coding region. **(B)** Domain structure of the FbxO1 protein and FbxO1-like sequences in *Toxoplasma* and closely related coccidian species obtained by BLASTP and COBALT analyses. GxxxS: predicted *N*-myristoylation motif; N: N-terminal; F: F-box motif; C: C-terminal. (**C**) Domain structure of FbxO1-like sequences in most other apicomplexans, *Vitrella*, and several ciliates. (**D**) Domain structure of FbxO1-like sequences in all other alveolates included in the non-redundant database search.

Table 4. Prediction of *N*-myristoylation of FbxO1-like proteins

Accession	Length (aa)	Species	Phylum	Clade	N-term 20 aa	Myristoylated?	ExPASy Myristoylator Score (Confidence)
XP_002364337.1	808	*Toxoplasma gondii* ME49	Apicomplexa	Coccidian A	mgntestaae lhdnylavlk	yes	0.24 (Low)
XP_008885908.1	807	*Hammondia hammondi*	Apicomplexa	Coccidian A	mgntestaae lhdnylavlk	yes	0.24 (Low)
XP_003885097.1	779	*Neospora caninum* Liverpool	Apicomplexa	Coccidian A	mgnaestasd lhdnylavlk	yes	0.61 (Medium)
PFH34091.1	802	*Besnoitia besnoiti*	Apicomplexa	Coccidian A	mgntestpsd lhdnylavlk	yes	0.78 (Medium)
PHJ16413.1	804	*Cystoisospora suis*	Apicomplexa	Coccidian A	mgntesappa lhdnylavia	no	-0.12
XP_013433823.1	764	*Eimeria necatrix*	Apicomplexa	Coccidian B	mgnnpshptv pldgylavra	yes	0.76 (Medium)
XP_026193228.1	681	*Cyclospora cayetanensis*	Apicomplexa	Coccidian B	mgnrpsyssv pldgylaara	yes	0.71 (Medium)
XP_002140319.1	527	*Cryptosporidium muris* RN66	Apicomplexa	Coccidian	mgsvtsapsh dkhvypknnn	yes	0.98 (High)
XP_668219.1	551	*Cryptosporidium hominis* TU502	Apicomplexa	Coccidian	mgntlnfdne eqlvlltshs	yes	0.95(High)
XP_009689732.1	573	*Theileria orientalis* strain Shintoku	Apicomplexa	Piroplasmid	msnytptnrr ircfsfrrrr	no N-term G	
XP_012766453.1	539	*Babesia bigemina*	Apicomplexa	Piroplasmid	manyrgfflr fkglcarrmd	no N-term G	
XP_021338828.1	426	*Babesia microti* strain RI	Apicomplexa	Piroplasmid	mgsvcsgick prsggknlqc	yes	0.73 (Medium)
EUD73303.1	587	*Plasmodium vinckei* petteri	Apicomplexa	Haemosporid	mgnkisdnkq kqlilykdik	yes	0.99 (High)
SBT77726.1	657	*Plasmodium ovale*	Apicomplexa	Haemosporid	mgnkvpenkq rqfilyrdik	yes	0.63 (Medium)
XP_004223305.1	416	*Plasmodium cynomolgi* strain B	Apicomplexa	Haemosporid	mvddtkdstv gdssigrtfe	no N-term G	
XP_011131538.1	187	*Gregarina niphandrodes*	Apicomplexa	Gregarinasina	mgnraskedv diplvsrlrd	yes	0.99 (High)
CEM03254.1	541	*Vitrella brassicaformis* CCMP3155	Chromerida		mgnvssgssr fdarkedrkf	yes	0.99 (High)
XP_004034674.1	357	*Ichthyophthirius multifiliis*	Ciliophora		mklpflaqnk iffflfdeqi	no N-term G	
XP_001432362.1	388	*Paramecium tetraurelia* strain d4-2	Ciliophora		mgqnnctpni pglencyary	no	-0.84
XP_001028005.3	470	*Tetrahymena thermophila* SB210	Ciliophora		mgidiskpnq tqgtnknsnl	yes	0.99002784 (High)
XP_001018140.1	640	*Tetrahymena thermophila* SB211	Ciliophora		mgqnevkpln qrsiyfgqte	no	-0.35
OMJ95062.1	386	*Stentor coeruleus*	Ciliophora		mgisnvkpsd seevitsrey	no	-0.97
OMJ86612.1	385	*Stentor coeruleus*	Ciliophora		mgivnskptd peviiarehr	yes	0.97 (High)
KRX05854.1	414	*Pseudocohnilembus persalinus*	Ciliophora		mgsnntkqle yqkekiynkd	yes	0.99 (High)
CDW85962.1	806	*Stylonychia lemnae*	Ciliophora		mgqnnsfsqd andkeikett	yes	0.94 (High)
CDW85380.1	679	*Stylonychia lemnae*	Ciliophora		mntnpsielf nnldyqrpsk	no N-term G	
EJY81828.1	1015	*Oxytricha trifallax*	Ciliophora		mggnnsknnd fynnpellak	yes	0.94 (High)
EJY65153.1	805	*Oxytricha trifallax*	Ciliophora		mysnfskeqq fqqqqqnnfq	no N-term G	
OLQ08676.1	1003	*Symbiodinium microadriaticum*	Dinophyceae		mqvrvdagdl apelllsvrv	no N-term G	

3.2 Verification of FbxO1 endogenous gene tagging

To enable immuno-detection of FbxO1 from *Toxoplasma* cells, the C-terminus of the FbxO1 gene of both the RHΔΔ and Δ*phyA* strains was endogenously tagged with 3×HA using a CRISPR/Cas9-mediated strategy described in Chapter 2 [32]. To verify the insertion of the 3×HA sequence at the desired genomic locus, the picked clones were analyzed by diagnostic PCRs. Clones A11 and D8 were from the same transfection of the Δ*phyA* strain, and clones D12 and H6 were from the same transfection of the RHΔΔ strain. The primer pair O1F1 and O1R4 were located just outside the expected insertion (Figure 6). The 4 clones all yielded a PCR product with increased size (4,600-bp) compared to the wildtype (243-bp) (Figure 9A), correlating to the expected size of the tagged locus and suggesting successful insertion of the 3×HA sequence.

To further confirm that there were no unintended mutations or deletions occurred during strain construction, the tagged locus of each clone was amplified with primers Seq For and Seq Rev (Figure 6) and the PCR products were analyzed by Sanger sequencing. After aligning the sequencing results with the expected query sequence of the tagged locus, it was confirmed that the 3×HA sequence properly integrated at the C-terminus of FbxO1 uniformly across all the sequenced clones. However, a nucleotide substitution (T to A) was detected in clone D8 on FbxO1 exon 7, and another substitution (G to A) was detected in clone D12 on the same exon, which resulted in point mutations annotated as I796K and D798N, respectively. Clones A11 and H6 did not have any mutations in the sequenced region (Figure 9B), thus they were used for the immuno-detection and comparison of FbxO1 abundance in RHΔΔ and Δ*phyA* strains to assess the effect of the Skp1 modifications. No sequence errors were detected in the strains used for

tagging or the primers used during transfection or sequencing, so it was possible that the error occurred during HDR with the template.

To verify that the C-terminally 3×HA tagged FbxO1 (FbxO1-3HA) was expressed in the clones, cells from each clone were extracted and probed with anti-HA by Western blot as described in Chapter 2. Briefly, the cell pellets were each resuspended in cold 1% NP-40 Lysis buffer. The supernatants were collected as S21 and each of the P21 was resuspended in the same lysis buffer and homogenized by probe sonication. The equivalence of ~3 million parasites was loaded on the gel for each sample. The predominant signal migrated at ~105 kDa as indicated on the blot, which was present in all clones but not the RHΔΔ and Δ*phyA* parental strains (Figure 9C, top), suggesting that this signal corresponded to FbxO1-3HA expression. The majority of the FbxO1 was present in the S21 fraction, suggesting that a large fraction of it could be extracted by mild, non-ionic detergent. The stronger P21 signal seen in clones H6 and D8 were attributed to relatively more sample loading. The size of FbxO1 was, based on migration, larger than the predicted size of 87 kDa, possibly due to post-translational modifications such as the predicted *N*-myristoylation and possible multi-phosphorylation that slowed down the migration. Phosphorylation of FbxO1 is also supported by mass spectrometry-based evidence of FbxO1 expression in tachyzoite phosphoproteome [36, 37]. Another explanation is that the predicted gene model for FbxO1 (Figure 8A) could have missed exons but no such error has been detected. The Skp1 blot showed that the majority of Skp1 from clones A11 and D8 and their Δ*phyA* parental strain, migrated a little faster than the modified Skp1 (GGFGGnO-Skp1) from clones D12 and H6 and their RHΔΔ parental strain, confirming the correct background of each clone (Figure 9C, middle).

A potential issue found with these FbxO1-3HA strains was that the signal intensity of FbxO1-3HA was about 50% weaker than the signal of FbxO1HA (data not shown) in the previously generated C-terminally 3×HA tagged strain (FbxO1HA) which was also under the endogenous FbxO1 promoter [17]. This FbxO1HA strain was able to complement FbxO1 depletion. Compared to the inserted sequence in the FbxO1-3HA strain, the inserted sequence in the FbxO1HA strain has a leading Ala in the linker region but lacks a Gly-Ser connecter between the second and third HA repeats (Figure 7B), which leads to a possible explanation that the slightly different tag sequences contribute to variance in affinity to the anti-HA antibody, and thus the discrepancy in the signal intensity of the tagged FbxO1. An attempt to knock out *phyA* in the FbxO1HA strain using the CRISPR/Cas9-mediated strategy [32] was not successful, so the FbxO1-3HA strains were used exclusively for examination of the effects of the Skp1 modifications on FbxO1, and the FbxO1HA strain was used for cellular fractionation and interactome studies of FbxO1.

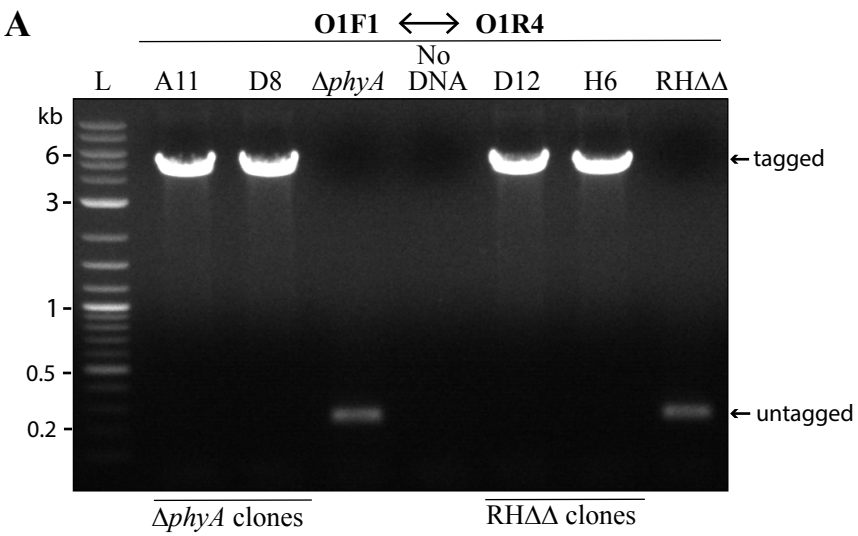
A
O1F1 ⟷ O1R4
No DNA
L
A11
D8
ΔphyA
D12
H6
RHΔΔ
kb
6
3
1
0.5
0.2
tagged
untagged
ΔphyA clones
RHΔΔ clones

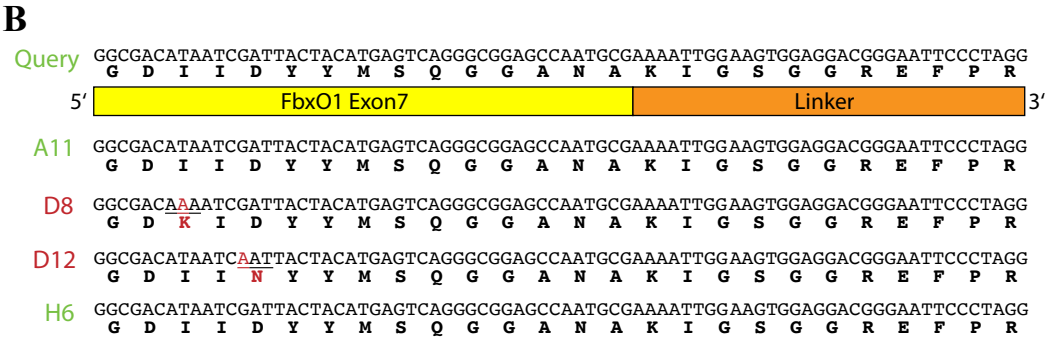
B
Query GGCGACATAATCGATTACTACATGAGTCAGGGCGGAGCCAATGCGAAAATTGGAAGTGGAGGACGGGAATTCCCTAGG
G D I I D Y Y M S Q G G A N A K I G S G G R E F P R
5′ FbxO1 Exon7 Linker 3′
A11 GGCGACATAATCGATTACTACATGAGTCAGGGCGGAGCCAATGCGAAAATTGGAAGTGGAGGACGGGAATTCCCTAGG
G D I I D Y Y M S Q G G A N A K I G S G G R E F P R
D8 GGCGACAAAATCGATTACTACATGAGTCAGGGCGGAGCCAATGCGAAAATTGGAAGTGGAGGACGGGAATTCCCTAGG
G D K I D Y Y M S Q G G A N A K I G S G G R E F P R
D12 GGCGACATAATCAATTACTACATGAGTCAGGGCGGAGCCAATGCGAAAATTGGAAGTGGAGGACGGGAATTCCCTAGG
G D I I N Y Y M S Q G G A N A K I G S G G R E F P R
H6 GGCGACATAATCGATTACTACATGAGTCAGGGCGGAGCCAATGCGAAAATTGGAAGTGGAGGACGGGAATTCCCTAGG
G D I I D Y Y M S Q G G A N A K I G S G G R E F P R

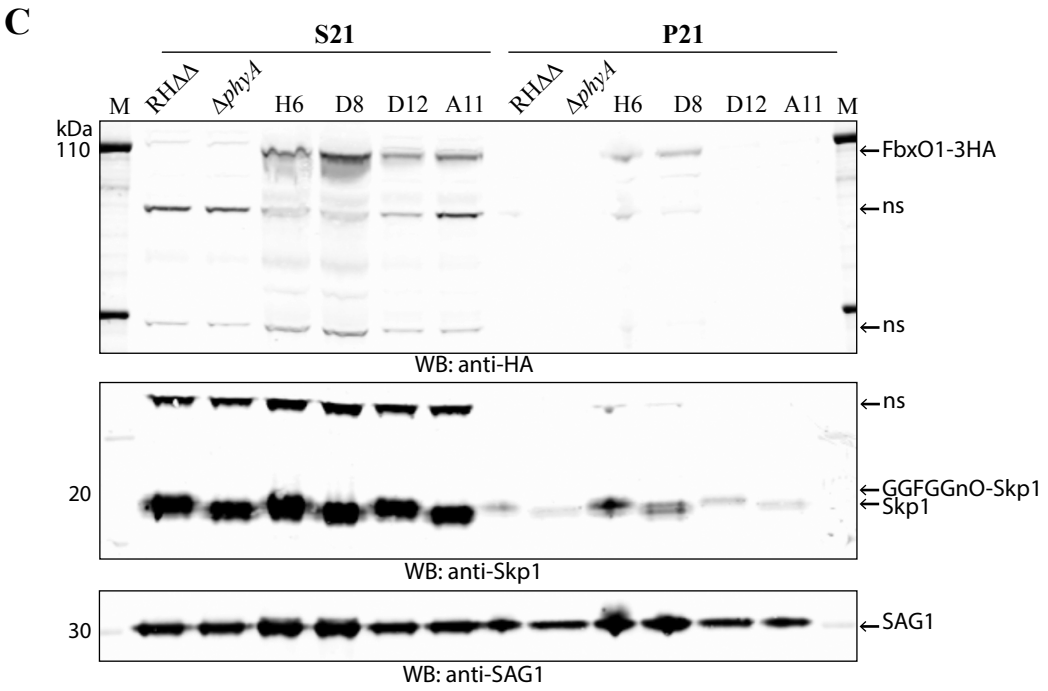
C
S21
P21
M
RHΔΔ
ΔphyA
H6
D8
D12
A11
RHΔΔ
ΔphyA
H6
D8
D12
A11
M
kDa
110
FbxO1-3HA
ns
ns
WB: anti-HA
ns
20
GGFGGnO-Skp1
Skp1
WB: anti-Skp1
30
SAG1
WB: anti-SAG1

Figure 9. Verification of FbxO1 3×HA epitope tagging. (A) The diagnostic PCR products from clones (A11, D8) in Δ*phyA* background, clones (D12, H6) in RHΔΔ background and controls (RHΔΔ and Δ*phyA* parental strains) were analyzed. L: 2-log DNA ladder from NEB. (**B)** A cropped view of the alignment of the sequencing results from the clones with the expected query sequence. For simplicity, only the FbxO1 exon 7 sequence followed by the inserted linker sequence is displayed. In clone D8 and D12, the mutated nucleotides and the resulting amino acid changes are highlighted in dark red. (**C)** The extracts equivalent to ~3 million parasites from the clones and controls were loaded on a gel and Western blotted with the indicated antibodies. SAG1 was used as the loading control. S21: the supernatant from 21,000 × g, 15 min centrifugation; P21: the pellet from 21,000 × g, 15 min centrifugation; M: Novex Sharp protein molecular marker; WB: Western blot; ns: non-specific signals.

3.3 Cellular fractionation of FbxO1

To investigate the solubility and localization of FbxO1 biochemically, a cell pellet consisting of about 80% EC and 20% IC parasites from the strain FbxO1HA was lysed and extracted sequentially in a series of buffers as described in Chapter 2, and the soluble material from each extraction step was immunoblotted with anti-HA to examine in which fractions FbxO1 resides. Briefly, the cell pellet was first probe sonicated in Sucrose buffer in order to retain osmolarity and help preserve intracellular components including the nuclei and organelles during cell lysis. Then the insoluble matter from the initial extraction was evenly distributed into three and extracted in parallel in Hypertonic buffer, Hypotonic buffer, and Detergent buffer. Lastly, the insoluble matter from each of the extractions was boiled in 2% SDS. A cell pellet from RHΔΔ was directly lysed in Detergent buffer and both the soluble and insoluble materials were collected as negative controls for the Western blot.

As observed on the blot, ~40% of the FbxO1 was extracted by Sucrose buffer, and about another 40% of FbxO1 was extracted by Detergent buffer. Hypotonic buffer did not seem to extract any of the FbxO1, while Hypertonic buffer extracted about another 10% of FbxO1 (Figure 10A). This result suggested that about half of the FbxO1 is relatively soluble and may reside in the cytosol, while the other half is less soluble and may be membrane-associated. A potential explanation for the partitioning of FbxO1 could be that the *N*-myristoylation anchors some FbxO1 onto membranes, and another FbxO1 population has the myristoyl group buried inside the protein, thus rendering these FbxO1 soluble. A caveat associated with this fractionation method is that the probe sonication step might be strong enough to partially disrupt membrane association of proteins or generate particles too small to sediment under the conditions employed. This disruption was evident with the presence of the loading control

SAG1, a glycosylphosphatidylinositol (GPI)-anchored membrane protein in *Toxoplasma*, in the 1-S100 fraction (Figure 10A), which may lead to overestimation of the amount of FbxO1 that was readily soluble.

To examine if Skp1 association with FbxO1 was different among the fractions, cells from RHΔΔ and FbxO1HA strain were fractionated using the same method, and FbxO1 was co-immunoprecipitated from sucrose extraction (fraction 1), hypertonic extraction (fraction 2) and detergent extraction (fraction 4). The anti-Skp1 antibody (UOK75) was used to detect Skp1 in the FbxO1HA co-IP eluates. Skp1 was associated with FbxO1 in all three fractions. Skp1 appeared more soluble than FbxO1 since more Skp1 was extracted by Sucrose buffer than Detergent buffer, yet, the amount of Skp1 that associated with FbxO1 was about equal in the sucrose extract and the detergent extract (Figure 10B), suggesting that the Skp1-FbxO1 association is equally present regardless of where FbxO1 resides in the cell.

Although no subcellular markers were used in the cellular fractionation experiments as controls to confirm the subcellular properties of the different soluble extracts, combining the results from the cellular fractionation and immunofluorescence experiments, it is reasonable to predict that around half of the FbxO1 resides in a soluble form in the cytosol, while the other half is less soluble and likely associates with membranes, either with the IMC or the DCS, depending on the stage of the parasites. However, with the robust association between Skp1 and FbxO1, a functional SCF^{FbxO1} E3 ubiquitin ligase complex could potentially form at any of the cellular locales to assist in signaling events that are related to endodyogeny. It is also possible that FbxO1 at the IMC is degraded in a SCF-dependent manner at the end of G1-phase to facilitate progression of the cell cycle.

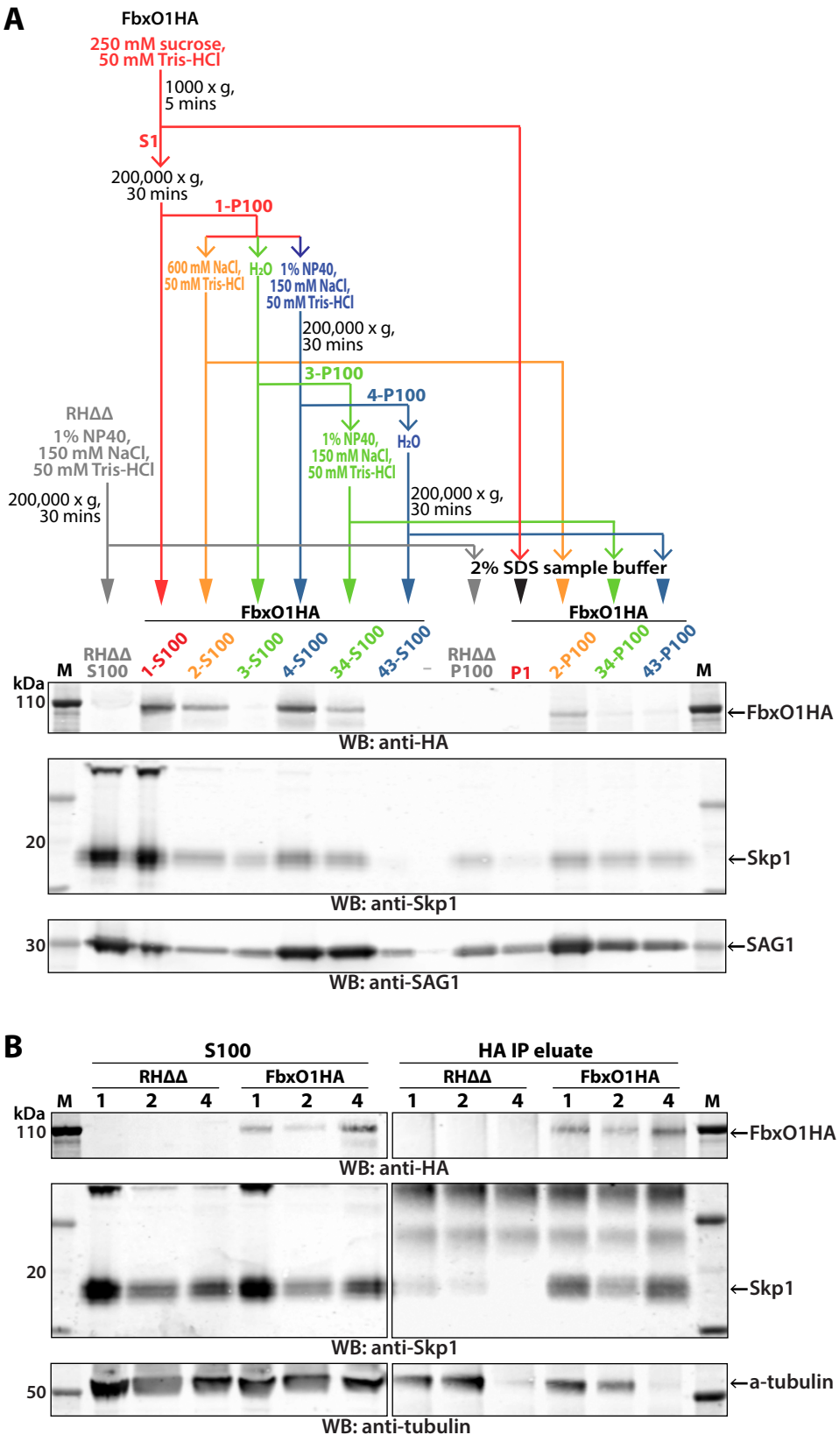
A
FbxO1HA
250 mM sucrose, 50 mM Tris-HCl
1000 x g, 5 mins
S1
200,000 x g, 30 mins
1-P100
600 mM NaCl, 50 mM Tris-HCl
H2O
1% NP40, 150 mM NaCl, 50 mM Tris-HCl
200,000 x g, 30 mins
3-P100
4-P100
RHΔΔ
1% NP40, 150 mM NaCl, 50 mM Tris-HCl
200,000 x g, 30 mins
H2O
1% NP40, 150 mM NaCl, 50 mM Tris-HCl
200,000 x g, 30 mins
2% SDS sample buffer
FbxO1HA
FbxO1HA
M
RHΔΔ S100
1-S100
2-S100
3-S100
4-S100
34-S100
43-S100
RHΔΔ P100
P1
2-P100
34-P100
43-P100
M
kDa
110
←FbxO1HA
WB: anti-HA
20
←Skp1
WB: anti-Skp1
30
←SAG1
WB: anti-SAG1
B
S100
HA IP eluate
RHΔΔ
FbxO1HA
RHΔΔ
FbxO1HA
M 1 2 4 1 2 4 1 2 4 1 2 4 M
kDa
110
←FbxO1HA
WB: anti-HA
20
←Skp1
WB: anti-Skp1
50
←a-tubulin
WB: anti-tubulin

Figure 10. Cellular fractionation of FbxO1. (**A)** Cellular fractionation experiment of FbxO1. Equal fractions of the total equivalent to ~6 million parasites were loaded into each lane of the SDS-PAGE gel, except for the RHΔΔ samples which were equivalent to ~4 million parasites. SAG1 was used as the loading control. (**B)** Co-IP of FbxO1 fractions generated in a separate experiment. **Fraction 1** represents extraction in Sucrose buffer, **fraction 2** represents extraction in Hypertonic buffer, and **fraction 4** represents extraction in Detergent buffer. For the S100, a sample equivalent to ~5 million parasites was loaded in each lane, and for the HA IP eluates, a sample equivalent to ~20 million parasites was loaded in each lane except for FbxO1HA-4, in which a sample equivalent to ~12.5 million parasites was loaded. α-tubulin was used as the loading control.

3.4 Investigation of the FbxO1 interactome by co-IP/MS

To examine the possibility of *Toxoplasma* FbxO1 as a substrate-type FBP even if it does not have any recognizable substrate-binding domains, the FbxO1 interactome was investigated by co-IP/MS. To optimize the condition of the co-IP to recover interactors of FbxO1, various NP-40 concentrations including 0.2%, 0.5% and 1% were tested, and both IC and EC parasites were tested. Samples including detergent extracts and fractionated extracts were both tested. Although the protein raw abundance of the FbxO1 bait in the FbxO1 co-IP/MS experiments ranged from a substantial value of 10^7 to 10^8 based on the sum of precursor ion intensities, and the peptide coverage of FbxO1 sequence was up to 72% among the series of experiments, no proteins except for Skp1 were detected as FbxO1 interactors in a consistent and replicable manner (Table 5).

Two potential pitfalls could have affected the results. The first is that the expression level of FbxO1 is too low for this experiment. Even though FbxO1 is one of the most highly expressed among all the predicted *Toxoplasma* FBPs, the expression level is still relatively low compared to Skp1. Thus, more than 100-200 million parasites may have been needed as the starting material to achieve better enrichment of FbxO1 and its potential interactors. The second pitfall is that the C-terminal tag placed on the highly conserved C-terminus of FbxO1 could interfere with its interaction with other proteins. Although the C-terminus lacks any recognizable substrate-binding domains (Figure 8), it could engage interactors in an yet to be determined manner. Thus, it will be necessary to explore other weakly conserved regions to tag on FbxO1 or develop antibodies against FbxO1.

Recently, a strain with an N-terminally 3×HA tagged FbxO1 expressed under the TetO7-SAG4 (T7S4) repressible promoter was generated [17]. The expression level of FbxO1 in this

strain (HAFbxO1) was ~2.3 times higher than that of the FbxO1HA strain which was expressed under the endogenous promoter (data not shown). The increased signal intensity of FbxO1 in HAFbxO1 strain could be attributed to the stronger T7S4 promoter, but the efficiency of anti-HA binding to the 3×HA tag at two distinct locations of FbxO1 may also play a role. The FbxO1 in the HAFbxO1 strain also migrated at ~105 kDa, which suggested that only phosphorylation possibly causes the molecular weight increase of *Toxoplasma* FbxO1, since HAFbxO1 could not be myristoylated. The HAFbxO1 strain was used for co-IP/MS experiment using similar number of parasites to discover FbxO1 interactors. From this experiment, Skp1 was reproducibly identified as an FbxO1 interactor as expected. No other relevant hits were discovered except for a small GTPase (Rab11b) which had 2 identified peptides at a relaxed FDR. Rab11b is one of the first factors to be recruited to the DCS and mediates the trafficking of IMC proteins to the DCS [3]. Intriguingly, the DCS localization of FbxO1 had been reported to be Rab11b-dependent [17]. Together with the evidence that IMC biogenesis requires Rab11b-dependent Golgi vesicular transport [38], these results suggested that Rab11b could interact with FbxO1 during the early stages of endodyogeny, and possibly regulates FbxO1 turnover in a similar manner. The presence of Rab11b in FbxO1 interactome supports their interaction, but more FbxO1 interactome studies are needed to confirm this finding.

Table 5. List of potential FbxO1 interactors.

Interactor	Strain	Cell stage	Extraction Method	Reproducible Result	Represented Trial	Sample Input (Number of Tachyzoites)	Exp. q-value: Sequest HT	Coverage [%]	PSMs	Unique Peptides	Absolute Abundance (x10^6)	Abundance/ 10^7 Tachyzoites
FbxO1 (bait)	FbxO1HA	Both EC and IC	0.2-1% NP-40, fractionation	yes	#2	4×10^7	0	51	86	30	56.8	**14.2**
	HAFbxO1				#4	1.5×10^7	0	72	521	46	139.3	**92.9**
Skp1	FbxO1HA	Both EC and IC	0.2-1% NP-40, fractionation	yes	#2	4×10^7	0	38	12	3	3	**0.8**
	HAFbxO1				#4	1.5×10^7	0	71	81	9	5.6	**3.7**
MORN2	FbxO1HA	~70% IC	1% NP-40	no	#1	1×10^7	0.022	17	4	3	1.2	**1.2**
Nuf2	FbxO1HA	~70% IC	fractionation	not yet repeated	#3	50×10^7	0.038	8	1	1	27	**0.5**
Rab11b	HAFbxO1	Mostly IC	0.5% NP-40	not yet repeated	#4	1.5×10^7	0.077	8	3	2	0.2	**0.1**

Note: PSMs – peptide spectrum matches

3.5 The effect of the Skp1 modifications on FbxO1 abundance and its association with Skp1

To investigate if the Skp1 modifications had an effect on Skp1 or FbxO1 abundance in cells, extracts of the Δ*phyA* and the RHΔΔ parental strains were compared by Western blotting or mass spectrometry after co-immunoprecipitation of Skp1 or FbxO1. Skp1 co-IP/MS experiments using both the native Skp1 and Skp1-SF as the baits were performed. As summarized in Table 6A, the relative abundance of Skp1 in Δ*phyA* extracts compared to RHΔΔ extracts varied considerably in the different experiments without a consistent trend, ranging from 1 to 2.26, however, averaging experiments 1-4 (n=9) yielded a Δ*phyA*/RHΔΔ ratio of 1.17 ± 0.43, suggesting that the Skp1 modifications do not significantly affect Skp1 abundance in cells. The comparison of FbxO1-3HA strains in both the Δ*phyA* and RHΔΔ background from the available co-IP/WB experiments (3 and 4) did not yield statistical difference to indicate an effect of the Skp1 modifications on FbxO1 abundance, as the average Δ*phyA*/RHΔΔ ratio for FbxO1 abundance from the two experiments (n=3) was 1.30 ± 0.29 (Table 6A), and the smaller S.D. compared to that for Skp1 abundance ratio indicated that these trials are more consistent. It was also observed that FbxO1 had modestly greater abundance ratio (Δ*phyA*/RHΔΔ) in EC cells compared to IC cells. Since it could be inferred from FbxO1 localization that the protein likely undergoes higher level of turnover at the EC stage, a higher Δ*phyA*/RHΔΔ ratio for FbxO1 abundance in EC parasites potentially indicated that the Skp1 modifications contribute to FbxO1 turnover during endodyogeny. More experiments are required to confirm if this trend is statistically significant.

The association between Skp1 and FbxO1 was interpreted from co-IP experiments queried by mass spectrometry or Western blotting. The amount of FbxO1 associated with Skp1 was calculated as a measure of the abundance of FbxO1 relative to that of Skp1 and compared

between the Δ*phyA* and RHΔΔ strains. The ratio of FbxO1:Skp1 between Δ*phyA* and RHΔΔ varied from 0.4 to 1.98 in various Skp1 pull-downs (n=8), and from 1.17 to 1.43 in FbxO1-3HA pull-downs (n=2), while both averaged to nearly 1 (Table 6A). The FbxO1-3HA pull-downs captured greater than 95% of FbxO1, whereas the efficiency of Skp1 capture in Skp1 pull-downs varied from 60-80% and was usually better in the Δ*phyA* cells than in RHΔΔ cells as observed from Skp1 co-IP experiments. A similar difference is reported in studies on *Dictyostelium* [28], suggesting that the pentasaccharide on Skp1 may interfere with antibody binding. In experiment 4 analyzed by Western blot, a search for trends suggested increased interactions between FbxO1 and Skp1 in the Δ*phyA* EC parasites that was not observed in IC parasites (Figure 11), but this trend was not observed in experiment 2 analyzed by mass spectrometry (Table 6A). Without evidence for effects that depended on particular experimental variables, an average of all data was taken and found to yield no statistically significant differences of either levels of Skp1 and FbxO1 or their association between the Δ*phyA* and RHΔΔ cells, thus, these results suggested that FbxO1 abundance or its association with Skp1 are not apparently under the regulation of the Skp1 modifications, at least as suggested by all the available results so far. But the occurrence of small differences (less than 1.7-fold) under certain conditions are not excluded.

During sequencing verification of the tagged FbxO1-3HA strains, clone D8, from which FbxO1 was tagged in the Δ*phyA* background, was found to have a point mutation (I796K) close to the C-terminus of FbxO1. Unexpectedly, the I796K point mutation significantly increased FbxO1 abundance in the Δ*phyA* strain by 2.9-fold (n=5) compared to the RHΔΔ strain, while no effects on Skp1 abundance was seen (Table 6B, Figure 9C). Although the single trial yielded an increased interaction of Skp1 with mutant FbxO1 in Δ*phyA* background relative to the interaction of Skp1 with normal FbxO1 in RHΔΔ background, it could be explained by the increased level

of FbxO1-3HA^{I796K} being pulled down. The mechanism of the effect of the point mutation and its dependence on the Skp1 modifications remains to be explored.

Table 6. Summary of the effect of the Skp1 modifications on Skp1 and FbxO1 abundance and their association.

Experiment	Quantification Method	Parasite Status	Description	Skp1			FbxO1		
				Abundance Δ*phyA*/RHΔΔ	FbxO1:Skp1 Δ*phyA*/RHΔΔ	Normalized to	Abundance Δ*phyA*/RHΔΔ	Skp1:FbxO1 Δ*phyA*/RHΔΔ	Normalized to
A. Skp1 co-IP/MS and FbxO1-3HA co-IP/WB									
1. UOK75 co-IP (EG)	MS-area under the curve	Δ*phyA* : 80% EC RHΔΔ: 40% EC	1% NP-40 lysis, 8 µl injection	0.86	1.38	non-specific proteins			
			1% NP-40 lysis, 4 µl injection	1.22	0.4	non-specific proteins			
			0.2% NP-40 lysis, 8 µl injection	1.00	1.98	non-specific proteins			
			0.2% NP-40 lysis, 4 µl injection	0.85	1.48	non-specific proteins			
2. Anti-FLAG co-IP (EG)	MS-area under the curve	EC (Skp1-SF & parental)	3× pooled 12 µl injections	2.26	0.43	non-specific proteins			
		IC (Skp1-SF & parental)	3× pooled 12 µl injections	1.23	0.36	non-specific proteins			
3. FbxO1-3HA WB	WB-densitometry	50% EC (H6 & A11)		1.11		Sag1	1.36		Sag1
4. Skp1 and FbxO1-3HA reciprocal co-IPs	WB-densitometry	EC (H6 & A11)		1.00	1.66	a-tubulin	1.55	1.43	a-tubulin
		IC (H6 & A11)		1.00	0.99	a-tubulin	0.98	1.17	a-tubulin
Average ± S.D. (1-4)				**1.17 ± 0.43**	**1.09 ± 0.63**		**1.30 ± 0.29**	**1.30 ± 0.18**	
B. FbxO1-3HA^I796K in ΔphyA co-IP/WB									
5. FbxO1-3HA WB	WB-densitometry	90% IC (H6 & D8)	1st SDS-PAGE	not probed			2.58		CBB
			Repeat	not probed			2.74		CBB
6. FbxO1-3HA co-IP/WB	WB-densitometry	50% EC (H6 & D8)	1st SDS-PAGE	0.84		CBB	3.13	2.05	CBB
			Repeat	0.99		Sag1	3.53		Sag1
7. FbxO1-3HA WB-2	WB-densitometry	50% EC (H6 & D8)		0.86		Sag1	2.89		Sag1
Average ± S.D. (5-7)				**0.90 ± 0.08**			**2.97 ± 0.37**	**2.05**	

Note: Results of expt. 4 are also shown Figure 11; The Skp1 co-IP/MS experiments were performed by Dr. Elisabet Gas-Pascual.

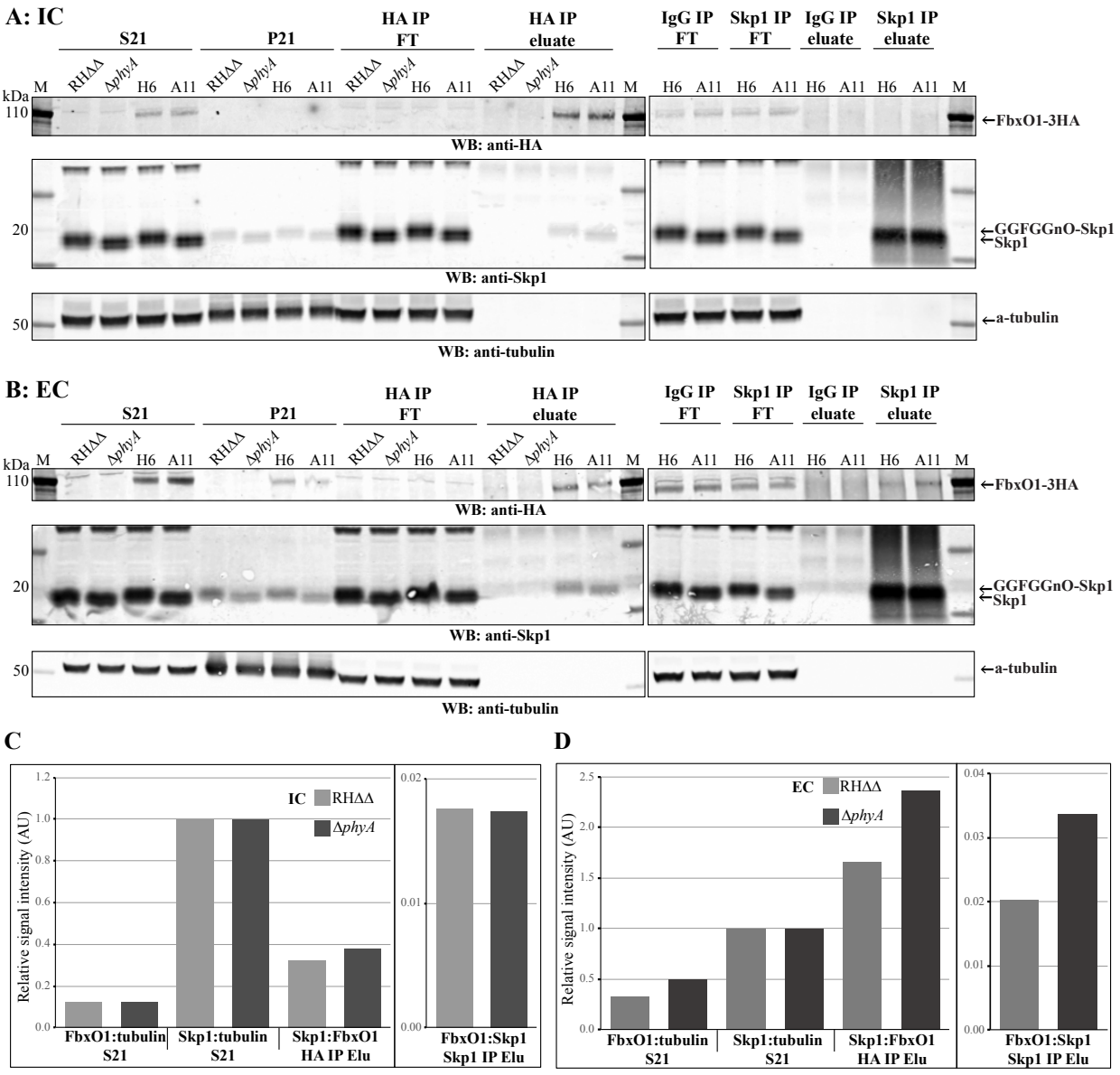

Figure 11. The effect of the Skp1 modifications on the abundance and association of Skp1 and FbxO1. (A) Reciprocal co-IP of Skp1 and FbxO1 from IC parasites. Loading was equivalent to ~3 million parasites for S21, P21, and IP flow-through (FT), and equivalent to ~10 million parasites for IP eluates. IgG IP was used as the negative control for Skp1 IP. α-tubulin was used as the loading control. **(B)** Reciprocal co-IP of Skp1 and FbxO1 from EC parasites, loading was equivalent to ~6 million parasites for S21, P21, and IP FT, and equivalent to ~20

million parasites for IP eluates. IgG IP was used as the negative control for Skp1 IP. α-tubulin was used as the loading control. **(C)** Quantitative comparison of strains A11 (Δ*phyA* background) and H6 (RHΔΔ background) from the results in panel A for IC parasites. **(D)** Quantitative comparison of strains A11 (Δ*phyA* background) and H6 (RHΔΔ background) from the results in panel B for EC parasites. AU: arbitrary unit.

3.6 Co-expression and purification of recombinant FbxO1

To recombinantly express sufficient amount of *Toxoplasma* FbxO1 as the antigen to generate anti-serum and to enable other biochemical studies, FbxO1 was expressed either alone or with *Toxoplasma* Skp1 in *E. coli* using the autoinduction protocol described in Chapter 2. The resulting *E. coli* extract was analyzed by SDS-PAGE and anti-His Western blot. About 50-60% of the putative 6His-FbxO1 was in the soluble fraction while the rest was likely in the insoluble inclusion bodies. In comparison, at least 80% of 6His-FbxO1 was soluble when co-expressed with Skp1, and the protein yield was significantly improved (Figure 12A). The effect of Skp1 on improving FBP solubility was observed previously with *Dictyostelium* Skp1 and JcdI, and it was hypothesized that Skp1 served as a chaperone or co-factor for JcdI, and JcdI required Skp1 to be functional in the soluble form (data not shown). This result indicated the improved solubility of *Toxoplasma* FbxO1 when co-expressed with *Toxoplasma* Skp1 and provides additional support for the importance of Skp1-FbxO1 interaction and the necessary role of Skp1 for FBP function.

The S21 and S100 fractions from the co-expression were used to purify the recombinant FbxO1 by the batch purification method described in Chapter 2. Briefly, the soluble extract was incubated with nickel charged Sepharose resin; then the resin was washed with 60 mM imidazole and eluted stepwise with 120 mM, 240 mM, 360 mM and 500 mM imidazole. Equal fractions of all samples were analyzed by SDS-PAGE and anti-His Western blot. As examined from Figure 12B, a predominant His-reactive band was observed at the expected molecular weight position for 6His-FbxO1 (calculated Mr = 89.6 kDa). At least 95% of the putative 6His-FbxO1 was captured by the resin. The first wash removed the excessive unbound material and the 60 mM imidazole wash removed some unspecific background. The elution with 240 mM imidazole released the most of the putative 6His-FbxO1 and another protein that migrated at the expected

position for *Toxoplasma* Skp1 consistent with expectation of formation and co-purification of a Skp1-FbxO1 complex. The remaining bound proteins were released by 360 mM and 500 mM imidazole elution. The amount of recombinant FbxO1 in each of the eluates was determined by A280 and densitometry of the protein gel. To remove the 6His tag, all of the 240 mM, 360 mM and 500 mM eluates were dialyzed into Thrombin Cleavage buffer and pooled for thrombin cleavage. At a 1:50 thrombin to recombinant FbxO1 molar ratio, at least 95% of the putative 6His-FbxO1 was cleaved which was evident with a molecular weight decrease of ~2 kDa on the protein gel and the absence of the cleaved product on the anti-His Western blot (Figure 12C). This result is consistent with the purified and digested protein being FbxO1. Comparing the molecular weights of the recombinantly expressed FbxO1 (~87 kDa) and the *Toxoplasma* expressed FbxO1 (~105 kDa), it further implied that FbxO1 is subject to posttranslational modifications in *Toxoplasma*. The cleaved sample was cleaned up and further gel purified as described in Chapter 2 for anti-serum production in rabbits.

The pre-bleeds and test bleeds from both rabbits were diluted 1:100 and used as the primary antibody for Western blotting of the purified FbxO1 sample and RHΔΔ extract. The test bleeds from rabbit UGA160 presented a prominent band at the expected Mr (87 kDa) of FbxO1 when probed with the purified FbxO1 sample, suggesting the presence of FbxO1 anti-serum in the test bleeds, however, no prominent band at the expected size of *Toxoplasma* FbxO1 (~105 kDa) was detected in the RHΔΔ extract. The other rabbit (UGA159) showed much weaker signal at 87 kDa than UGA160 in the positive control, and it did not show prominent signal at the expected size for *Toxoplasma* FbxO1 (Figure 13). More antigen related to the purified FbxO1 was sent for a boost in both of the rabbits and the final exsanguinations will be tested. Also, the

FbxO1HA strain will be compared with the RHΔΔ strain in the next screening experiment to help differentiate the 3×HA tagged FbxO1 from the native FbxO1.

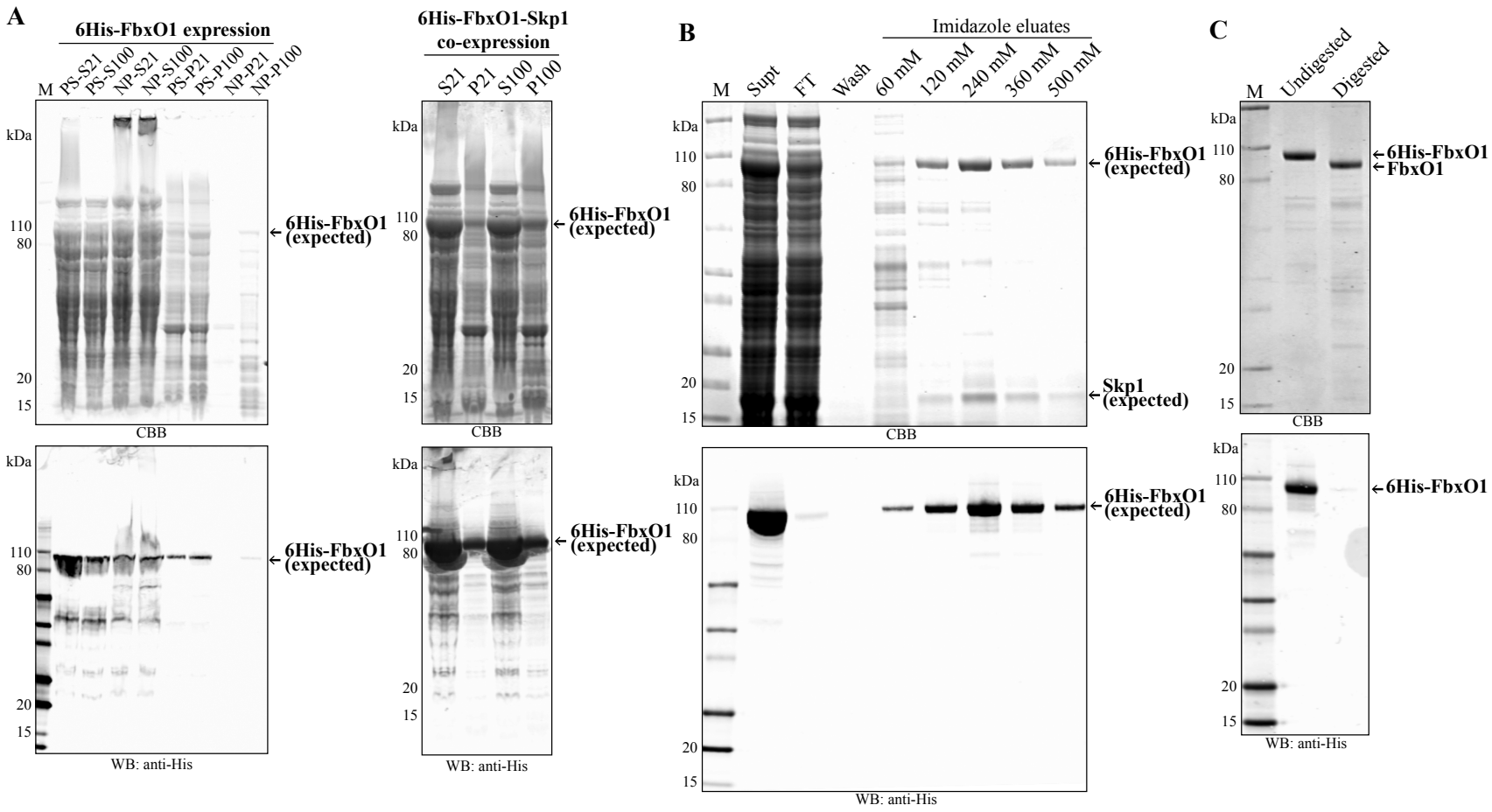
A
6His-FbxO1 expression
M
PS-S21
PS-S100
NP-S21
NP-S100
PS-P21
PS-P100
NP-P21
NP-P100
kDa
110
80
20
15
6His-FbxO1 (expected)
CBB
WB: anti-His
6His-FbxO1-Skp1 co-expression
S21
P21
S100
P100
B
Imidazole eluates
Supt
FT
Wash
60 mM
120 mM
240 mM
360 mM
500 mM
Skp1 (expected)
C
Undigested
Digested
6His-FbxO1
FbxO1

Figure 12. Co-expression and purification of recombinant FbxO1. (A) The solubility of the 6His-FbxO1 was examined by comparing the amount of the protein in supernatant and pellet fractions. In 6His-FbxO1 lone expression, both probe sonication in *E. coli* Lysis buffer (PS) and lysis in 1% NP-40 buffer (NP) were compared. In 6His-FbxO1 and Skp1 co-expression, the *E. coli* pellet was only extracted by probe sonication in *E. coli* Lysis buffer. All gel loadings were equal in each experiment. **(B)** The samples from a batch purification of 6His-FbxO1 were analyzed on an SDS-PAGE gel alongside the soluble fraction of the extract from the transformed *E. coli* strain. The protein gel was Western blotted with anti-His (1:1,000) to detect 6His-FbxO1. Loading of the supernatant was equal to about 0.06% of the total sample, and all other samples represented an equal fraction of the total. **(C)** Purified samples before and after thrombin digestion were analyzed on an SDS-PAGE gel and Western blotted to detect the recombinant 6His-FbxO1. M: Novex Sharp protein standard.

A **Screening with purified recombinant FbxO1**

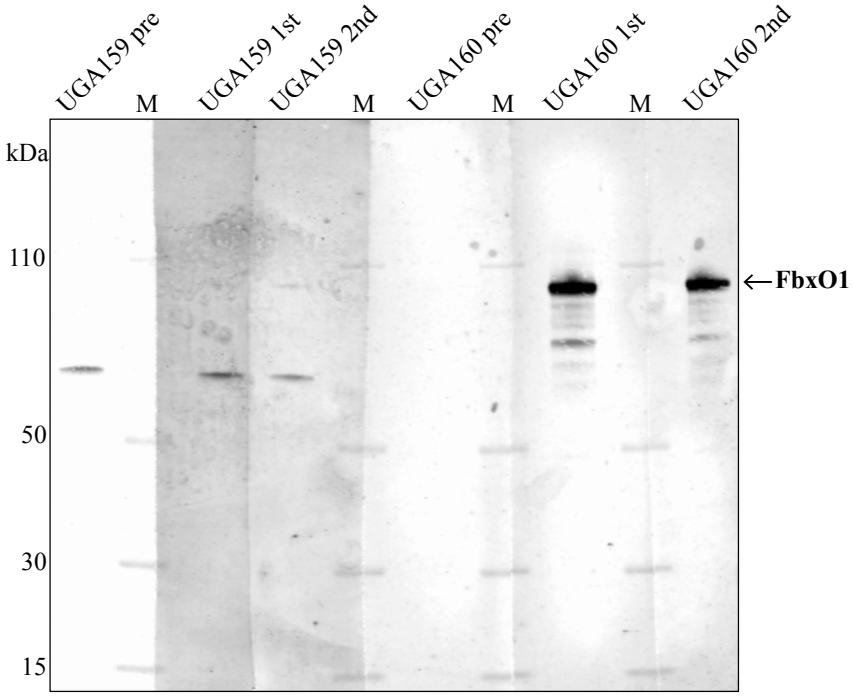

WB (1:100 of each serum)

B **Screening with *Toxoplasma* RHΔΔ lysate**

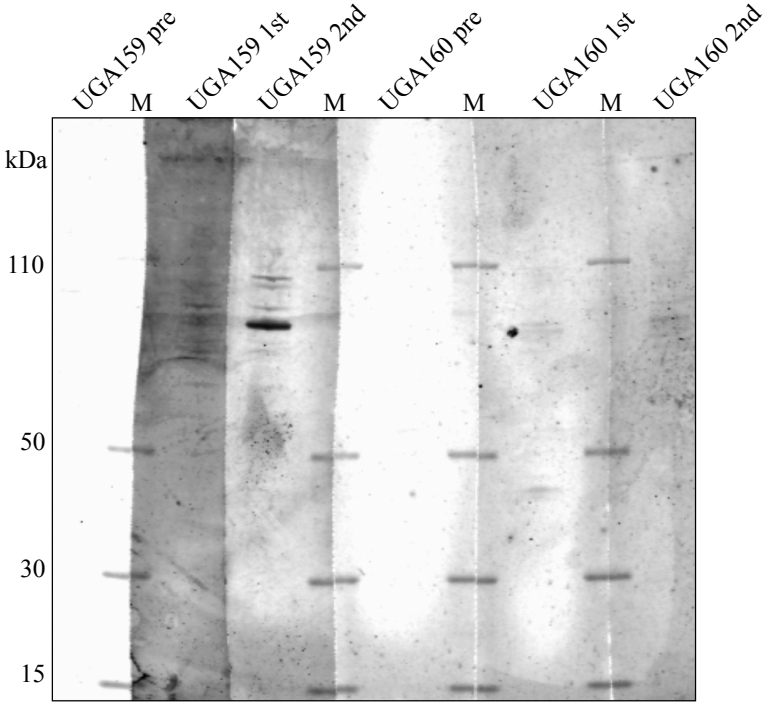

WB (1:100 of each serum)

Figure 13. Screening of serum samples from rabbits immunized with purified *Toxoplasma* FbxO1. (A) Screening of serum samples including the pre-bleeds (obtained before immunization with FbxO1), 1st bleeds and 2nd bleeds from both of the immunized rabbits, named UGA 159 and UGA 160, respectively, with purified *Toxoplasma* FbxO1 sample. About 100 ng of the sample was loaded in each lane. **(B)** Screening of the same serum samples with whole cell lysate S21 from RHΔΔ strain. The loading was equivalent to ~3 million parasites. A dilution of 1:100 of each serum sample was used for primary antibody incubation of the blots. M: Novex Sharp protein standard.

CHAPTER 4

SUMMARY AND FUTURE DIRECTIONS

4.1 Summary

The purpose of this study is to investigate if the *Toxoplasma* Skp1 modifications affect the association between Skp1 and its interactors. Based on the Skp1 interactome results, *Toxoplasma* FbxO1, one of the 18 predicted *Toxoplasma* FBPs, was consistently detected as the main Skp1 interactor. The interaction between FbxO1 and Skp1 was determined to be robust by reciprocal FbxO1 co-IP studies. The largely improved efficiency in recombinant expression of FbxO1 when it was co-expressed with Skp1 further indicated the importance of the Skp1-FbxO1 interaction and suggested that their interaction is direct *in vitro*. This interaction was further supported by the finding that truncation of the *Toxoplasma* FbxO1 F-box motif did not allow for complementation in the parasites. Together, these results suggested that Skp1 directly interacts with FbxO1 and their interaction is important for FbxO1 function.

Toxoplasma FbxO1 was further analyzed for its potential function, and more importantly, whether the association between Skp1 and FbxO1 was affected by the Skp1 modifications. Domain analysis of FbxO1 revealed that its sequence was well conserved among apicomplexan species, implying a specialized function of FbxO1-like proteins in this group of protists. FbxO1 was also predicted to be *N*-myristoylated, which could transform at least part of the FbxO1 into peripherally membrane-associated protein. Cellular fractionation of FbxO1 showed that about equal amounts of FbxO1 in the parasites were either cytosolic or membrane-associated, which

supported the *N*-myristoylation prediction of FbxO1, and coincided with the evidence that the myristoyl group could be either exposed or buried inside the protein to change protein solubility [35]. FbxO1 localization was dynamic during the cell cycle, indicating its regulated turnover or trans-localization, and it was involved in DCS formation in a Rab11b-dependent manner during early endodyogeny [17], similar to what was observed for IMC [5, 38]. The presence of *Toxoplasma* Rab11b in the FbxO1 interactome, although needing further confirmation, provided support to the Rab11b-dependent mechanism. Though the FbxO1 interactome studies did not identify stable interactors, a role as a substrate-receptor type FBP could not be excluded as such interactions are expected to be transient and eliminate the interactor. The dynamic localization and possible turnover indicated that alternatively, FbxO1 could potentially play a signaling role and be regulate by the SCF^{FbxO1}.

There was no significant effect of the Skp1 modifications on either FbxO1 abundance or its association with Skp1 based on all the available co-IP results. However, it is important to know that these were static and steady state measurements, and there could be altered turnover of FbxO1 facilitated by the Skp1 modifications, which was too subtle to be detected. Thus, more experiments are needed to explore the effect of the Skp1 modifications on SCF assembly and the underlying mechanism for PhyA regulation of the SCF.

4.2 Future directions

The *Toxoplasma* FbxO1 interactome needs to be further investigated by co-IP/MS with increased starting material to improve enrichment of FbxO1 and its interactors. And since the C-terminus of FbxO1 is potentially important for protein-protein interactions, an alternative approach is to tag FbxO1 in the less conserved region in the N-terminal domain. Previous BioID

trials expressed FbxO1 tagged with the C-terminal 3×HA-BirA* but did not show above-background labeling of biotinylated species in biotin-treated parasites (Figure 14), potentially due to below background labeling or inactivation of the tag. An improved version of BioID, known as TurboID, is smaller and requires less activation time [39], thus it may be a better option for future tagging and interactome studies of FbxO1. Another ongoing approach is to generate polyclonal antibodies against *Toxoplasma* FbxO1 to circumvent problems with using epitope tags. The FbxO1 anti-serum could be used in future FbxO1 co-IP studies. To exploit the possibility of FbxO1 as a substrate receptor, the improved FbxO1 co-IP workflows mentioned above will also be combined with either *in vivo* crosslinking to stabilize complexes or proteasomal inhibitor treatment to stabilize interactors of FbxO1 that are potentially polyubiquitinated by the SCF^{FbxO1}.

Although the Skp1 modifications did not significantly affect FbxO1 abundance or its association with Skp1, some other Skp1 interactors including Cullin1, TGGT1_259880, and another *Toxoplasma* FBP (JmjD6b) had >10-fold difference between the Δ*phyA* and RHΔΔ strains in their abundance relative to Skp1. JmjD6b was detected in recent Skp1-SF co-IP/MS experiments and was annotated as a histone lysine demethylase (toxodb.org). JmjD6b has a predicted F-box motif and is also a homolog to one of the *Dictyostelium* FBPs, JcdI, whose abundance was influenced by the Skp1 modifications [28]. Thus, JmjD6b is a relevant target FBP to study the effect of the Skp1 modifications on Skp1 and FBP association and SCF assembly in *Toxoplasma*.

As one of the major components of the SCF complex, it has been suggested that Cul1 plays an important role in keeping the equilibrium between Skp1-FBP subcomplexes and cellular substrates by exchanging the Skp1-FBP subcomplexes that interact with Cul1 [12]. Though in

need of confirmation, it had been observed from Skp1 co-IP/MS experiments that Cul1 interaction with Skp1 decreased in the Δ*phyA* strain, suggesting that the interaction between Cul1 and Skp1-FBP subcomplexes could be regulated by the Skp1 modifications. Thus, the reverse investigation of Cul1 interactome in the Δ*phyA* and RHΔΔ strains will be a future approach to understand the effect of the Skp1 modifications on *Toxoplasma* SCF assembly.

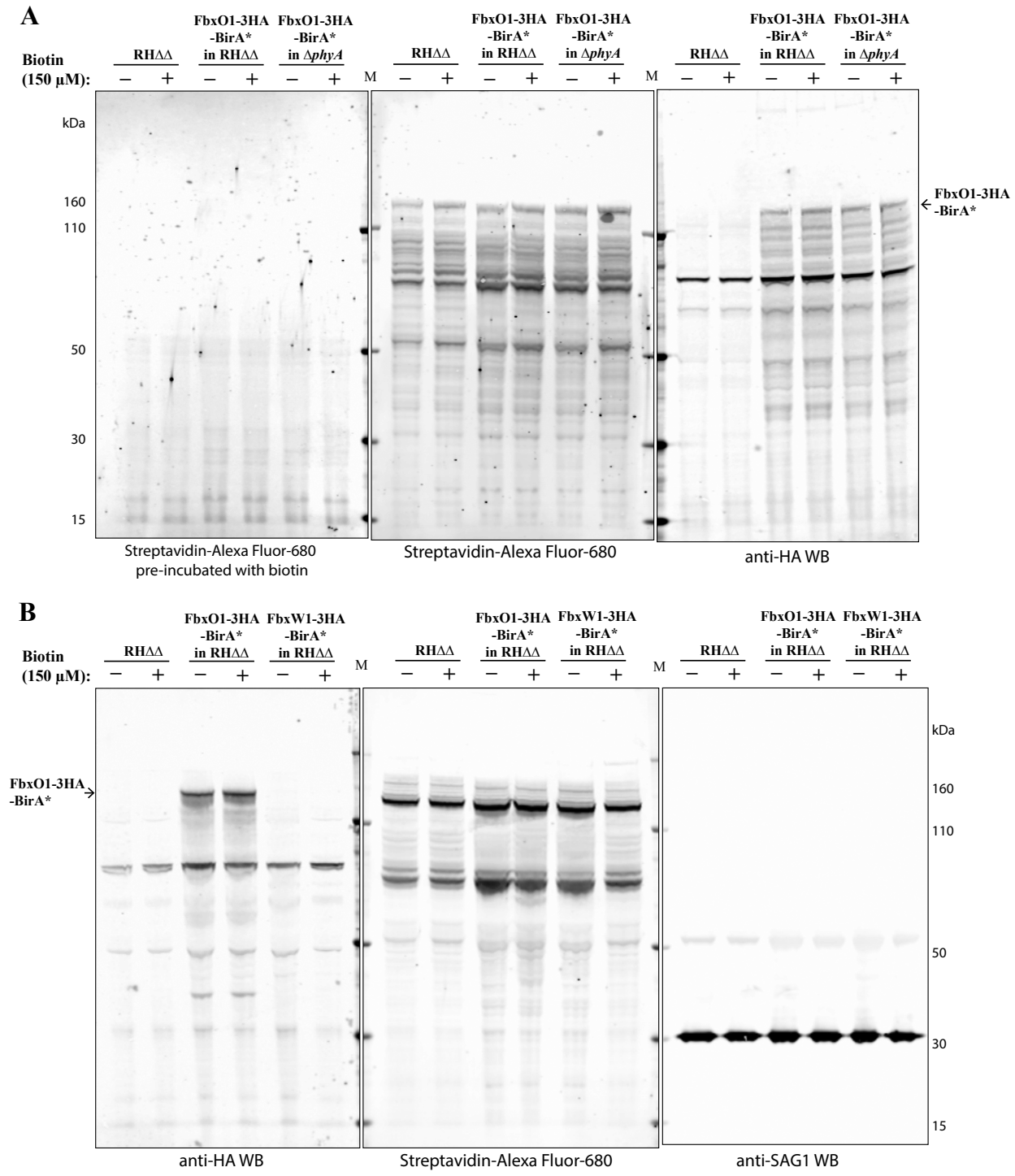

Figure 14. Western blot analysis of BirA* tagged strains. The FbxO1-3HA-BirA* and FbxW1-3HA-BirA* strains were generated as described in Chapter 2. **(A)** The FbxO1-3HA-BirA* strains in both the RHΔΔ and Δ*phyA* background were treated with 150 µM biotin for 24

hours and compared with the non-treated group. As a control to verify the specificity of streptavidin-Alexa Fluor-680, it was incubated with excess biotin in dark for 30 mins before being used for blotting. The FbxO1-3HA-BirA* has an expected molecular weight of ~140 kDa and was indeed observed on the anti-HA Western blot. No obvious differences were observed for the parasites either treated with biotin or not. **(B)** The FbxO1-3HA-BirA* and FbxW1-3HA-BirA* strains, both in the RHΔΔ background, were treated in the same way as shown above. The size of the tagged FbxO1 was replicated on the anti-HA Western blot. But the tagged FbxW1 was not detected. Similarly, no obvious differences were observed for the parasites either treated with biotin or not. SAG1 was used as the loading control. M: Novex Sharp protein standard.

Publications

Baptista CG, Lis A, **Deng B**, Gas-Pascual E, Dittmar A, Sigurdson W, West CM, Blader IJ. *Toxoplasma* F-box protein 1 is required for daughter cell scaffold function during parasite replication. PLoS Pathog. 2019;15(7)*

* **Note**: I contributed to Ref. 17 by investigating *Toxoplasma* FbxO1 domain and evolution using tools including BLASTP search and COBALT alignment. I was involved in the Skp1 interactome result analysis and update of the list of predicted *Toxoplasma* FBPs.

Gas-Pascual E, Ichikawa HT, Sheikh MO, Serji MI, **Deng B**, Mandalasi M, Bandini G, Samuelson J, Wells L, West CM. CRISPR/Cas9 and glycomics tools for *Toxoplasma* glycobiology. Journal of Biological Chemistry. 2018;294(4):1104–1125.**

Note: I contributed to reference 32 by performing knockout trials of two *Toxoplasma* glycogenes, TGGT1_266320 and TGGT1_280400, using the CRISPR/Cas9-mediated double gRNA strategy developed in this study.

REFERENCES

1. Dubey JP. The history and life cycle of *Toxoplasma gondii*. In: Weiss LM, Kim K, editors. Toxoplasma gondii, the Model Apicomplexan: Perspectives and Methods. 2007;1-17.
2. Flegr J, Prandota J, Sovičková M, Israili ZH. Toxoplasmosis – A Global Threat. Correlation of Latent Toxoplasmosis with Specific Disease Burden in a Set of 88 Countries. PLoS ONE. 2014;9(3):1-22.
3. Blader IJ, Coleman BI, Chen CT, Gubbels MJ. Lytic Cycle of *Toxoplasma gondii*: 15 Years Later. Annu Rev Microbiol. 2015;69:463-85.
4. Francia ME, Striepen B. Cell division in apicomplexan parasites. Nat Rev Microbiol. 2014;12(2):125-36.
5. Ouologuem DT, Roos DS. Dynamics of the *Toxoplasma gondii* inner membrane complex. J Cell Sci. 2014;127(15):3320–3330.
6. Ciechanover A, Orian A, Schwartz AL. Ubiquitin-mediated proteolysis: biological regulation via destruction. Bioessays. 2000;22(5):442-451.
7. Silmon de Monerri NC, Yakubu RR, Chen AL, Bradley PJ, Nieves E, Weiss LM, Kim K. The Ubiquitin Proteome of *Toxoplasma gondii* Reveals Roles for Protein Ubiquitination in Cell-Cycle Transitions. Cell Host & Microbe. 2015; 18(5):621-633.
8. Zheng N, Shabek N. Ubiquitin Ligases: Structure, Function, and Regulation. Annual Review of Biochemistry. 2017;86:129-157.

9. Sheikh MO, Schafer CM, Powell JT, Rodgers KK, Mooers BH, West CM. Glycosylation of Skp1 affects its conformation and promotes binding to a model f-box protein. Biochemistry. 2014;53(10):1657-1669.
10. West CM, Blader IJ. Oxygen sensing by protozoans: how they catch their breath. Current Opinion in Microbiology. 2015;26:41-47.
11. Wu JT, Lin HC, Hu YC, Chien CT. Neddylation and deneddylation regulate Cul1 and Cul3 protein accumulation. Nature Cell Biology. 2005;7(10):1014-1020.
12. Pierce NW, Lee JE, Liu X, Sweredoski MJ, Graham RL, Larimore EA, Rome M, Zheng N, Clurman BE, Hess S, Shan S, Deshaies RJ. Cand1 promotes assembly of new SCF complexes through dynamic exchange of F box proteins. Cell. 2013;153:206-215.
13. Skowyra D, Craig KL, Tyers M, Elledge SJ, Harper JW. F-box proteins are receptors that recruit phosphorylated substrates to the SCF ubiquitin-ligase complex. Cell. 1997;91(2):209-219.
14. Bai C, Sen P, Hofmann K, Ma L, Goebl M, Harper JW, Elledge SJ. SKP1 Connects Cell Cycle Regulators to the Ubiquitin Proteolysis Machinery through a Novel Motif, the F-Box. Cell. 1996;86(2):263-274.
15. Schulman BA, Carrano AC, Jeffrey PD, Bowen Z, Kinnucan ER, Finnin MS, Elledge SJ, Harper JW, Pagano M, Pavletich NP. Insights into SCF ubiquitin ligases from the structure of the Skp1-Skp2 complex. Nature. 2000;408(6810):381-386.
16. Kipreos ET, Pagano M. The F-box protein family. Genome Biology. 2000;1(5):1-7.
17. Baptista CG, Lis A, Deng B, Gas-Pascual E, Dittmar A, Sigurdson W, West CM, Blader IJ. *Toxoplasma* F-box protein 1 is required for daughter cell scaffold function during parasite replication. PLoS Pathog. 2019;15(7)

18. Neer EJ, Schmidt CJ, Nambudripad R, Smith TF. The ancient regulatory-protein family of WD-repeat proteins. Nature. 1994;371(6495):297-300.
19. Kobe B, Deisenhofer J. The leucine-rich repeat: a versatile binding motif. Trends in Biochemical Sciences. 1994;19(10):415-421.
20. van der Wel H, Ercan A, West CM. The Skp1 prolyl hydroxylase from *Dictyostelium* is related to the hypoxia-inducible factor-alpha class of animal prolyl 4-hydroxylases. Journal of Biological Chemistry. 2005;280(15):14645-14655.
21. Teng-umnuay P, Morris HR, Dell A, Panico M, Paxton T, West CM. The Cytoplasmic F-box Binding Protein SKP1 Contains a Novel Pentasaccharide Linked to Hydroxyproline in *Dictyostelium*. Journal of Biological Chemistry. 1998;273:18242-18249.
22. West CM, van der Wel H, Wang ZA. Prolyl 4-hydroxylase-1 mediates O2 signaling during development of *Dictyostelium*. Development. 2007;134(18);3349-3358.
23. Wang ZA, Singh D, van der Wel H, West CM. Prolyl hydroxylation- and glycosylation-dependent functions of Skp1 in O2-regulated development of *Dictyostelium*. Developmental Biology. 2011;349(2):283-295.
24. Xu Y, Brown KM, Wang ZA, van der Wel H, Teygong C, Zhang D, Blader IJ, West CM. The Skp1 protein from *Toxoplasma* is modified by a cytoplasmic prolyl 4-hydroxylase associated with oxygen sensing in the social amoeba *Dictyostelium*. Journal of Biological Chemistry. 2012;287(30):25098-25110.
25. Rahman K, Zhao P, Mandalasi M, van der Wel H, Wells L, Blader IJ, West CM. The E3 Ubiquitin Ligase Adaptor Protein Skp1 Is Glycosylated by an Evolutionarily Conserved Pathway That Regulates Protist Growth and Development. Journal of Biological Chemistry. 2016;291(9):4268-4280.

26. West CM, Wang ZA, van der Wel H. A cytoplasmic prolyl hydroxylation and glycosylation pathway modifies Skp1 and regulates O2-dependent development in *Dictyostelium*. Biochimica et Biophysica Acta. 2010;1800(2):160-171.
27. Rahman K, Mandalasi M, Zhao P, Sheikh MO, Taujale R, Kim H, van der Wel H, Matta K, Kannan N, Glushka JN, Wells L, West CM. Characterization of a cytoplasmic glucosyltransferase that extends the core trisaccharide of the *Toxoplasma* Skp1 E3 ubiquitin ligase subunit. Journal of Biological Chemistry. 2017;292:18644-18659.
28. Sheikh MO, Xu Y, van der Wel H, Walden P, Hartson SD, West CM. Glycosylation of Skp1 promotes formation of Skp1-cullin-1-F-box protein complexes in *dictyostelium*. Mol Cell Proteomics. 2014;14(1):66–80.
29. Xu X, Eletsky A, Sheikh MO, Prestegard JH, West CM. Glycosylation Promotes the Random Coil to Helix Transition in a Region of a Protist Skp1 Associated with F-Box Binding. Biochemistry. 2018;57(5):511-515.
30. Sheikh MO, Thieker D, Chalmers G, Schafer CM, Ishihara M, Azadi P, Woods RJ, Glushka JN, Bendiak B, Prestegard JH, West CM. O2 sensing-associated glycosylation exposes the F-box-combining site of the *Dictyostelium* Skp1 subunit in E3 ubiquitin ligases. Journal of Biological Chemistry. 2017;292(46):18897-18915.
31. Sidik SM, Huet D, Ganesan SM, Huynh MH, Wang T, Nasamu AS, Thiru P, Saeij JPJ, Carruthers VB, Niles JC, Lourido S. A Genome-wide CRISPR Screen in *Toxoplasma* Identifies Essential Apicomplexan Genes. Cell. 2016;166(6):1423-1435.
32. Gas-Pascual E, Ichikawa HT, Sheikh MO, Serji MI, Deng B, Mandalasi M, Bandini G, Samuelson J, Wells L, West CM. CRISPR/Cas9 and glycomics tools for *Toxoplasma* glycobiology. Journal of Biological Chemistry. 2018;294(4):1104–1125.

33. Shen B, Brown K, Long S, Sibley LD. Development of CRISPR/Cas9 for efficient genome editing in *Toxoplasma gondii*. Meth. Mol. Biol. 2017;1498:79-103.

34. Martin DD, Beauchamp E, Berthiaume LG. Post-translational myristoylation: Fat matters in cellular life and death. Biochimie. 2011;93(1):18-31.

35. Schlott AC, Holder AA, Tate EW. N-Myristoylation as a Drug Target in Malaria: Exploring the Role of N-Myristoyltransferase Substrates in the Inhibitor Mode of Action. ACS Infect Dis. 2018;4:449-457.

36. Treeck M, Sanders JL, Elias JE, Boothroyd JC. The phosphoproteomes of *Plasmodium falciparum* and *Toxoplasma gondii* reveal unusual adaptations within and beyond the parasites' boundaries. Cell Host Microbe. 2011;10(4):410–419.

37. Nebl T, Prieto JH, Kapp E, Smith BJ, Williams MJ, Yates JR 3rd, Cowman AF, Tonkin CJ. Quantitative in vivo analyses reveal calcium-dependent phosphorylation sites and identifies a novel component of the *Toxoplasma* invasion motor complex. PLoS Pathog. 2011;7(9)

38. Agop-Nersesian C, Egarter S, Langsley G, Foth BJ, Ferguson DJ, Meissner M. Biogenesis of the inner membrane complex is dependent on vesicular transport by the alveolate specific GTPase Rab11B. PLoS Pathog. 2010;6(7).

39. Branon TC, Bosch JA, Sanchez AD, et al. Efficient proximity labeling in living cells and organisms with TurboID [published correction appears in Nat Biotechnol. 2020 Jan;38(1):108]. Nat Biotechnol. 2018;36(9):880–887.